UNIVERSITY OF GAZİANTEP

GRADUATE SCHOOL OF

NATURAL & APPLIED SCIENCES

INVESTIGATION OF IMPACT BEHAVIOR OF LAMINATED HYBRID COMPOSITE PLATES

Ph.D THESIS

IN

MECHANICAL ENGINEERING

BY

MEHMET BULUT

JANUARY 2017

Investigation of Impact Behavior of Laminated Hybrid Composite Plates

University of Gaziantep

Ph. D. Thesis

In

Mechanical Engineering

Supervisor

Assoc. Prof. Dr. Ahmet ERKLİĞ

Co-Supervisor

Assist. Prof. Dr. Eyüp YETER

By

Mehmet BULUT

January 2017

REPUBLIC OF TURKEY
UNIVERSITY OF GAZİANTEP
GRADUATE SCHOOL OF NATURAL & APPLIED SCIENCES
MECHANICAL ENGINEERING DEPARTMENT

Name of thesis: Investigation of Impact Behavior of Laminated Hybrid Composite
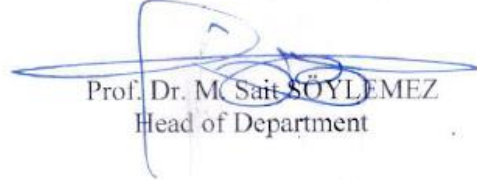
Plates

Name of the Student: Mehmet BULUT

Exam Date: 09.01.2017

Approval of the Graduate School of Natural and Applied Sciences

Prof. Dr. A. Necmeddin YAZICI
Director

I certify that this thesis satisfies all the requirements as a thesis for the degree of
Doctor of Philosophy.

Prof. Dr. M. Sait SÖYLEMEZ
Head of Department

This is to certify that we have read this thesis and that in our consensus/majority
opinion it is fully adequate, in scope and quality, as a thesis for the degree of Doctor
of Philosophy.

Assist. Prof. Dr. Eyüp YETER   Assoc. Prof. Dr. Ahmet ERKLİĞ
Co-Supervisor   Supervisor

Examining Committee Members: Signature

Prof. Dr. İ. Hüseyin FİLİZ

Prof. Dr. M. Kemal APALAK

Assoc. Prof. Dr. Ahmet ERKLİĞ

Assist. Prof. Dr. Veysel ÇAKIR

Assist. Prof. Dr. M. Murat YAVUZ

I hereby declare that all information in this document has been obtained and presented in accordance with academic rules and ethical conduct. I also declare that, as required by these rules and conduct, I have fully cited and referenced all material and results that are not original to this work.

Mehmet BULUT

ABSTRACT

INVESTIGATION OF IMPACT BEHAVIOR OF LAMINATED HYBRID COMPOSITE PLATES

BULUT, Mehmet
Ph. D. In Mechanical Engineering
Supervisor: Assoc. Prof. Dr. Ahmet ERKLİĞ
Co-Supervisor: Assist. Prof. Dr. Eyüp YETER
January 2017, 126 Pages

Present study investigates the impact and damage characteristics of hybrid composite laminates using quasi-static penetration (QSPT), quasi-static indentation (QSI) and low velocity impact tests (LVI) conditions. For this purpose, ASTM D732, ASTM D 6264 and ASTM D 7136 international test standards were used. Woven Carbon, Kevlar and S-glass fabrics were used as reinforcing fibers for production of hybrid and non-hybrid composite laminates. During the QSPT experiments, punch shear test procedures were employed until the perforation and complete plugging shear out of the laminate. A flat end punch with diameter of 12.7 mm has been used for two different support spans (25.4 and 63.5 mm) having two different support span (Ds) to punch diameter (Dp) ratios (SPR = Ds/Dp = 2 and 5).

The goal of QSI tests from this study is to develop basic understanding low velocity impact events. QSI tests were performed by a hemispherical indenter having 12.7 mm size of diameter to the coupons having 76.2 mm diameter circular opening. LVI tests were performed by an instrumented and controlled drop weight impact machine. Impact and damage characteristics of the samples were compared with observing the impacted and non-impacted surfaces under the constant impact energies (15 and 30J). The degree of the hybridization effects was evaluated with reference to the rule of mixture in terms of absorbed energy and maximum force.

The results from this study showed that failure mechanisms of the hybrid samples were significantly affected by stacking sequence of the fibers. It is possible to increase impact resistance and energy absorption capacity by hybridization of Kevlar and Carbon fibers while incorporation of more economic S-glass fibers contributed to decrease cost of the hybrid composite.

Keywords: Quasi-static, hybrid composite, impact behavior, fiber

ÖZET

TABAKALI HİBRİT KOMPOZİT PLAKALARIN DARBE DAVRANIŞININ ARAŞTIRILMASI

BULUT, Mehmet
Doktora Tezi, Makine Mühendisliği
Tez Yöneticisi: Doç. Dr. Ahmet ERKLİĞ
Yardımcı Tez Danışmanı: Yrd. Doç. Dr. Eyüp YETER
Ocak 2017, 126 sayfa

Bu çalışma tabakalı hibrit kompozitlerin darbe ve hasar özelliklerini yarıstatik penetrasyon, yarı statik batma ve düşük hızlı darbe altındaki darbe özelliklerini araştırmaktadır. Bu amaç için, sırasıyla ASTM D732, ASTM D 6264 ve ASTM D 7136 uluslararası standartlar kullanılmıştır. Hibrit ve hibrit olmayan kompozitlerin üretiminde güçlendirici fiber olarak örgülü karbon, kevlar ve S-camı fiberler kullanılmıştır. Yarı statik penetrasyon deneyleri sırasında, kompozit tabakanın tamamen delinmesi ve oluşan artık parçanın nümunelerden çıkmasına kadar panç-kesme prosedürleri uygulanmıştır. Düz ve 12.7 mm çapında panç, iki farklı destek/panç çapı oranını (SPR = Ds/Dp = 2 ve 5) elde etmek için iki farklı destek genişliği (25.4 ve 63.5 mm) kullanılmıştır.

Yarı statik batma testlerindeki amaç, düşük hızlı darbe olaylarını temel olarak anlamayı geliştirmektir. Yarı statik batma testleri üzerinde 76.2 mm çapında açıklık bulunan test nümunelerine 12.7 mm çapındaki küresel uçlu panç ile gerçekleştirilmiştir. Ağırlık düşürme darbe cihazı yardımı ile düşük hızlı darbe testleri gerçekleştirilmiştir. Malzemelerin darbe ve hasar toleransları sabit 15J ve 30J darbe enerjileri altında darbe yapılan yüzey ve arka kısımlardaki yüzeyleri gözlemlenerek karşılaştırılmıştır. Hibridizasyon etkilerinin derecesi emilen enerji ve maksimum kuvvet cinsinden karıştırma kuralına göre hesaplanmıştır.

Bu çalışma sonucunda, hibrit kompozitlerde oluşan hasar mekanizmalarının fiber dizilimlerinden oldukça fazla etkilenmiştir. Kevlar ve karbon fiberlerinin hibridizasyonu ile darbe dayanımı ve enerji emme kapasitesini artırmak mümkün olmakla birlikte daha ekonomik S-camı fiberin katılması hibrit kompozitin maliyetinin düşmesine yardımcı olmaktadır.

Anahtar kelimeler: Yarı statik, hibrit kompozit, darbe davranışı, fiber

ACKNOWLEDGEMENT

TABLE OF CONTENTS

LIST OF FIGURES

x

LIST OF TABLES

CHAPTER 1

INTRODUCTION

1.1 Composite Materials and Applications

Composite materials are defined as mixtures of two or more different materials with different physical properties. Different materials can be mixed together with the purpose of generating superior materials which have better properties than those of the individual materials. In the most general case, composite materials are composed of one or more discontinuous phases distributed within the continuous phases. Continuous phase is called as "matrix" and discontinuous phase is called as reinforcing material or the reinforcement as described in Figure 1.1. In the case of several continuous phases for different natures, composite material is called as "hybrid composite." In general, discontinuous phase is harder with mechanical properties, which are much higher than those of continuous phase.

For composite materials in which reinforcement is composed of fibers, the fiber orientation is a major factor for the anisotropy of the material. This aspect continues the ability to tailor the composite structure according to the concept and fabrication of the structure in order to obtain desired structure properties [1].

Composite materials can be classified according to the form of the constituent materials or the nature of constituent materials. Since the fiber reinforced composites lead high mechanical properties and possibility to develop an extensive study of their mechanical characteristics, composite type dealt with throughout this study has been chosen as the fiber reinforced composites in which matrix resins are the polymeric materials. There can be found a variety of fibers used in several industries, some of most commonly used fibers and their mechanical properties are presented in Table 1.1.

In fiber reinforced composites, woven in two dimensional plane fibers are the popular due to their weaving advantageous in terms of impact strength and mechanical properties.

Woven fabric differ by the type of the fibers (strand, yarn, roving. etc.), and therefore by the linear density of the warp, as well as by the type of weave. Different types of the weaves can be made according to the repeating pattern of the warp and fill interlacing [1]. Figure 1.2 presents the most commonly used weave styles. In the present study, plain and twill weave of the fibers have been used.

Table 1.1 Some fibers and resin properties [2]

Matetial	Density (Mgm^{-3})	Tensile modulus (GPa)	Tensile strength (MPa)	Strain to failure (%)
Glass fibre	2.49-2.55	73-86	3400-4500	3.5-5.4
Carbon fibre	1.7-2.0	160-827	1400-7070	0.27-1.9
Aramid fibre	1.39-1.45	73-160	2400-3400	1.4-4.6
Inorganic fibre	2.0-3.97	152-462	1720-3900	
Phenolic fibre	1.0-1.35	3.1-4.6	50-75	1.0-6.5
Epoxy resin	1.2-1.2	2.6-3.8	60-85	1.5-8
Bismaleimide resin	1.2-1.32	3.2-5	48-110	1.5-3.3
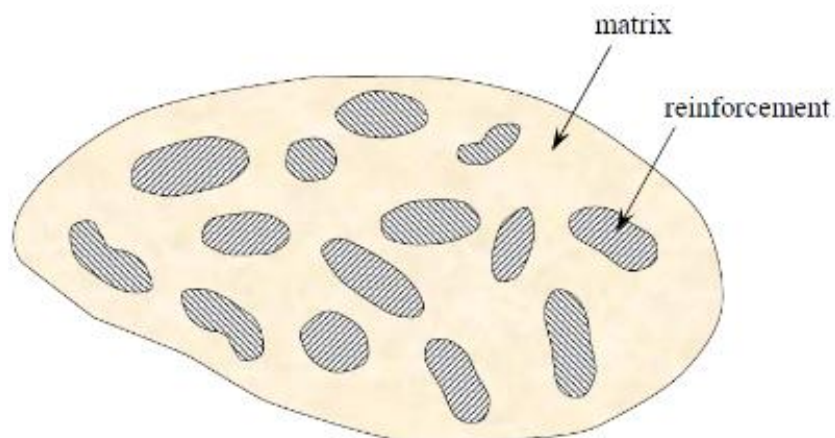
Figure 1.1 Composition of a composite material [1]

Plain weave or taffeta   2×2 twill weave or serge   8 satin weave

Cross-ply weave   Unidirectional cloth

(a)   (b)
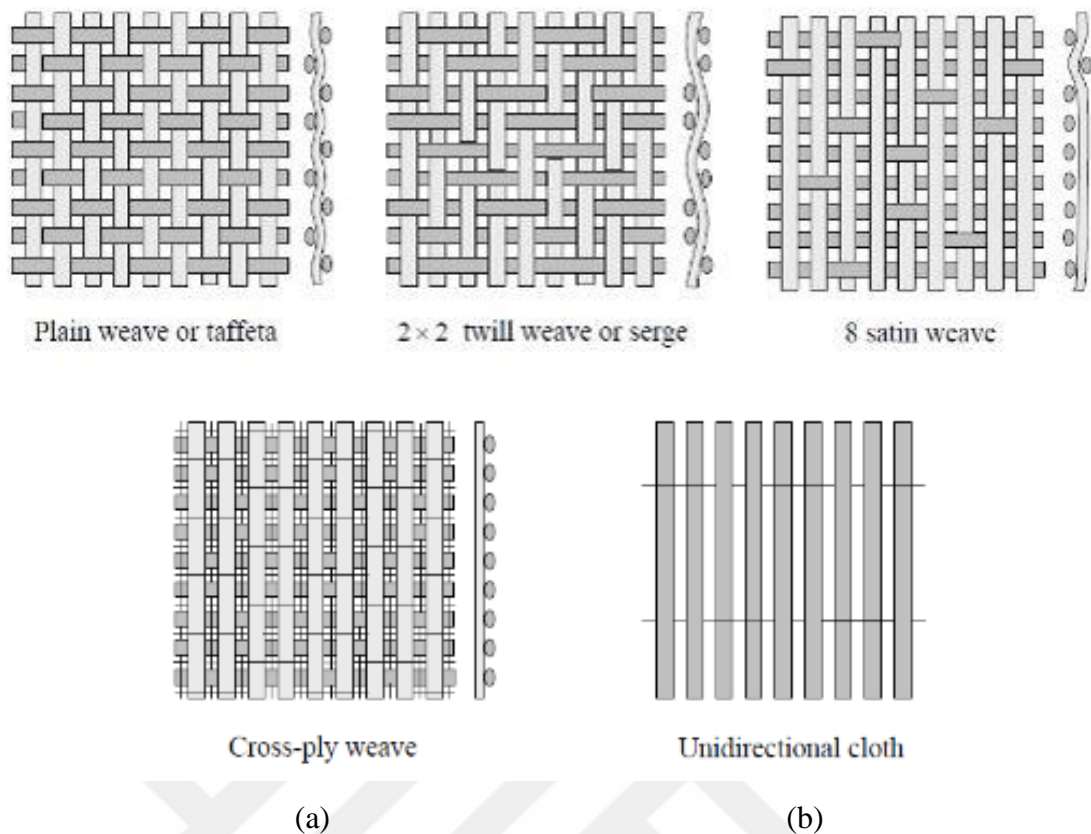
Figure 1.2 Several weaving architecture of the fibers [1]

1.1.1 Advantages and disadvantages of composites

The main advantages of composites can be summarized as follows [4]:

- Light-weight due to high specific strength and stiffness,
- Good fatigue and corrosion resistance,
- Low thermal conductivity,
- High creep resistance,
- Low density,
- High capability of optimization to tailored the directional stiffness and strength,
- It is possible to make composites with desired properties. A suitable reinforcement, matrix, and processing method can be selected from the wide variety of reinforcements, matrices, and processing methods.
- Complex shapes can be made very easily with composites.
- It is possible to produce composites with combination of desired properties.

While these composites have following disadvantages [4];

- Laminated composites having the poor interphases exhibit the poor resistance to out of plane tensile loadings,

- They have poor impact resistance with strong possibility of internal damages undergoing impact events,

- Composite materials are generally expensive compared with conventional metals,

- The recycling of composites is another difficulty compared to the conventional metallic materials,

- Manufacturing methods for shaping composite materials are often slow and costly,

1.1.2 Some applications of composites

Composites are candidate for next generation materials and their some applications in the aerospace, marine and automotive industries are listed below [5];

- Automotive body parts are constructed by mainly carbon and glass fiber reinforced composites,

- Many civil and military aircrafts now equipped inevitable quantities of lightweight, high-strength carbon-, glass- and Kevlar- fiber composite laminates, as laminated panels, plates and molding, and as composite honeycomb structures with metallic or resin-impregnated paper honeycomb core materials,

- Formula one extensively uses the carbon fiber reinforced composites,

- Carbon fiber reinforced composites are used in road and mountain bikes and also in road bikes made of Aluminum the seat posts handle bars, and forks,

- Carbon fiber and honeycomb composites are used for construction of Chassis,

- Fuel tanks are made up of Kevlar reinforced rubber,

- Offshore structures, underwater and surface vessels are the marine applications and they are mainly made of glass fiber reinforced composites for fishing boats, military, and transportation vessels.
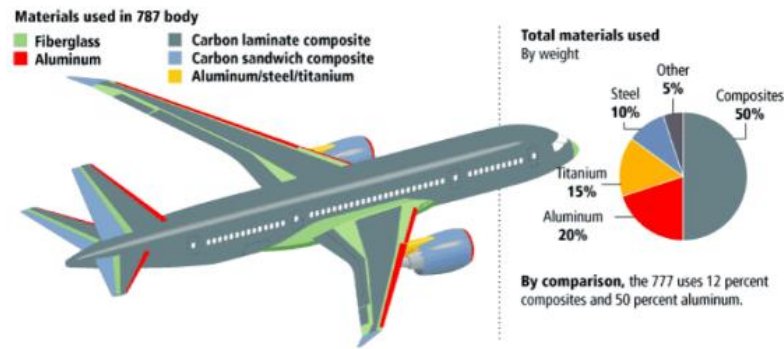
Figure 1.3 The parts of the Boeing-787 Dreamliner made of carbon and glass fibers [3]

As Figure 1.3 illustrates the composite ratio of components in the new made of airplanes (Boeing-787 Dreamliner). More than 50 % of the total material is made of the composite used in airplanes. Carbon and glass fibers are the major reinforcing materials, but the biggest part of the airplane is constructed by the carbon fibers.

1.1.3 Hybrid Composites

Reference to hybrid composites related with the kinds of fiber reinforced composites, generally resin based, in which two or more different fibers are combined within the single matrix. By the application of hybrid concept with combining two or more materials, it is possible to optimize their value to the engineer, permitting the exploitation of their better qualities while lessening the effects of their less desirable properties. As such, the definition is much more restrictive than the reality. Any combination of dissimilar materials could in fact be thought of as a hybrid.

 A classic example is the type of structural material in which a metal or paper honeycomb or a rigid plastic foam is bonded to thin skins of some high-performance FRPs, the skins carrying the high surface tensile and compressive loads and the core providing lightweight (and cheap) structural stability. The combination of sheets of aluminum alloy with laminates of fiber-reinforced resin, as in the commercial product ARALL is a related variety of layered hybrid and the mixing of fibrous and particulate fillers in a single resin or metal matrix produces another species of hybrid composite.

Some hybrids of current interest represent attempts to reduce the cost of expensive composites containing reinforcements like carbon fiber by incorporating a proportion of cheaper, lower-quality fibers such as glass without too seriously reducing the mechanical properties of the original composite. Of equal importance is the reverse

principle that of stiffening a GRP structure with a small quantity of judiciously placed carbon or aromatic polyamide fiber, without inflicting too great a cost penalty.

In high-technology fields, the question of cost may be insignificant by comparison with the advantages of optimizing properties. In aerospace applications, a familiar purpose of using hybrids is to utilize the natural toughness of GRP or of Kevlar-fiber-reinforced plastics (KFRP) to offset a perceived brittleness of typical CFRP. From the designer's point of view the important aspect of using hybrids is that provided there is adequate understanding of the underlying mechanisms of stiffening, strengthening and toughening, they allow even closer tailoring of composite properties to suit specific requirements than can be achieved with single-fiber types of composites [5]

1.1.4 Impact Behavior of Composites

Fiber-reinforced laminated composites have been used extensively in load bearing structures due generally to their lightweight, high strength-to weight and stiffness-to-weight ratios, excellent fatigue strength, good corrosion resistance and reduced parts count. Applications of such structures are abundant in aircraft, high-performance vehicles, high-speed boats, and marine vessels. These composite structures may encounter a transverse impact load in scenarios such as: tool-dropping, hailstones, runway or road debris. Such events may induce damage in the form of matrix cracking, fiber fracture and delamination. This damage can alter the structural response during impact and reduce subsequent structural performance.

Both strength and stiffness can be affected and in-plane compression strength is especially sensitive to this kind of damage. Therefore, a current and important design requirement in load-bearing composite structures is the ability to tolerate impact damage. There are five basic mechanical failure modes that can occur in a composite after initial elastic deformation. These are [6]:

• Fiber failure, fracture, and, for Aramids, defibrillation.

• Resin crazing, micro cracking and gross fracture.

• Debonding between the fiber and matrix.

• Delamination of adjacent plies in a laminate.

• Fiber pull out from the matrix and stress relaxation.

Composite structures impacted by a foreign object may lead to cause external and internal damages, and these failures will reduce stiffness and structural load carrying capacity. For example, a dropped foreign object may cause the delamination in the composites which sometimes visible or not. Even such a structures are in still in service without any failure, the initiation of damage can cause to extend the damage and result in the ultimate failure of the mechanism

As a result, it is needed to investigate damage and impact characteristics of fiber reinforced composite structures under the different loading conditions. When high velocity impact on composite laminates is assisted by the quasi-static penetration tests, the damage characteristics of the composite laminates can be altered due to dynamic effects, especially in large strains.

Figure 1.4 shows the effects of strain rate on impact behavior of woven Carbon/epoxy composite laminates. It is observed that the force has been increased at a much faster displacement rate before it has reached the peak value. This is due to the fact that the laminate deflection is very local when the laminate has been struck by a projectile at a much higher loading rate. On the other hand, the relatively lower force peak shown for the impact case, as compared to the quasi-static counterpart, was considered to be due to the occurrence of spallation damage that reduced the laminate stiffness [6].

Impact events are generally categorized as low-, high-, or hyper-velocity. Figure 1.5 shows possible impact types and corresponding to impact damage mechanisms. The type of impact may be distinguished by the response that it creates in the target material. The responses are dominated by stress wave propagation through the material, to which the structure does not have time to respond, resulting in much localized damage. Boundary condition effects can be ignored because the impact event is over before the stress waves have reached the edge of the structure [7].
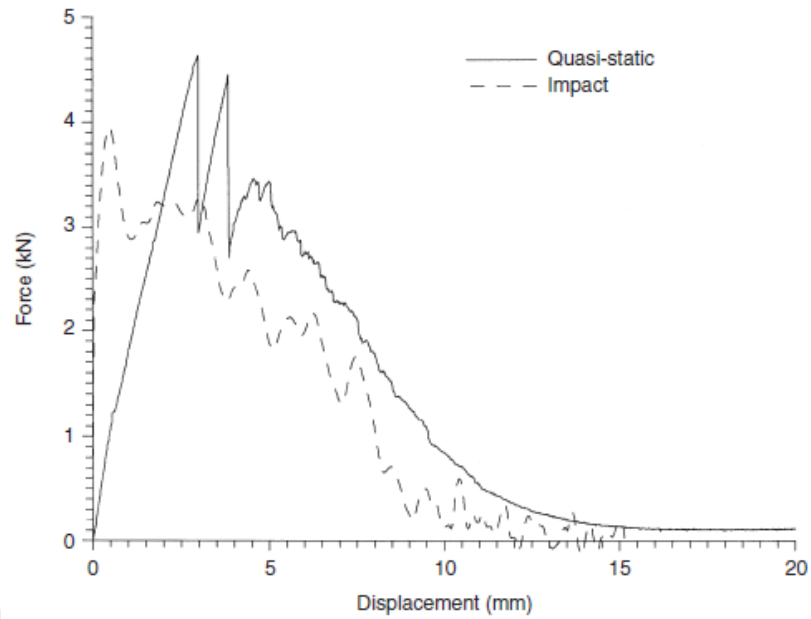
Figure 1.4 Effect of strain rate on the tensile stress-strain curve for woven Carbon/epoxy [6]

(a)   (b)
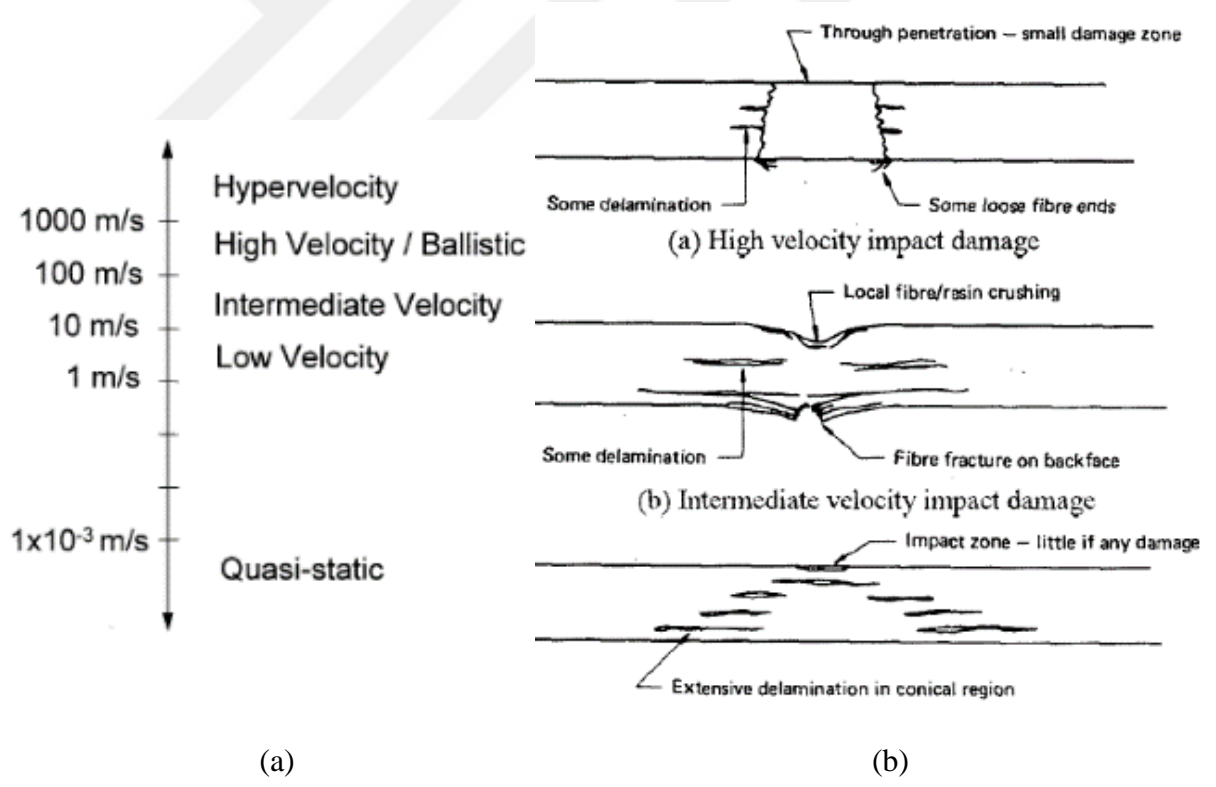
Figure 1.5 Types of damage and impacts with extend of projectile velocity. (a) Standard velocity classification for impact event. (b) Failure modes corresponding to impact velocity [8]

As shown in Figure 1.5, impact velocity below which 10 m/s can be considered as low velocity impact, while high velocity impact events are occurred more than 100 m/s velocity of projectile. Therefore, impact events by means of velocity can be divided into two parts, namely, low and high velocity impact, respectively. For a thick composite plate subjected to out of plane loading by a flat end striker, there would be three damage sequences through the thickness of the laminate. These stages are illustrated in Figure 1.6 [6]. Force to time responses and corresponding to damage shapes are also comparatively provided. As shown in Figure 1.6, the load increases linearly until the damage section, then follows the formation of delamination until the maximum load has reached. After the maximum load is exceeded, the failures of fiber breakage and plugging shear out reveal in the composite laminates.The impact response of materials can be classified by low (large mass) velocity, intermediate velocity, high/ballistic (small mass) velocity and hyper velocity regimes. For low velocity impact tests, the commonly used mechanisms are Izod-Charpy impact (Figure 1.7) and drop weight impact machine (Figure 1.8).
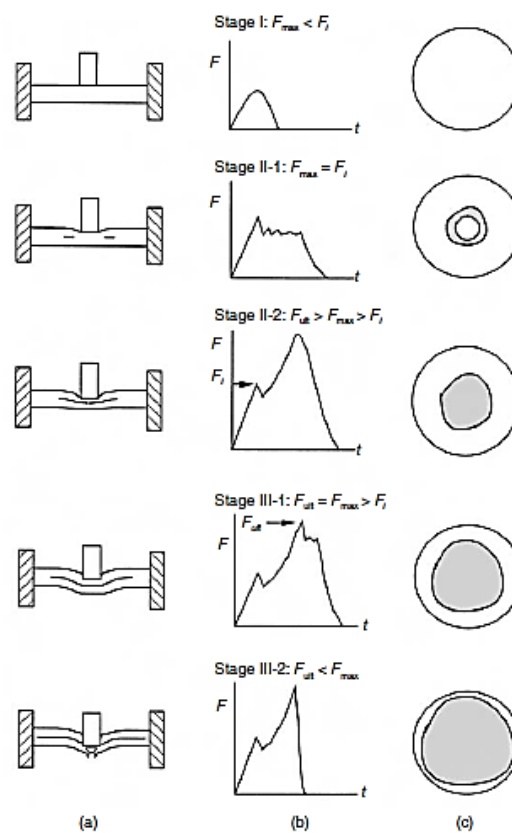
Figure 1.6 Three-stage damage sequence in thick laminate plates under low velocity impact described by (a) deformation sketches, (b) impact response curves and (c) C-scan graphs [6]

9
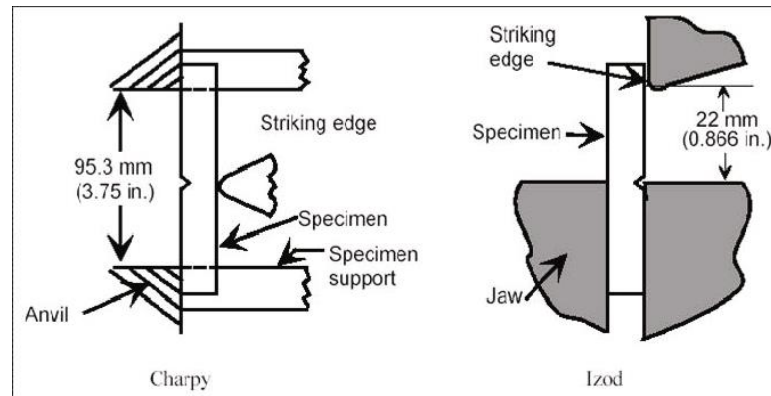
Figure 1.7 Izod and Charpy impact test mechanisms [9]
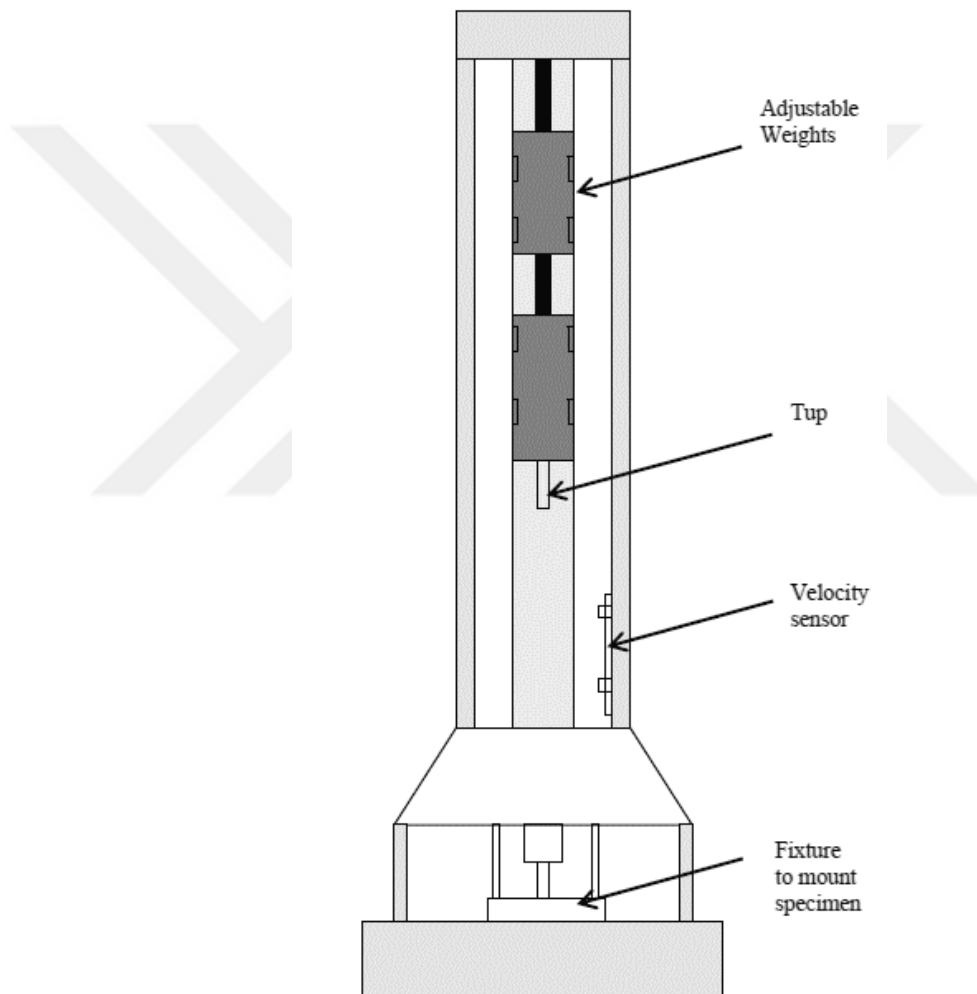
Figure 1.8 Drop weight impact machine for low velocity impact tests [9]

Polymer matrix composites are very sensitive to internal and external damage induced by low velocity impact. Internal damages may not be visible over the surfaces, but damage can be significant, resulting reduction of stiffness and residual strength in the composite structures.

The measurement of dynamic contact force during the impact event is not easy due to wide range of impact velocities, the limitation of experimental technique and other parameters. The static test methods would provide a very beneficial method to researchers for modelling low velocity impact events since much more data could be obtained from a quasi-static test rather than impact test [9].

The need for a static (or more commonly referred to as quasi-static) test method for modeling low velocity foreign object impact events would prove to be very beneficial to researchers since much more data can be obtained from a quasi-static test than from an impact test. An American Standard Testing Materials ASTM D6264/D6264M [10] standard has been proposed for transverse quasi-static loading of composite laminates, although the standard stops short of claiming to represent low-velocity impacts.

It would be very beneficial to simulate an impact event using a "quasi-static" loading test. By using this test, damage initiation and propagation can be more easily detected, deflection can be directly measured with great accuracy, and maximum transverse force can be better controlled. Thus, the focus of the work in this technical publication (TP) was to examine if drop-weight impact tests and quasi-static loading tests give the same size, shape, and location of damage for a given maximum transverse load [11]. Figure 1.9 shows the indentation damage mechanism of the structure.
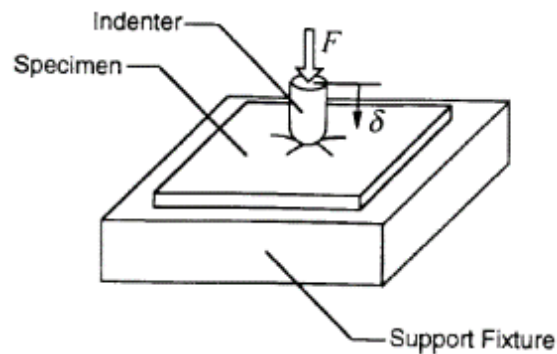
Figure 1.9 Quasi-Static Indentation Test

1.2 Scope of the Thesis

With the expanding field of composite materials, a greater knowledge of damage and impact mechanisms is needed. While a satisfactory understanding of the conventional materials as like metals has developed, the little of knowledge is devoted to fiber reinforced composites in today's industry. The demand and replacement of fiber

reinforced composites by metals are increasing due to their superior properties. The property of high strength to weight ratio of carbon and glass fiber reinforced composite structures has made them attractive for production of next generation materials. The understanding of impact resistance in fiber reinforced composites is quite important for design considerations against the foreign impact event.

An experimental procedure has been performed to evaluate progressive damage assessment in hybrid composite laminates. This effort comes from identifications of similar damage behavior resulting in quasi static and impact loading conditions since the behavior of fiber reinforced hybrid composites under the quasi static impact conditions has not been investigated adequately.

This work focuses on impact resistance and resulting development of damage modes in the fiber reinforced hybrid composites. The plain woven S-glass, kevlar and carbon fibers were used as primary reinforcing material for hybrid arrangements. A series of indentation and penetration tests were conducted by cylindrical indenters with hemispherical and flat ends, respectively. In addition, low velocity impact tests were performed by hemispherical end indenter with a constant impact energy level (30 J). The extension and development of damage modes were identified by comparing indentation test results.

General introduction and definitions on composite materials and their impact behavior are given in the first chapter. First chapter also covers the importance and outline of the study.

Literature survey is given in chapter 2. Literature survey has been grouped in five sections; Studies about glass fiber, studies on carbon fiber, studies of Kevlar fiber, studies on hybrid composites, and studies on high velocity impact/quasi-static penetration tests.

Chapter 3 presents the experimental procedures for production and preparation of test samples in order to use QSPT, QSI, and LVI experiments.

Chapter 4 presents the experimental studies for measurement of QSPT. The background and procedures from QSPT in this study have been discussed in this section.

Chapter 5 presents the experimental studies for measurement of QSI. The background, procedures and all results from QSI in this study have been discussed in this section.

Chapter 6 presents the experimental studies for measurement of LVI. The background, procedures, and all results from LVI in this study have been discussed in this section.

General conclusions and future works are given in chapter 7 and 8, respectively.

1.3 Aims and Objectives

The objective of this thesis is to develop basic understanding of impact behavior of fiber reinforced hybrid composite laminates under the quasi-static penetration and low velocity impact loading conditions. Present study attempts to identify the damage modes in the three different fibers and accurately describe the penetration, indentation and low velocity impact process. This information may in turn be used for modelling the ballistic impact and low velocity impact response of hybrid composites reinforced with Kevlar, carbon and glass fibers.

There is a quite need for a measurement system that is low cost, needs easy to operation and set-up. With the use of this system (quasi-static test) which capable of doing this purpose, force-displacement curves can be easily obtained, and these results enables the modelling of ballistic and low velocity impact events.

The goal of quasi-static penetration tests is to investigate energy absorption and maximum load carrying capacity of hybrid composites reinforced by combination of two and three different fibers. A second purpose is to perform quasi-static indentation tests by a hemispherical indenter in order to simulate low velocity impact events in hybrid and non-hybrid composite samples. QSI tests will be performed by instrumented tensile test machine, and damage assessment through the thickness will be identified by cutting of composite samples.

A third purpose is to carry out low velocity impact tests using an instrumented drop-weight impact test machine. By the use of international ASTM standards, impact behavior of composite samples will be identified in terms of force-time, force-displacement, and absorbed energy captured in the samples. With QSI tests, correlations and similarities with will be evaluated for different configurations of hybrid composite laminates.

1.4 Main Contributions

The main novelties of this thesis are:

- To identify the damage characteristics in hybrid composites reinforced with two and three different fibers by using quasi-static penetration, quasi-static indentation and low velocity impact tests.
- To evaluate the degree of hybrid effect concept in terms of rule of mixture,
- To show the failure mechanisms in the hybrid composite laminates for different stacking sequences,
- To determine the maximum load carrying capacity and absorbed energy of hybrid and non-hybrid composite laminates showing hybridization effects,

CHAPTER 2

LITERATURE SURVEY

In this section, an overview of the literature review dealing with the impact behavior of composite materials will be presented. Firstly, chapter discusses the general properties on the topic, including the classification of impact behavior of composites according to fiber types. Then literature review focuses on the factors those of influencing the behavior of hybrid composites under the quasi-static penetration process. Accordingly, literature follows the quasi-static indentation tests on hybrid composite laminates. Finally, conclusions on literature review will be presented.

2.1 Introduction

With rapidly expanding application of composite materials, a greater knowledge of properties is needed to meet design requirement in the structural applications. High mechanical properties per weight for lightweight structural applications are the main reasons for choosing these materials instead of traditional metals.

The requirement for understanding of impact behavior has been increased by the crucial areas in which fiber reinforced composites are found in today's industry. The main weakness in fiber reinforced composites is their ability to resist impact damage and could be improved by hybridization of different fibers. The carbon, aramid, and glass fibers are extensively used as reinforcing materials and combining of these fibers for exploit of each fiber advantage can increase the mechanical properties of the structure with high performance of impact strength and load carrying capacity. Natural fibers are also being increasingly used.

In the present study, the effort is devoted to examine the damage tolerance and impact behavior of fiber reinforced hybrid composites in the view of quasi-static penetration, quasi-static indentation and low velocity impact tests. In this context, present literature review related with impact behavior of composite laminates was grouped according to fiber types and test procedures used as damage mechanism.

2.2 Studies Using Glass Fiber

Hosseinzadeh et al [12] studied on the impact and damage behavior of fiber reinforced composite plates subjected by drop-weight impact tests with different impact energies having four different configurations using carbon and glass fibers. In addition, overall impact mechanism was modelled by ANSYS LS DYNA software to predict the threshold of damage in composite laminates. It is concluded that at higher impact energies, diameter of damaged area on the samples were increased while no collapse was occurred, and for carbon fiber laminates, there wasn't any damage observed under the 30 J impact energy level.

Agrawal et al. [13] examined comprehensive study on impact behavior of fiber reinforced polymer matrix composites. Their study covered the effects of striker shape, weight of striker, velocity of impact and environment undergoing impact tests. In addition, the damage area, energy absorbed, contact time, and environmental effects during the impact event were parameters to be handled properly. It is asserted that impact damage modes firstly initiated the matrix cracking, and then followed by the fiber breakage and penetration. Especially, unidirectional fiber reinforced composites were highly sensitive to impact damage by means of matrix cracking, delamination between layers and fiber breakage.

Atas [14] studied on the impact response of Glass fiber/Aluminum composite laminates under the drop-weight impact tests. In order to assess failure and impact characteristics of composite laminates, an energy profiling method showing the correlations between absorbed and impact energies were used. After a series of impact tests with different impact energies, damage mechanisms were inspected by observing over the front and rear surfaces. It is shown that plastic deformation and shearing in Aluminum layers and fiber breakage and delamination in the composite laminates were mostly effective in energy absorption capacity.

Ji et al. [15] handled the impact damage of 3D orthogonal woven composite circular plates. E-Glass fibers having warp, weft and Z yarns were used for impact tests. Low velocity impact tests were performed under the quasi-static and dynamic loading conditions with four different energy levels. Impact mechanisms were also simulated by finite element software ABAQUS to show the evaluation of damage and impact

events in the composite samples. Good correlation was found between experimental and numerical predictions.

Fan et al. [16] conducted low velocity impact tests on glass fiber/metal with epoxy composite laminates. The fiber/metal laminates comprised of a layer of glass fiber-reinforced plastics sandwiched between two layers of aluminum alloy. Impact tests were conducted on the test samples under the projectile velocity of 5 m/s. The effects of various parameters such as laminate thickness, striker size and impacted area were examined for prediction of energy absorption capacity. After the experiments, impacted sections were highlighted in order to predict impact events in the samples. It is shown that fiber/metal reinforced composite laminates sufficiently improved perforation resistance compared with plain composite counterparts. In addition, increasing of projectile diameter and thickness of the samples resulted in increase of perforation energy levels.

Caprino et al. [17] conducted low velocity impact tests on fiberglass (S2-glass)-aluminum (2024 T3 sheets) laminated composites to study the parameters of mass, impact energy and velocity those influencing material behavior. They asserted that load-displacement curves were strictly dependent on the energy, rather than mass and speed of the impactor. It was also found that a low was required energy for the first failure, while the energy level corresponding to first fiber fracture was similar to those of first failure in the Aluminum sheets.

Mathivanan and Jerald [18] studied on low-velocity impact behavior of composite laminates reinforced with glass fibers, experimentally. Impact tests were conducted for different thickness of the specimens and different velocities of projectiles according to ASTM standards using an instrumented impact testing machine. For the prediction of damage modes and extension, a correlation in terms of residual deformation in the middle of the samples was provided. It was shown that glass/epoxy composite laminates exhibited poor sensitivity to the mechanical behavior in terms of strain rate effects.

Mili and Necib [19] investigated impact and damage characteristics of cross-ply E-glass/epoxy laminated composites subjected to low velocity impact tests. Impact tests were carried out below the velocity of 3.1 m/s for three different lay-up configurations,

namely, $[0_2/90_6/0_2]$, $[0_3/90_4/0_3]$ and $[0_4/90_2/0_4]$. Influence of striker velocity and lay-up sequence on impact of composite plate was also studied. It is found that impact forces and deflections at the middle of plate were increased while increasing the striker velocity, and impact resistance of cross ply composite plates could be altered with increasing number of outer layers while remaining the total number of layers used in the lamina.

Shyr and Pan [20] investigated damage characteristics of composite laminates by drop-weight impact tests. E-glass, non-crimp, and nonwoven e-glass were primary reinforcing fibers during the testing of composites plates. Optical microscope was used to examine the damage characteristics in the cross-section of the impacted laminates. Results showed that the major damage on composite samples was recorded as fiber breakage when the impact energy was exceeded the threshold energy. Failure mechanisms of matrix cracking, delamination, and fiber breakage were also seen at the back surfaces. Finally, number of layer was major factor for the energy-absorption capability of composite laminates.

Atas et al. [21] studied impact behavior of repaired and unrepaired glass/epoxy composite plates. Samples were produced by the vacuum assisted resin infusion process and hand lay-up technique. Impact tests with different impact energies were performed for comparison of repaired and unrepaired samples. According to load-deflection curves obtained from impact tests, main damage modes for repaired samples were recorded as matrix and fiber breakage, but delaminations along with fiber directions were more dominant for unrepaired samples. Perforation energy of repaired samples was nearly 120 J while that of intact samples was larger than 150 J.

Zainuddin et al. [22] studied on low-velocity impact properties of e-glass/epoxy composites with hollow glass fibers. Two different energy levels as 40 and 56 J were applied to the samples with multiple times. Results indicated that significant improvement and recovery in impact properties were obtained with 53.6% gain in peak load after second impact in self-healing agent filled hollow glass fibers samples over control samples.

Baucom et al. [23] investigated low-velocity impact damage of woven 2-D and 3-D S2-glass reinforced composite laminates under repeated transverse impact loads.

Impact results were obtained in terms of energy dissipation capacity and impact force. Results indicated that the radial spread of damage was detected smallest and maximum for 2D and 3D composite laminates, respectively. The energy absorption capacity and penetration resistance in 3D composite laminates were better than those of 2D composite laminates.

Icten et al. [24] examined the effect of impactor diameter on impact resistance of woven Glass/epoxy composite plates under the low velocity impact tests. Four different impactor sizes were used, namely, 12.7, 20.0, 25.4 and 31.8 mm, respectively. Impact tests were conducted on composite samples with a range of energy levels from 5 J to perforation thresholds. It is indicated that impactor diameter was a key factor for the impact behavior of composite plates.

Santos et al. [25] studied on evaluation of low velocity impact damage in fiber Glass composite plates using piezoelectric sensors. Impact effect was examined by two parameters; amplitude response and time shift. It is asserted that two evaluated parameters were capable to characterize the damage types and amplitude predicted defect size, whenever fiber breakage occurred.

Belingardi and Vadori [26] investigated low velocity impact tests of laminated glass/epoxy composite. Both with unidirectional layers and with woven layers stacking, with three different layers orientations were considered. Impact tests were conducted on the samples using drop weight impact testing method according to ASTM standards. It is concluded that glass/epoxy laminates exhibited the poor sensitivity to the strain rate effect for considered speed range and type of loading.

Davies and Hitchings [27] examined impact resistance and residual strength of woven glass/polyester laminates under the low velocity impacts. Flat end striker was used up to energy level of 3100 J to evaluate impact damage on composite samples. The behavior of energy absorption and impact response was determined in terms of absorbed energy and impact force histories. The residual compressive strength values were also measured as well as damage tolerances. The failure surfaces on composites were determined by the sectioning of the samples and ultrasonic C-scanning. It is remarked that damage force and energy applied not only initiated the unstable fashion, but also caused the increase of damage size up to the maximum load bearing capacity.

Residual compressive strength values were decreased as the increasing in applied load as a result of delaminations between layers.

2.3 Studies Using Carbon Fiber

Ghelli and Minak [28] studied on damage and impact characteristics of thin carbon/epoxy composite laminates considering low velocity impact and compression after impact (CAI) tests. Impact tests according to ASTM standards were experimentally conducted on samples with different stacking sequences to the square and circular impacted areas. CAI tests were also simulated with a finite element software to predict critical buckling loads. Results showed that relationship between absorbed energy and delamination area was independent of stacking sequence and test configurations.

Rio et al. [29] investigated impact behavior of carbon/epoxy composite laminates under the low velocity impact tests with different laminate structures (unidirectional, cross-ply, quasi-isotropic and woven laminates) at temperature range from 20 ^{0}C to -150 ^{0}C. The amount of damage in the composite samples was evaluated by C-Scan ultrasonic inspection machine, optical and scanning electron microscopy. It is shown that cooling of samples before impact tests caused to decrease in energy absorption capacity, resulting severe matrix cracking, delamination, indentation on the impacted surface, fiber–matrix debonding and fiber fracture on the opposite surface.

Quaresimin et al. [30] studied on energy absorption capacity of woven carbon/epoxy composite laminates having different stacking sequences under the low velocity impact tests. Ultrasonic C-scan device was used for damage evaluation through the laminate thickness. A methodology based on simple physical considerations was developed to predict damage and energy absorption capacity of the composite samples. This methodology was based on a parabolic function which describes the absorption coefficient. Results showed that damage initiation, delamination threshold load and the associated energy were not affected by lay-up stacking sequence and impact energy, and they were highly depended on laminate thicknesses. Meanwhile, it is possible to improve the absorbed energy by the presence of 0/45 lay-up sequence.

Pegoretti et al. [31] optimized the impact energy absorption and inter-laminar fracture toughness of carbon/epoxy composite laminates using charpy impact test. Mode I

fracture toughness of the carbon/epoxy laminates was measured in the range from 40 to 260 J/m^2 by interleaving and perforated PET foils. There point bending tests were performed to study quasi static and impact responses. It was found that bending modulus was independent of inter laminar strength under the quasi static and impact conditions. It is also asserted that inter-laminar fracture toughness contributed the reverse effect on the initiation and propagation energy under the impact loading.

Bull et al. [32] studied on the effects of particle-filler in order to increase impact damage resistance in carbon fiber reinforced polymer composite laminates. Composite samples were designed as five layers of carbon fibers as reinforcement toughened with thermoplastic particles as well as without toughened matrices. Tests samples were subjected to impact energies ranging from 25 J and 50 J. Damage characteristics of samples were determined. It is found that addition of particle as a toughened material to the composite samples was caused to increase the impact and damage resistance resulting a bridge between layers.

Hosur et al. [33] investigated influence of cold–dry and cold–moisture conditioning on low velocity impact behavior of woven carbon/epoxy laminates. Test samples were subjected to different hydrothermal conditions for a period of 3 and 6 months, and they were also subjected to different impact energies, 15, 30 and 45 J, respectively. The amount of damages was evaluated by ultrasonic nondestructive evaluation. It is found that the samples in the cold moist condition had better energy absorption capacity and higher peak load. However, in the case of cold dry conditions, 3 months of period time are needed to obtain the better impact and load properties.

Tiberkak et al. [34] investigated impact behavior of carbon fiber/epoxy composite plates subjected to low velocity impact tests. A finite element analysis based on Mindlin's plate theory was used for impact tests. A parametric study including size and velocity of striker, in-plane dimensions of target, stacking sequence of samples and boundary condition of the supports was adopted. It is found that contact stress corresponding to maximum force was increased as plane dimensions of impacted area were decreased, both force and deflection in the middle of plate were increased by increasing the mass and velocity of striker. In addition, the increase of ply angle at 90^0 caused to reduce the rigidity of the laminates.

Zabala et al. [35] studied effects of impact velocity on the delamination of woven Carbon–epoxy plates under the drop-weight impact test. During the impact tests, different mass and velocity combinations were considered. Results showed that delamination area can be increased by the 45 % while increasing impactor velocity of projectile from 0.94 to 1.98 m/s and this delamination spread can decreased 20 %, resulting the reduction of the residual stiffness in the structure for a curtain the analyzed energy and velocity ranges.

Qiu et al. [36] investigated modelling of low velocity impact on composite laminates. Delamination between layers, fiber and matrix breakage were modelled by a finite element method under the different impact tests. Effects of impactor diameter, size of plate and velocity and of projectile were examined for impact tests. A numerical model including the composite fracture and delamination was proposed to study impact events in the composite laminates. Intra-laminar and inter-laminar crack models based on stress-criteria were used for modelling the impact behavior of test samples. It is found that clustering fibers contributed to reduce of the interphase damage. The maximum resulting interaction force by flat end striker was much greater than those of hemispherical end striker depending upon the boundary conditions.

Belingardi and Vadori [37] studied effect of laminate thickness on impact behavior of carbon fiber-epoxy composite laminates. Composite laminates exhibit the different thickness and stacking sequences, and subjected to both dynamic and quasi-static loading conditions. Energy absorption capacity obtained from load to deflection curves was determined for different striker velocities. Stacking sequences of $[0/60/-60]_i$ and the $[0/90]_i$ were considered during the evaluation of energy absorption and impact resistance. Results indicated that the carbon/epoxy composite laminates showed the poor sensitivity of its mechanical behavior to the strain rate effect. Stacking sequence of $[0/90]_i$ showed the better energy absorption and maximum peak force compared with others.

Moura and Marques [38] investigated low velocity impact behavior of carbon/epoxy composite laminates. Two different laminates $(0_4/90_4)s$ and $(0_2/\pm45_2/90_2)s$ were tested using a drop weight testing machine. Experimental and numerical studies were performed for prediction of damage in composite laminates having different stacking sequences. Damages in composites were measured by X-rays radiography. It is

concluded that numerical results were in good agreement with experimental results and samples with stacking sequence of $(0_2/\pm45_2/90_2)s$ provided the better impact resistance compared with stacking sequence of $(0_4/90_4)s$.

2.4 Studies Using Kevlar Fiber

Kevlar fibers were introduced the early 1970 as the high-strength, high-modulus materials and were desirable for their outstanding strength-to-weight ratios, which are superior to metals. Chemically, this group of materials is known as poly (paraphenylene terephthalamide). This material is known for its high toughness, impact resistance, and resistance to creep and fatigue failure.

The Kevlar fibers are most often used in composites having polymer matrices; common matrix materials are the epoxies and polyesters. Since the fibers are relatively flexible and somewhat ductile, they may be processed by most common textile operations. Typical applications of these kevlar composites are in ballistic products (bullet proof vests and armor), sporting goods, tires, ropes, missile cases, pressure vessels, and as a replacement for asbestos in automotive brake and clutch linings, and gaskets [39]

Singh and Samanta [40] presented a comprehensive literature review about thermal, mechanical and impact properties of Kevlar fiber and its composite laminates. It was concluded that Kevlar fibers with composites exhibited the high ratio of tensile to compression strength due to anisotropic nature of Kevlar fiber. It was also shown that hybridization of Kevlar fibers could increase the good interfacial fiber-matrix adhesion strength, resulting the increase in mechanical and impact properties.

Das et al. [41] investigated the influence of inter-yarn friction effects on ballistic performance of para-aramid woven fabrics. For ballistic tests, numerical and experimental studies were performed to show static and kinetic friction coefficient effects in a plain woven fabrics. They concluded that high inter-yarn friction was not highly influenced to get higher impact performances, and the nose shape of impacted is the major factor for higher friction coefficients.

Aswani et al. [42] studied ballistic impact behavior of composite armor reinforced with Kevlar fiber and polypropylene matrix. Different architectures (2D plain woven, 3D orthogonal and 3D angle interlock) with 9 mm full metal jacket were used for

production of composite amour plates. Results of ballistic tests showed that composite amours with 3D orthogonal and 3D angle interlock exhibited 16.44 % and 20 % respectively higher ballistic limit than those of compared with 2D woven fiber reinforced composites.

Kumar et al. [43] performed numerical studies for prediction of ballistic impact response of Kevlar/epoxy composite laminates. Samples were subjected to different velocities ranging from 100 to 1000 m/s. Numerical simulations were carried out using commercial software of ANSYS AUTODYN 11 for general purpose non-linear impact analysis. It is found that damage mechanisms in the composite samples changes below and after ballistic limit, and internal energy were increased after the sample was struck.

Yang et al. [44] both experimentally and numerically investigated the impact response of aramid fiber reinforced epoxy resin composite laminates by using low velocity impact tests. Drop weight impact tests with different energy levels (10, 11, 12, 15, 18, 21, 24, 28, and 32 J) conducted on composite laminates having different thicknesses. Force to time histories of samples was determined by measuring the degree of damage using the ultrasonic C-scan technology. It is found that impact energy highly effecting the force to time histories, and it was increased as increasing the thickness of samples. For small impact tests, force-time history was smooth and analogous to a sine curve. However, more oscillations were observed during the high velocity impact tests.

Taraghi et al. [45] studied low-velocity impact behavior of Kevlar/epoxy composite laminates with multi-walled carbon nanotubes for different nanotube contents. Energy profile diagrams were used to predict the penetration threshold. The effect of Carbon nanotube addition on impact behavior was investigated at the same impact energy level of 45 J at ambient and low temperatures. It is found that carbon nanotube addition significantly improved the impact strength.

Reis et al. [46] investigated influence of nano-clay addition on impact behavior of kevlar/epoxy composite laminates under the low velocity impact. Different weight contents of nano-clays, namely, 1.5, 3 and 6 % were incorporated to study optimum impact performance of composite laminates. It is found that the maximum impact performance was obtained with weight content of 6 % in terms of elastic recuperation and penetration threshold compared to the neat laminates. In addition, nano-clays with

3 % and 6 % composite laminates had high benefits. Finally, benefits from experiments were obtained about 1.15 % and 32.22 % in terms of penetration threshold.

Mishra et al. [47] studied impact properties of three-dimensional woven Kevlar fabric structures before and after toughening with epoxy resin. Three-dimensional shape of the composite fabric was modelled using Solidworks software, and then their impact responses were simulated by using ANSYS software. A series of low velocity impact tests were performed experimentally for different impact velocities of striker, and then results were compared with those of obtained numerical results. It is found that three-dimensional shape of woven Kevlar/epoxy composite laminates was proved sufficiently better impact resistance due to high interface strength between matrix and fiber in the lamina.

2.5 Studies on Hybrid composite laminates

The use of hybrid composite materials has been increasing in structural and engineering applications in which strength to weight considerations are the major design requirements. Hybrid composites provide the flexibility in designing of innovative systems and damage tolerant structures subjected to high differences in strain rate, pressure, and temperature [48]. Hybrid composites may be composed of artificial or natural fibers, which can help us to reach a better combination of properties than constituent fibers. Nunna et al. [49] presented a comprehensive review study about impact and mechanical behavior of natural fiber reinforced hybrid composites. It was indicated that factors those effecting impact and mechanical characteristics of the hybrid structure are the fiber volume/weight fraction, stacking sequence of the fibers and environmental conditions.

In the literature, the extensive studies on impact behavior of composite laminates can be found with variety of experimental, numerical, and analytical approaches [6, 50-57]. It is well known that composite materials are vulnerable to damage resulting from foreign objects due to the inherent brittleness of both the fiber and the matrix.

When the object is significantly rigid and small, the extensive damage causes around the contact region within the shorter contact time. Hence, the extension damage through the composites is strictly depend on the contact force between target and object [58]. In most cases, this type of impacts reveals the failure that is hardly

detectable by visual inspections, resulting a significant reduction of the structural performance under service loads [59-60], and these defects may trigger the sudden collapse of the structures as a result of different failures in terms of delamination [61-62], matrix cracking [63], interfacial debonding and fiber rupture. Impact behavior of composite laminates depends on different parameters such as laminate thickness [60-64], size and shape of impactor [65-66], laminate configuration [67], and so forth. Although these results showed that impact resistance of composites could be increased by using thicker laminates, one effective way to increase the impact resistance and energy absorbing capacity of composite materials is to incorporate high strain to-failure fibers to the host laminates, thus referring hybrid composites [68].

Hybridization is one of the effective ways to increase impact resistance and energy absorption capability of composites using high strength fibers like carbon and Kevlar, also to decrease cost using more economic fibers like glass. The advantages with usage of this approach are to balance the strength and stiffness, improved impact strength and reduction of weight and cost [60]. Several researchers [69-70] have shown the significance of hybridization effect to improve mechanical properties and damage resistance of composite laminates.

Bandaru et al. [69] investigated the effect of hybridization on the ballistic performance of hybrid composite armor reinforced with various combinations and stacking sequences of Kevlar, glass and carbon fibers. It is found that stacking sequence of the fibers showed the major factor for ballistic performance. For example, it is revealed the good ballistic performance in the case of Kevlar fiber at the rear side, glass fiber in the exterior side and carbon fiber at front side.

Naik et al. [70] performed low velocity impact tests on glass/carbon hybrid composites having different stacking sequences. Impact and post impact compressive behavior of test samples showed that they exhibited lower notch sensitivity when carbon layers were placed at outer and glass layers were placed at inner surfaces. In this context, the analysis of the damage assessment involved in the impact event is thus needed considering hybrid effect concept.

Sevkat et al. [71] studied impact behavior of hybrid S2 Glass-IM7 graphite fibers/toughened epoxy composite laminates using drop weight impact tests. Three different size and shape of strikers, spherical, flat-ended cylindrical and straight-line

were used during the impact tests for prediction of force-time histories and impact-induced dynamic strains. In addition, impact mechanism was simulated using 3-D dynamic finite element software by LS-DYNA. It is found that experimental and finite element results were in close agreement each other by means of dynamic force, strain histories, damage patterns inside the composites. The resulting damage and corresponding to maximum contact force increase by using higher size of strikers.

Sevkat et al. [72] investigated ballistic impact behavior of hybrid and non-hybrid S2 Glass/ graphite fibers with epoxy resin composite laminates. The influence of hybridization on ballistic limit was inspected under the various impact velocities. 3D nonlinear finite element was used to simulate experimental results. The variation of strain inside the lamina was determined by considering hybridization effects. It is concluded that ballistic limit of composite laminates was not significantly affected by using glass fibers those placed at the inner and outer layers. In addition, delamination area around the impacted surfaces was increased with increasing impact velocity of the striker.

González et al. [73] studied the drop-weight impact response of inter ply hybrid laminates made of polymer-matrix composite materials. Woven carbon and glass fabrics, and unidirectional carbon tape, were used as reinforcements in the lamina manufactured by the resin transfer molding process. Impact and CAI tests were performed for different pair of fiber/epoxy laminates and stacking sequences under the different impact loads. Results indicated that hybrid composites could improve damage and impact resistance of composite laminates. For same materials, the shift of fiber stacking sequence through the thicknesses resulted the significant changes in CAI and impact properties of samples.

Hosur et al. [74] studied experimentally on the low-velocity impact response of woven hybrid composites using drop weight impact testing machine. Hybrid composites used in impact tests were made of fibers with twill weave of Carbon fabric and plain weave of S2-Glass fabric. Samples were subjected to the different impact energies, namely, 10, 20, 30 and 40 J, respectively. It is found that arrangement of hybrid composite provided better load carrying capacity and impact resistance.

Evci and Gülgeç [75] investigated impact behavior of composite laminates reinforced by unidirectional E-Glass, woven E-Glass, and Aramid fibers. Test samples were subjected to drop weight impact loading with an instrumented impact test machine. Energy absorption curves, the limits of rebound and on-set of perforation were determined. Results indicated that woven laminates showed the better damage spread capacity than unidirectional one, also strength of samples was affected by the dynamic effects during the low velocity impact tests while dynamic effects were found at minimum level in the static loadings as a result of strain rate.

Sarasini et al. [76-78] studied low-velocity impact behavior of woven kevlar/basalt, carbon/basalt and glass/basalt with epoxy hybrid composite laminates. Hybrid composite samples having different stacking sequences were subjected to different impact energy levels, that is, 5, 12.5, and 25 J, respectively. Residual post-impact properties of the aramid/basalt hybrid laminates were determined by quasi-static four point bending tests. Post-impact flexural tests were monitored by using acoustic emission in order to predict impact mechanism. It is found that alternating sequence of Basalt and Aramid fabrics induced to increase impact resistance. Basalt laminates showed the poor impact resistance compared to aramid laminates and their impact resistances were increased by the hybridization with aramid fibers. For glass/carbon arrangements, glass fiber composite laminates had better peak load than those of basalt fiber composite laminates, but its impact resistance were lower than Basalt fiber composite laminates. For basalt/carbon hybrid arrangements, Basalt fiber hybridization caused the increase of impact strength and reduction of penetration while enhancing the peak forces.

Wang et al. [79] investigated impact behavior of 3D woven basalt/aramid/epoxy hybrid composite laminates under the low velocity impact tests. Test samples were prepared inter-ply and intra-ply laminates having different type of yarns. It is shown that the inter-ply hybrid laminates had higher ductility, lower peak load, and higher specific energy absorption capacity in both warp and weft directions compared with the intra-ply hybrid laminates.

A standard test ASTM D7136 [80] is available to measure the damage resistance of a fiber-reinforced polymer matrix composites subjected to the drop weight impact test. Force to displacement and force to time response curves are obtained by hemispherical

and cylindrical strikers. Impact forces are applied to a rectangular shape of impact area on the surface of the composite samples.

Sayer [81] examined the impact behavior of hybrid Aramid/Glass/epoxy, hybrid Aramid/Carbon/epoxy and hybrid Carbon/Glass/epoxy composite laminates under the different impact energy levels at room temperature. An instrumented drop-weight impact machine was used in order to predict penetration and perforation thresholds of composite laminates. In addition, the effects of stacking sequence on impact response were examined. It is found that damage level captured in the hybrid composites was increased according to applied impact load. The increase of carbon fiber content inside the hybrid composites was not significantly increased the perforation threshold. During the impact tests, contact force to deformation values was reached maximum level at perforation threshold.

Sayer et al. [82] studied the impact behavior of Glass/Carbon with epoxy hybrid composite laminates using drop weight impact tests. Penetration and perforation thresholds of hybrid laminates were determined by means of load to deflection curves. Energy absorption and impact energy values were also obtained for different impact energy levels. The extent and spread of damages were also investigated. It is concluded that the hybrid composites impacted to the surface of Carbon fiber face sheets showed better perforation threshold energy than those of hybrid composites impacted to the surface of Glass fiber face sheets.

Sayer et al. [83] investigated the influence of temperature on Carbon/Glass/epoxy hybrid composite laminates under the impact loading. Perforation energies of hybrid samples were inspected the temperature range from -20 to +60 ^{0}C. The energy profiling diagrams were used for prediction of penetration and perforation thresholds of hybrid composite samples. Impact properties and energy absorption capacity of hybrid composites were determined in terms of maximum load, contact time and permanent deflection. The results showed that impact energy and perforation energies were significantly affected by variation of temperature. As a result, the optimum impact characteristics of hybrid composite laminates were obtained at room temperatures.

Park and Jang [84] studied impact behavior of aramid/Glass fiber reinforced hybrid composites. The effects of stacking sequence and fiber volume fraction of the Aramid

fiber were examined. They found that composite laminates exhibited the higher impact energy and delamination area when aramid layers were placed on surface of back sides. However, impact energy of hybrid laminates was not significantly affected by the position of aramid layers.

Tjong et al. [85] investigated the impact properties of Polyimide 6 hybrid composites reinforced with short glass fibers with different ratios. It is indicated that hybrid composites exhibited higher impact strength and absorbed energy compared with Polyimide 6 hybrid laminates, particularly those with low- short glass fibers content.

Salehi-Khojin et al. [86] showed that impact behavior of glass/Kevlar composite laminates were highly sensitive to the role of the temperature at different energy levels (8, 15, and 25 J). It is indicated that impact resistance of the composite laminates were highly sensitive to temperature.

Sreekala et al. [87] investigated the influence of hybridization of oil palm fibers with glass fibers on mechanical properties of hybrid composite laminates. They showed that hybridization of glass fibers contributed to the significant increase in mechanical properties.

Erkliğ and Bulut [88] presented the effects of impacted side on low velocity impact resistance and damage tolerance of Kevlar/glass/epoxy hybrid composites by using charpy impact tests. It was shown that hybrid samples exhibited higher absorbed energy with lower damage tolerance when they were impacted at the Kevlar side of the surface.

Bozkurt et al. [89] assisted the charpy impact tests on Basalt/Aramid/epoxy hybrid composites to study hybridization effects for different fiber configurations. It was reported that damage tolerances and impact resistance in terms of absorbed energy were strictly dependent on impacted surface of the hybrid sample, which was designed as asymmetric structure.

2.6 Quasi-static Penetration Tests

The use of quasi-static tests to determine the material behavior and damage mechanisms related with impact behavior may seem questionable at first. However, studies have shown that the information obtained from these tests can be quite useful

for modelling and simulation of impact events. Not only possible easy to observe material behavior and damage mechanisms during the loading and interrupted evaluation, but also values of peak load and energy absorbed can often be used to predict impact resistance. Finally, it is a method to measure contact stiffness, which was required for theoretical analysis and finite element modelling [6]

Quasi-static penetration test is a method to measure impact characteristics of the structures by controlled indenters under the out of plane loadings. By the controlling of energy absorption capacity of structures as the small strain rates, it is possible to predict accurately damage and impact properties of the composite materials. As a result of applying load to the out of plane of the composite structures, their failure characteristics undergoes shearing, plugging and accordingly perforation.

Quasi-static penetration tests can be conducted by quasi-static punch shear test (QPST). A QPST fixture has a cover plate with a circular hole at the center and a cylindrical punch with a flat end tip as shown in Figure 2.1. In addition, a square base plate is also used in addition to cover plate of the fixture.

As can be seen in Figure 2.1, two parameters are considered for QPST, namely punch diameter (D_p) and punch diameter (D_s). QPST experiments are performed with different shear punch ratios (SPR) between D_p and D_s (D_p/D_s).

A displacement controlled instrumented test machine is needed in order to collect force and displacement relation. Figure 2.2 shows a set-up for quasi-static penetration tests with different shear punch ratios and their failure mechanisms and force to deflection curves were shown in Figure 2.3.
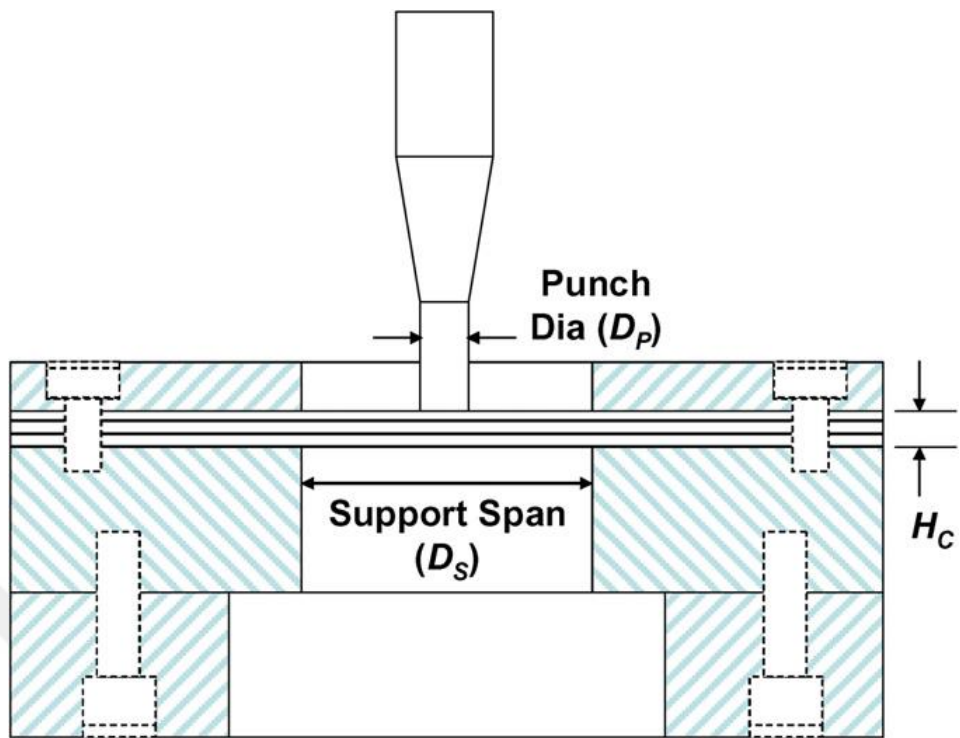
Figure 2.1. Schematic illustration of punch shear test fixture [90]
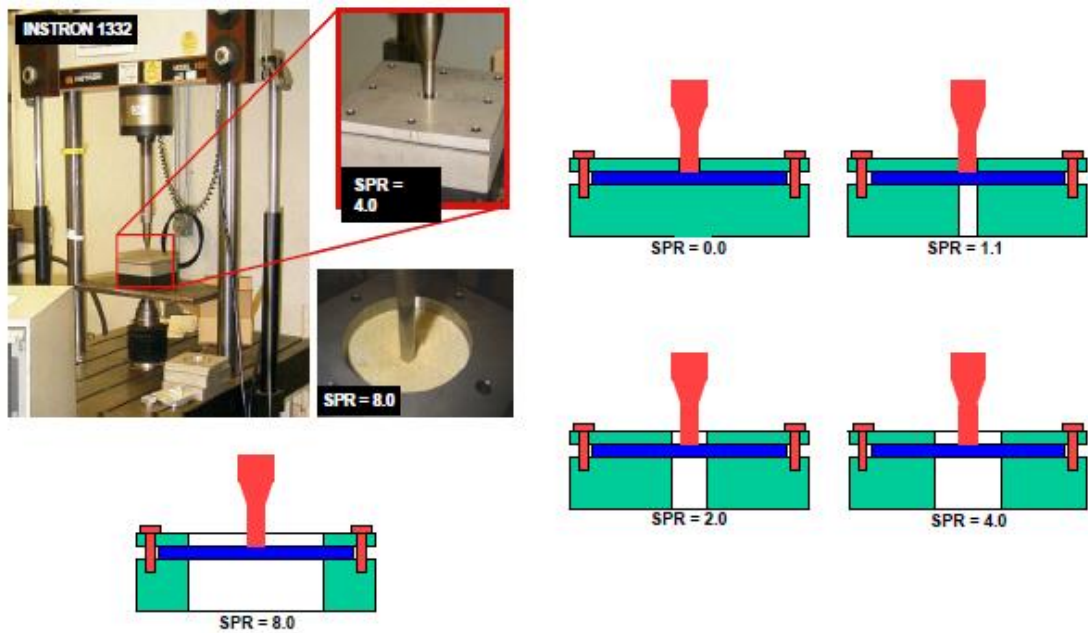
Figure 2.2. A quasi static penetration test set-up [91]
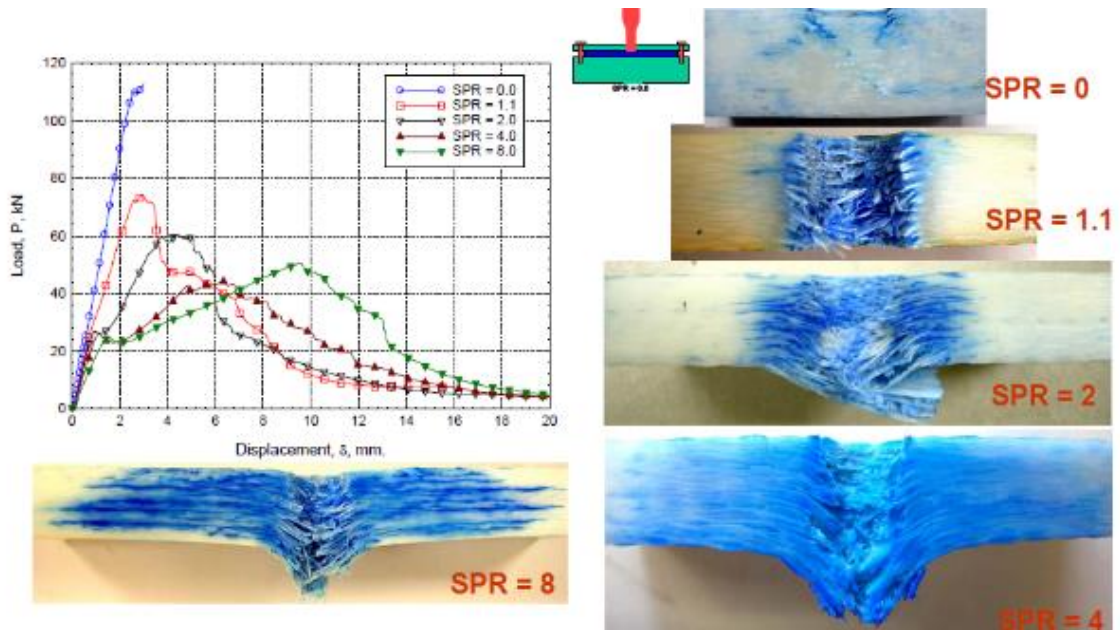
Figure 2.3. Failure behavior of quasi-static penetration test for different SPR ratios [91]

Sun and Potti [92] studied residual velocities of thick composite laminates considering high velocity impact tests (dynamic energy model) and Quasi-static impact tests. Impact tests were conducted on Graphite-epoxy laminates using different size of strikers. Number of layers used in this study was chosen as 32, 48, and 64 to show the effects of laminate thickness. It is concluded that both dynamic and experimental results through which quasi-static punch test model were in good agreement and dynamic response model could be used to predict high velocity impact test on information of quasi static penetration test for different thicknesses and sizes.

Nemes et al. [93] investigated influence of deformation on penetration of graphite/epoxy and quasi-isotropic laminates for different thicknesses and stacking sequences under the quasi-static penetration and high strain rate loading. The results showed that stacking sequence and specimen thicknesses were significant parameters to displacement and load responses of samples. Based upon the result obtained from experiments, it is clear that both peak load and absorbed energy are proportional to laminate thickness. In addition, high strain rate loading tests significantly increased transverse shear strength of the laminates.

Gama and Gillespie [94] developed a quasi-static penetration model for estimating ballistic behavior of composite materials. It is asserted that ballistic impact could be

33

modelled by performing a series of quasi-static tests. In the case of ballistic impact events, the penetration of a composite laminate followed by five stages, Stage I – Impact–contact and stress wave propagation, Stage II – Hydrostatic compression and local punch shear, Stage III – Shear plug formation under compression-shear, Stage IV – Large deformation under tension-shear, and Phase V – End of penetration and structural vibration.

Xiao et al. [95] investigated progressive damage and delamination of plain weave (PW) S-2 Glass/SC-15 epoxy composite laminates using quasi-static penetration tests to identify damage modes of compression and tension shear properties. The damage and energy absorption capacity of laminates were determined for different laminate thicknesses. In addition to experimental studies, numerical studies using LS-DYNA 970 software were performed. Good agreement was found from comparison of numerical simulations and experimental results by means of load to displacement curves. It is indicated that delamination and fiber breakage were more dominantly observed damage mechanisms in composite laminates.

Potti and Sun [96] proposed "structural constitutive model" to predict impact induced penetration and delamination in thick composite laminates. This model was based on highly nonlinear behavior of the laminate in the penetration process. It is remarked from the study that the delamination area of target was increased as the velocity of projectile was approached to the ballistic limit, but it was decreased beyond the ballistic limit. Plug formation and deformations were highly sensitive to strain rates.

Goldsmith et al. [97] examined quasi-static and ballistic impact behavior of Carbon fiber composite laminates by cylindrical indenters. Load-deflection curves were obtained under the quasi-static tests by a standard testing machine, and displacement of striker was ranging from 0.012 and 6.5 s^{-1}. In ballistic impact tests, composite laminates were subjected by strikers having 12.7 mm diameter and velocity ranging from 30 to 310 m/s. It is indicated that maximum perforation energies of quasi-static tests were less than ballistic tests for the same specimen thicknesses. In addition, perforation energy values were increased linearly as a function of thickness of the composite laminate.

He et al. [98] investigated penetration and perforation resistance of fiber reinforced composite laminates by conical nosed strikers. Quasi-static penetration and dynamic penetration models were used over the wide range of projectile velocity. It is shown that both quasi-static and dynamic predictions were in good agreement with each other.

Wen [99] derived analytical methods to predict penetration and perforation of thick FRP laminates by different type of nose shapes. Formulations used in analytical methods were based on dynamic and quasi-static penetration loading conditions. Penetration depth and ballistic velocity limit of composite laminates were obtained from experimental and analytical solutions with a close agreement.

Caprino et al. [100] studied the behavior of Carbon fiber reinforced plastic plates having different thicknesses under the indentation and penetration by hemispherical steel indenters. The experimental tests were carried out until the compete penetration. Force to displacement curves and penetration energies were determined for different diameters of indenters and results were compared with information obtained from low velocity impact tests. The results showed that both penetration and indentation energies were not significantly affected by loading speed rate of the punch. Penetration energy can be calculated by an empirical equation by taking into account the total fiber areal weight and the indenter diameter. Indentation is expected to be valid only when the material-indenter contact conditions are well beyond those governed by the Hertzian contact law.

Wardle and Lagace [101] investigated impact damage resistance of graphite/epoxy composite shell structures under the quasi-static penetration tests. Composite structures had $[(\pm 45)_n / 0_n]_s$ layup configuration and they include convex and concave shell U sections of plates, and full cylinders. For the given same load conditions, impact damage evaluations of composite samples were determined using X-radiograph comparisons of the damage states. It is asserted that quasi-static tests were more accessible, easier to conduct, and provide consistent and controlled data acquisition of damaged and undamaged structures in the case of unavailable or inaccessible in impact events.

Yahaya et al. [102] studied quasi-static penetration and ballistic properties of non-woven Kenaf/Kevlar epoxy hybrid laminates. Experimental studied were conducted

for different thickness of hybrid composite laminates ranging from 3.1 mm to 10.8 mm. Quasi static experiments were performed on the samples using a instrumented tensile testing machine with velocity of 1.27 mm/min and 2.54 mm/min. Results showed that maximum force to critical penetration energy values of hybrid composite laminates were greater than full Kevlar/epoxy and Kenaf/epoxy laminates. In addition, hybridization of Kenaf or Kevlar fiber caused to increase in energy absorption capacity (penetration), while resulting the increase in maximum load.

Jordan et al. [103] examined quasi-static penetration, low velocity impact and ballistic impact behavior of plain weave E-Glass/phenolic composite laminates. Mechanical properties, density, Poisson's ratio, tensile, compressive and shear strengths, and the elastic and shear modulus of the material were determined according to ASTM standards. Quasi-static punch shear and crushing tests were performed. Ballistic limits (V_{50}) and perforation depth of the samples were obtained using a right circular cylinder (RCC). It is concluded that results obtained from experiments could be used for structural design and also to satisfy both numerical solutions of low velocity and ballistic impact.

2.7 Quasi-static Indentation Tests

It is well known that composite materials are vulnerable to damage resulting from foreign objects due to the inherent brittleness of both the fiber and the matrix. During the impact loading, soft and hard materials result in different failure modes in the impacted materials. When the object is significantly rigid and small, the extensive damage causes around the contact region within the shorter contact time. Hence, the extension damage through the composites are strictly depend on the contact force between target and object [104].

The influence of foreign object impact needs to be predicted as the component may be subjected to a low velocity impact like a dropped tool during the service life. This localized loading is generally caused to propagate a damaged area and resulted in strength and stiffness degradation. In most cases, this type of impacts reveals the failure that is hardly detectable by visual inspections, resulting a significant reduction of the structural performance under service loads. It should be noted here that amount of impact damage is effected by many parameters like geometry of support and

projectile parameters such as material, size, shape, and angle of incidence, stacking sequence, thickness of the plate and shape of the impactor [55, 105].

Herb et al. [105] presented the damage assessment in 3D woven SiC/SiC composites subjected to indentation tests. The extent of damage in the composites was explored by the use of optical and microscopic electro scanning devices. Post-tensile strength of the samples was also identified after the indentation tests. Results indicated that damage was remained as a localized while 3D fibers prevented the delamination. It was noted also that the reduction of tensile strength is proportional to the indenter diameter influencing the size of the damage.

The measurement of dynamic contact force during the impact event is not easy due to wide range of impact velocities, the limitation of experimental technique. During the modelling of low velocity impact, static test methods provide much more data with high accuracy compared with impact tests [11]. The several researchers [106-111] showed the similarities between low velocity impact and QSI tests, while others [32, 112-114] have indicated the disadvantages and limitations of quasi static tests for impact events.

Several studies [115-120] have been carried out to indicate the hybrid concept for enhancement of impact resistance in fiber reinforced composites. The main reason to utilize the hybrid technique is to provide the combination of different fibers for requirement of structural design, while increasing mechanical properties with low cost of composite production.

Lee et al. [120] examined the hybrid effect concept to study indentation behavior of carbon fiber reinforced fibers and nonwoven carbon tissue reinforced hybrid composites. Delamination and absorbed energy values were determined in terms of hybrid effect. Damaged parts were observed along the half sectioned parts using a microscopic device. It was indicated that the delamination area after the indentation tests was decreased to a half of carbon fiber reinforced composites, and this was attributed the predominant Mode II interlinear fracture during the delamination by impact event.

From the studies examined thus far, it appears that many studies have been performed to investigate the hybrid composites for their impact and mechanical properties. To the

best of our knowledge, there have been no study related with the influence of stacking sequence configurations on indentation behavior of fiber reinforced hybrid composites and presently it has being considered in this study.

2.8 Conclusion on Literature Review

A comprehensive literature review has been carried out in order to investigate impact and energy absorption characteristics of laminated hybrid and non-hybrid composites. Following conclusions can be drawn from this literature review:

- The studies about impact behavior of composite laminates are mainly focused on reinforcements of glass, kevlar and carbon fibers in the view of reinforcing fibers,
- Impact behavior of composite laminates has been especially investigated by the low and high velocity impact conditions,
- In the literature, the effects of impactor type, velocity of impactor, weight of the impactor and laminate stacking sequence are the major parameters dealing with the impact behavior of composite laminates,
- It is concluded that low and high velocity impact behavior of composite materials can be investigated by using quasi-static indentation and quasi-static penetration tests, respectively,
- In hybrid composites, the studies about hybrid composites reinforced by two different fibers, especially carbon/glass, carbon/kevlar and glass/kevlar can be found in previous studies. The studies of natural fiber reinforced composites investigating the mechanical, impact and damage tolerances are existing also in literature. However, studies about hybrid composites reinforced by three different fibers are limited,
- Previous studies showed that the behavior of hybrid composite laminates has not been adequately investigated under the quasi-static penetration and quasi-static indentation conditions, showing the damage modes in the samples.

The present study dealing with the damage characteristics and impact behavior of hybrid composites is organized to investigate study energy absorption and load carrying capacity of the hybrid composite laminates. Quasi-static penetration, quasi-static indentation and low velocity impact responses of the fiber reinforced hybrid composite laminates will be identified to study the parameters of hybridization effect

and stacking sequence configurations. Meanwhile, the failure modes and extension of damage mechanisms will be characterized by observing the surfaces of composite samples. For the purpose of stacking sequence effects and hybridization effects, three different fibers will be used as reinforcing materials.

CHAPTER 3

MATERIALS, PRODUCTION AND METHODS

3.1 Introduction

This section is devoted the production and preparation of test samples for QSPT, QSI and LVI tests. Test samples, projectiles (indenters), boundary conditions, and procedures for experimental measurements will be discussed.

3.2 Production of Composite Samples

As shown in Figure 3.1, twill 2x2 woven Aramid, woven plain carbon fiber and woven plain S-glass fibers were used in the production of hybrid composites. The areal densities of the reinforcing fabrics are 173, 200 and 200 g/m^2 per ply respectively. Table 3.1 represents the mechanical properties of these fibers.
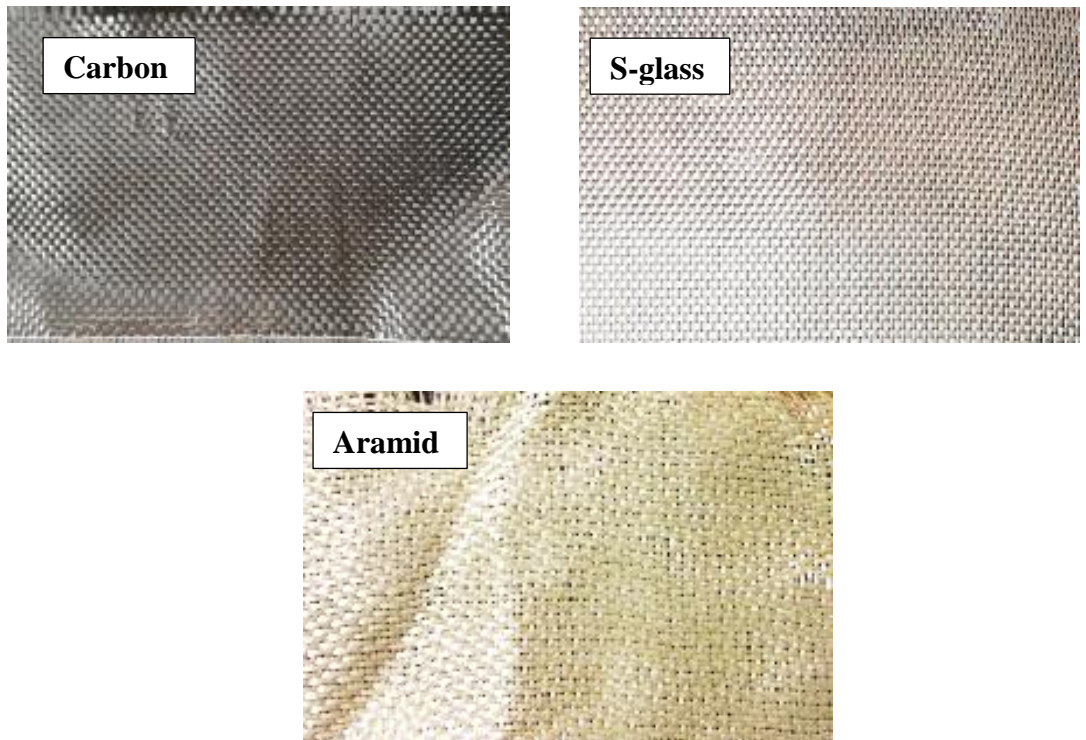
Figure 3.1 Fibers used as major reinforcing materials

Table 3.1 Mechanical properties of fibers [121]

Fiber Type	Areal density (g/m²)	Tensile strength (MPa)	Elastic modulus (GPa)	Density (g/cm³)
S-glass	200	3000-5000	72-82	2.48-2.61
Carbon	200	2500-3000	200-700	1.75-1.96
Kevlar	173	2750-3000	82-124	1.44

Composite laminates were manufactured by using hand lay-up process at the room temperature of 25^0C. The epoxy, hardener, and all of fibers were supplied from Dostkimya Company in Istanbul. Figure 3.2 represents the chemical materials used during the production process. An epoxy (Hexion MGS-L285) with hardener (Hexion MGS-H285) was used by the mixing ratio of 100:40. For the purpose of mixing the epoxy and hardener, a mechanism as shown in Figure 3.3 was used before impregnation of epoxy resin to the fibers. Fibers were cut in the sizes of 350 x 250 mm in order to meet required dimensions and number of specimens. Fabrics were laid the layer by layer by the application of epoxy resin for each step. All layers were impregnated by epoxy resin using a roller before curing process.

A hot mold press with flat molds was used for curing, subjecting the samples to 0.4 MPa pressure for 1 hour curing time with 80 °C temperature. At the end of process, test coupons were prepared from bulk laminates in the size of 100x100mm. The process was completed until laminates reached to room temperature. A flow chart for production process is illustrated in Figure 3.4.

Volume fractions of fibers were determined from equation 3.1, 3.2 and 3.3, respectively. Stacking sequence and fiber volume fractions for QSPT and QSI/LVI samples are presented in Table 3.2, and Table 3.3, respectively.

$$V_{f,G} = \frac{\dfrac{W_{f,G}}{\rho_G}}{\dfrac{W_m}{\rho_m} + \dfrac{W_{f,G}}{\rho_G} + \dfrac{W_{f,K}}{\rho_K} + \dfrac{W_{f,C}}{\rho_C}} \qquad (3.1)$$

$$V_{f,C} = \cfrac{\cfrac{W_{f,C}}{\rho_G}}{\cfrac{W_m}{\rho_m} + \cfrac{W_{f,G}}{\rho_G} + \cfrac{W_{f,K}}{\rho_K} + \cfrac{W_{f,C}}{\rho_C}} \tag{3.2}$$

$$V_{f,K} = \cfrac{\cfrac{W_{f,K}}{\rho_G}}{\cfrac{W_m}{\rho_m} + \cfrac{W_{f,G}}{\rho_G} + \cfrac{W_{f,K}}{\rho_K} + \cfrac{W_{f,C}}{\rho_C}} \tag{3.3}$$

Where ρ_m and W_m are the density and weight of epoxy, $W_{f,G}$, $W_{f,C}$ $W_{f,K}$ and ρ_G, ρ_C and ρ_K are weight and density of S-glass, carbon and Kevlar fibers, respectively. $V_{f,G}$, $V_{f,C}$ and $V_{f,K}$ denote the volume fractions of S-glass, carbon and Kevlar fibers, respectively.

Figure 3.2 Hardener and laminating resin
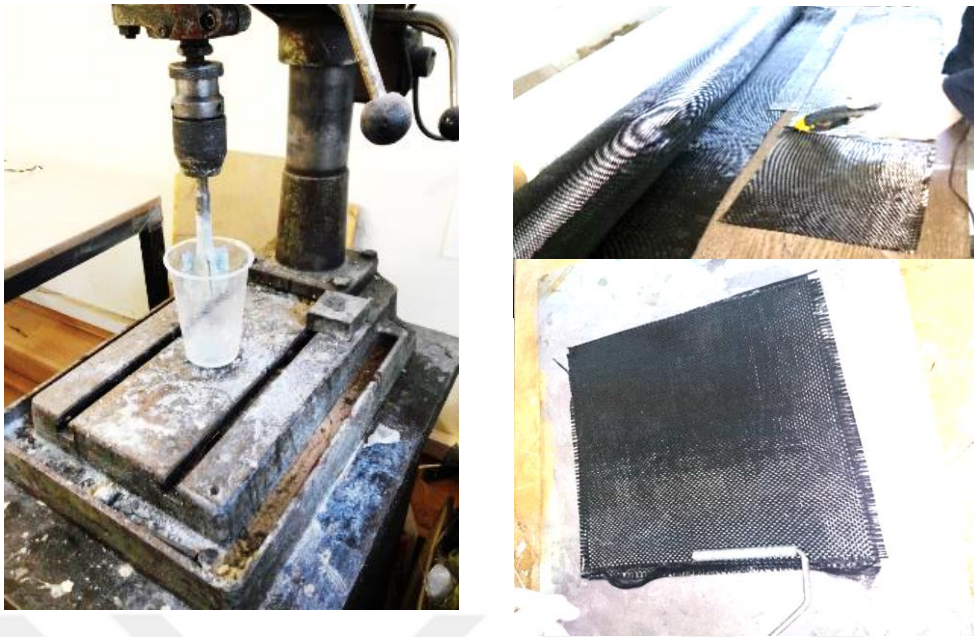
Figure 3.3 Preparing of impregnated fibers
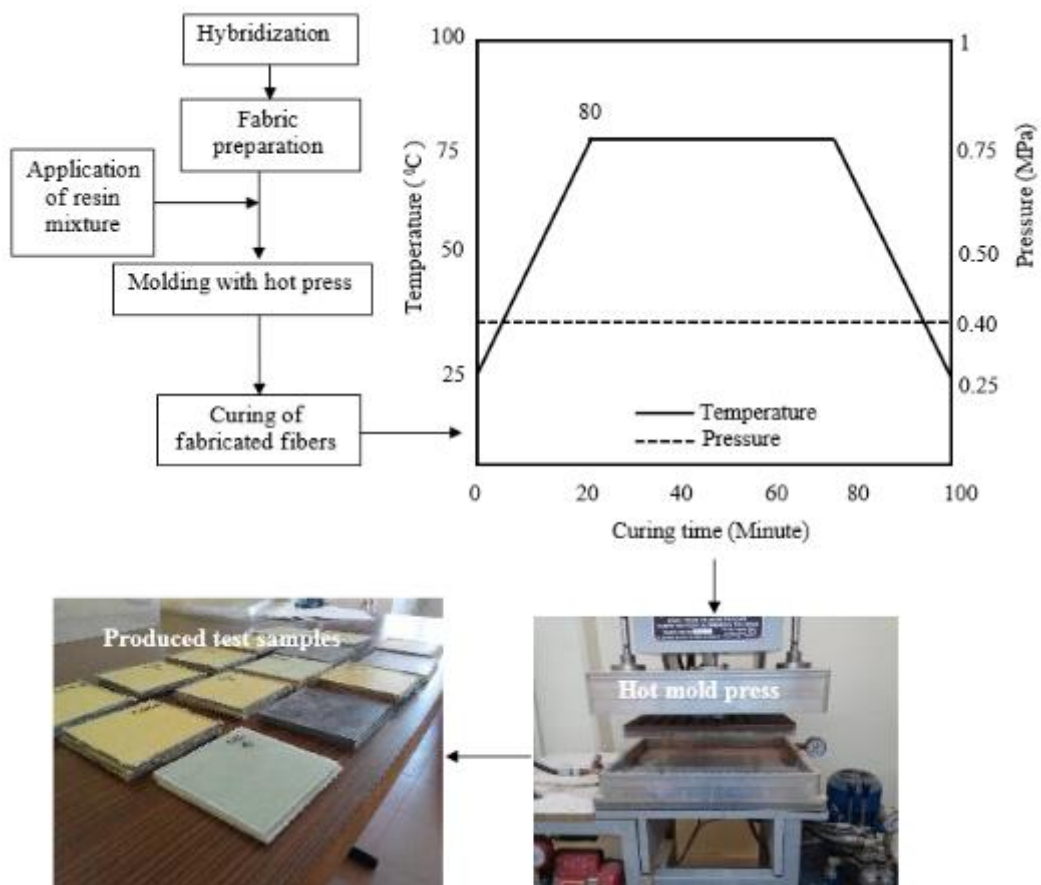
Figure 3.4 Production process

Number of layers used for production of QSPT samples was totally 24 resulting an average thickness of 5.8±0.3 mm. Each sample used for QSI and LVI experiments has totally 12 layers resulting an average thickness of 2.7±0.3 mm. The test samples for experiments were prepared from the laminates by cutting in the sizes of the 100x100 mm, having quasi-isotropic structure in accordance with ASTM D6264/D6264M [10] standard.

Table 3.2 Stacking sequence and fiber volume fractions of the composites for QSPT

Material	Stacking sequence and fiber configurations	$V_{f,G}$ (%)	$V_{f,C}$ (%)	$V_{f,K}$ (%)	Density (kg/m³)
GGG	$[(0°_G/90°_G)_2/(±45°_G)_2/(0°_G/90°_G)_2/(±45°_G)_2/(0°_G/90°_G)_2/(±45°_G)_2]_s$	73.95	0	0	1633
CCC	$[(0°_C/90°_C)_2/(±45°_C)_2/(0°_C/90°_C)_2/(±45°_C)_2/(0°_C/90°_C)_2/(±45°_C)_2]_s$	0.00	74.51	0.00	1367
KKK	$[(0°_K/90°_K)_2/(±45°_K)_2/(0°_K/90°_K)_2/(±45°_K)_2/(0°_K/90°_K)_2/(±45°_K)_2]_s$	0	0	68.57	1212
GCK	$[(0°_G/90°_G)_2/(±45°_G)_2/(0°_C/90°_C)_2/(±45°_C)_2/(0°_K/90°_K)_2/(±45°_K)_2]_s$	23.86	26.67	28.07	1360
GKC	$[(0°_G/90°_G)_2/(±45°_G)_2/(0°_K/90°_K)_2/(±45°_K)_2/(0°_C/90°_C)_2/(±45°_C)_2]_s$	23.29	26.03	27.40	1399
CGK	$[(0°_C/90°_C)_2/(±45°_C)_2/(0°_G/90°_G)_2/(±45°_G)_2/(0°_K/90°_K)_2/(±45°_K)_2]_s$	23.05	25.76	27.12	1362
CKG	$[(0°_C/90°_C)_2/(±45°_C)_2/(0°_K/90°_K)_2/(±45°_K)_2/(0°_G/90°_G)_2/(±45°_G)_2]_s$	23.86	26.67	20.88	1421
KCG	$[(0°_K/90°_K)_2/(±45°_K)_2/(0°_C/90°_C)_2/(±45°_C)_2/(0°_G/90°_G)_2/(±45°_G)_2]_s$	24.03	26.86	28.27	1380
KGC	$[(0°_K/90°_K)_2/(±45°_K)_2/(0°_G/90°_G)_2/(±45°_G)_2/(0°_C/90°_C)_2/(±45°_C)_2]_s$	23.37	26.12	27.49	1346
CKC	$[(0°_C/90°_C)_3/(±45°_C)_3/(0°_K/90°_K)_3/(±45°_K)_3]_s$	0	35.22	32.54	1318
KCK	$[(0°_K/90°_K)_3/(±45°_K)_3/(0°_C/90°_C)_3/(±45°_C)_3]_s$	0	33.86	34.52	1290
GCG	$[(0°_G/90°_G)_3/(±45°_G)_3/(0°_C/90°_C)_3/(±45°_C)_3]_s$	38.35	32.86	0	1548
CGC	$[(0°_C/90°_C)_3/(±45°_C)_3/(0°_G/90°_G)_3/(±45°_G)_3]_s$	38.78	33.35	0	1517
KGK	$[(0°_K/90°_K)_3/(±45°_K)_3/(0°_G/90°_G)_3/(±45°_G)_3]_s$	35.29	0	32.52	1405
GKG	$[(0°_G/90°_G)_3/(±45°_G)_3/(0°_K/90°_K)_3/(±45°_K)_3]_s$	32.05	0	31.47	1454

Table 3.3 Stacking sequence and fiber volume fractions of the composites for QSI and LVI

Material	Stacking sequence and fiber configurations	$V_{f,G}$ (%)	$V_{f,C}$ (%)	$V_{f,K}$ (%)	Density (kg/m³)
GG	$(\pm45°_G)_2 /(0°_G/90°_G)_2/(\pm45°_G)_2$ $/(0°_G/90°_G)_2/(\pm45°_G)_2 /(0°_G/90°_G)_2$	63.91	0	0	1632.09
CC	$(\pm45°_C)_2 /(0°_C/90°_C)_2/(\pm45°_C)_2$ $/(0°_C/90°_C)_2/(\pm45°_C)_2 /(0°_C/90°_C)_2$	0.00	64.51	0.00	1283.85
KK	$(\pm45°_K)_2/(0°_K/90°_K)_2/(\pm45°_K)_2/(0°_K/90°_K)_2/$ $(\pm45°_K)_2/(0°_K/90°_K)_2$	0	0	68.59	1297.31
GCK	$(\pm45°_G)_2/(0°_G/90°_G)_2/(\pm45°_C)_2/(0°_C/90°_C)_2/$ $(\pm45°_K)_2/(0°_K/90°_K)_2$	21.82	26.62	20.07	1398.44
GKC	$(\pm45°_G)_2/(0°_G/90°_G)_2/(\pm45°_K)_2/(0°_K/90°_K)_2/$ $(\pm45°_C)_2/(0°_C/90°_C)_2$	23.29	26.13	20.40	1467.71
CGK	$(\pm45°_C)_2/(0°_C/90°_C)_2/(\pm45°_G)_2/(0°_G/90°_G)_2/$ $(\pm45°_K)_2/(0°_K/90°_K)_2$	23.05	20.26	22.12	1304.05
CKG	$(\pm45°_C)_2/(0°_C/90°_C)_2/(\pm45°_K)_2/(0°_K/90°_K)_2/$ $(\pm45°_G)_2/(0°_G/90°_G)_2$	23.86	21.67	20.88	1398.93
KCG	$(\pm45°_K)_2/(0°_K/90°_K)_2/(\pm45°_C)_2/(0°_C/90°_C)_2/$ $(\pm45°_G)_2/(0°_G/90°_G)_2$	24.03	21.82	21.27	1396.11
KGC	$(\pm45°_K)_2/(0°_K/90°_K)_2/(\pm45°_G)_2/(0°_G/90°_G)_2/$ $(\pm45°_C)_2/(0°_C/90°_C)_2$	23.37	26.12	27.43	1462.84
CK	$(\pm45°_C)_3/(0°_C/90°_C)_3/(\pm45°_K)_3/(0°_K/90°_K)_3$	32.78	33.35	0	1511.95
KC	$(\pm45°_K)_3/(0°_K/90°_K)_3/(\pm45°_C)_3/(0°_C/90°_C)_3$	35.29	0.00	32.50	1437.81
GC	$(\pm45°_G)_3/(0°_G/90°_G)_3/(\pm45°_C)_3/(0°_C/90°_C)_3$	33.35	32.86	0	1526.85
CG	$(\pm45°_C)_3/(0°_C/90°_C)_3//(\pm45°_G)_3/(0°_G/90°_G)_3$	0.00	35.17	30.22	1338.29
KG	$(\pm45°_K)_3/(0°_K/90°_K)_3//(\pm45°_G)_3/(0°_G/90°_G)_3$	35.29	0.00	32.55	1398.21
GK	$(\pm45°_G)_3/(0°_G/90°_G)_3//(\pm45°_K)_3/(0°_K/90°_K)_3$	0	35.51	31.46	1302.22

In order to compare the hybridization effects, two different hybrid structures were designed and tested. First one is the double fiber combinations by interplay hybridization of two different fibers, another is the triple fiber combinations by interplay hybridization of three different fibers as shown in Figure 3.5 and Figure 3.6.

GGG CCC KKK

GCK GKC CGK

CKG KCG KGC

S-Glass//epoxy
$(0°_G/90°_G)_2 /(\pm 45°_G)_2$

Carbon/epoxy
$(0°_C/90°_C)_2/(\pm 45°_C)_2$

Kevlar/epoxy
$(0°_K/90°_K)_2/(\pm 45°_K)_2$

Stacking sequences with two different fibers

CKC KCK GCG

CGC KGK GKG

S-Glass//epoxy
$(0°_G/90°_G)_3 /(\pm 45°_G)_3$

Carbon/epoxy
$(0°_C/90°_C)_3/(\pm 45°_C)_3$

Kevlar/epoxy
$(0°_K/90°_K)_3 /(\pm 45°_K)_3$

Figure 3.5 Hybrid and non-hybrid configurations of composite laminates for QSPT

Stacking sequences with three different fibers

GG CC KK

GCK GKC CGK

CKG KCG KGC

S-Glass//epoxy
$(0°_G/90°_G)_2 /(\pm 45°_G)_2$

Carbon/epoxy
$(\pm 45°_C)_2 /(0°_C/90°_C)_2$

Kevlar/epoxy
$(\pm 45°_K)_2 /(0°_K/90°_K)_2$

Stacking sequences with two different fibers

S-glass/epoxy
$(\pm45°_G)_3 / (0°_G/90°_G)_3$

Carbon/epoxy
$(\pm45°_C)_3 / (0°_C/90°_C)_3$

Kevlar/epoxy
$(\pm45°_K)_3 / (0°_K/90°_K)_3$
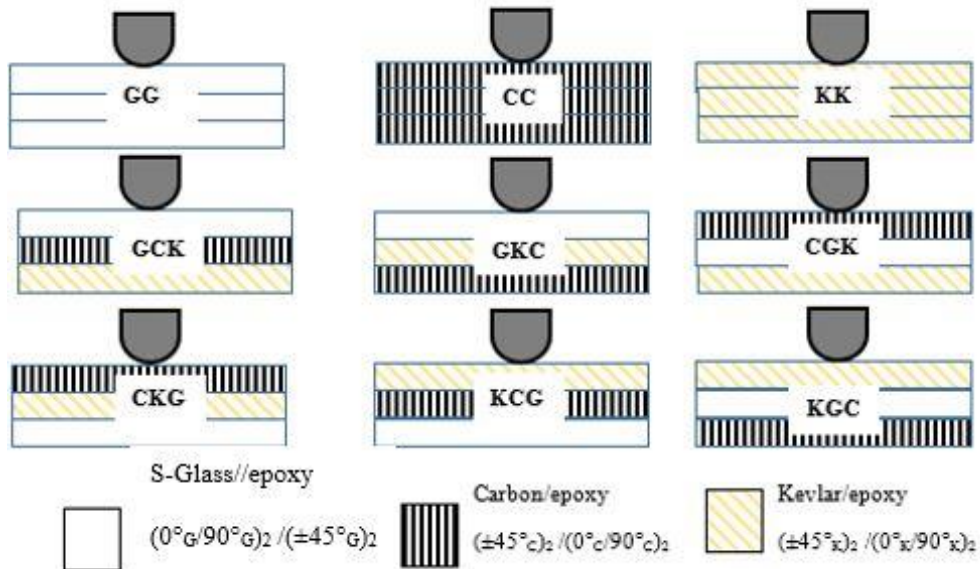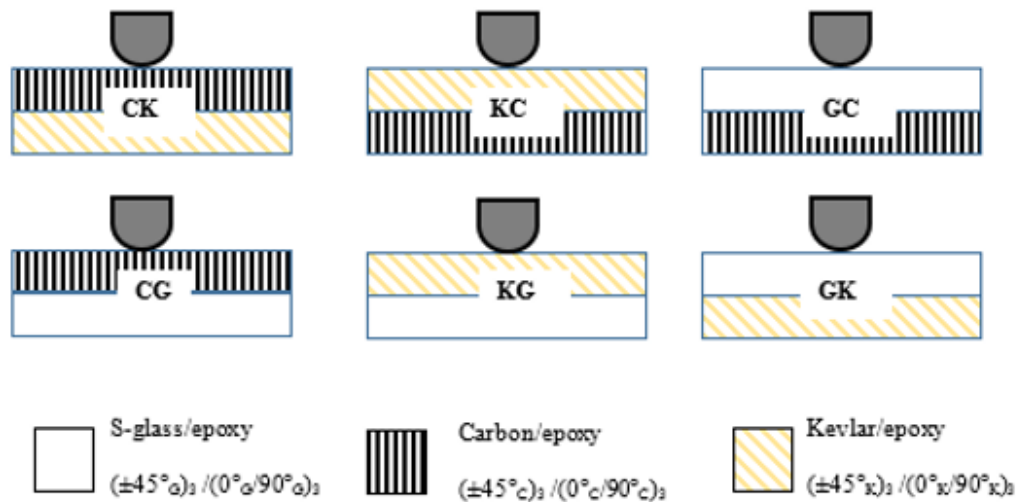
Figure 3.6 Hybrid and non-hybrid configurations of composite laminates for QSI and LVI

3.3 Procedures for QSPT Experiments

The quasi static punch methodology through the penetration tests was conducted by a controlled tensile testing machine Shimadzu AGX with a load frame of 300 kN (Figure 3.7 (a)). The test fixture is schematically shown in Figure 3.7 (b). It consists of a cover plate (20 mm thick) having a circular cutout at the center, a thick support plate (40 mm thick) having a central cutout those similar to the cover plate, and a cylindrical indenter.

Twelve different hybrid composite laminates with different stacking sequences were tested for two different support spans (D_S) of 25.4 mm and 63.5 mm by using a 12.5 mm diameter indenter. The crosshead-loading rate of the indenter was 1.25 mm/min in accordance with ASTM D732 [122]. Five samples were tested for each SPR and their average values were taken as result.
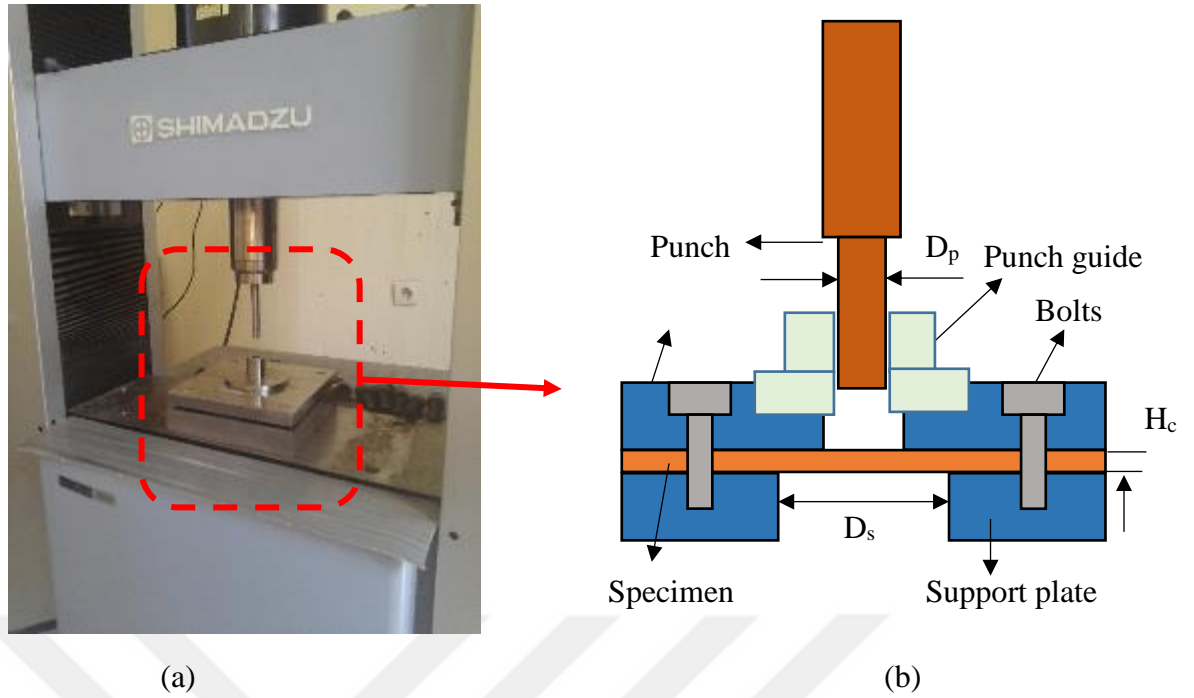
Figure 3.7 Damage mechanism for QSPT. (a) Punch shear test fixture, (b) Schematic illustration of test fixture

The initiation and formation of the damage mechanism in the hybrid laminates were characterized at a constant crosshead displacements of 8 (for SPR=2) and 10 mm (for SPR=5), and compared with non-hybrid composite laminates. The goal of the attempt is to show the progressive damage modes of composite laminates, and to obtain penetration force to displacement relation. During the penetration process, critical value of the transverse shear strength or punch shear strength around the indenter was resulted in the delamination formation and followed by a plug formation. The punch shear strength (PSS) of the samples is the maximum force (P_{max}) required to resist shear out of the plug from the material, and can be calculated by using equation (3.4)

$$PSS = \frac{P_{max}}{\pi D_p H_c} \qquad (3.4)$$

Where, D_p is the diameter of the punch and H_c is the thickness of the laminate. For the punch shear based damage mechanism of the toughened polymer matrix composites, force-displacement characteristic of structure is schematically illustrated as shown in Figure 3.8.

During the QSPT, load increases linearly within the elastic region up to point A. In this region, the laminate is subjected to elastic bending by the out of plane of punch load. After the point A, the formation of damage is followed by the delamination and matrix cracking until the plug has formed at point B. At point B, load abruptly drops due to rupture of fibers on the back surface of the laminates.

The load drop from B to C is quite important for the loss of the load carrying capacity of the laminates. Plugging formation has been completed at point C, then follows the frictional force between the cylindrical indenter and plug.
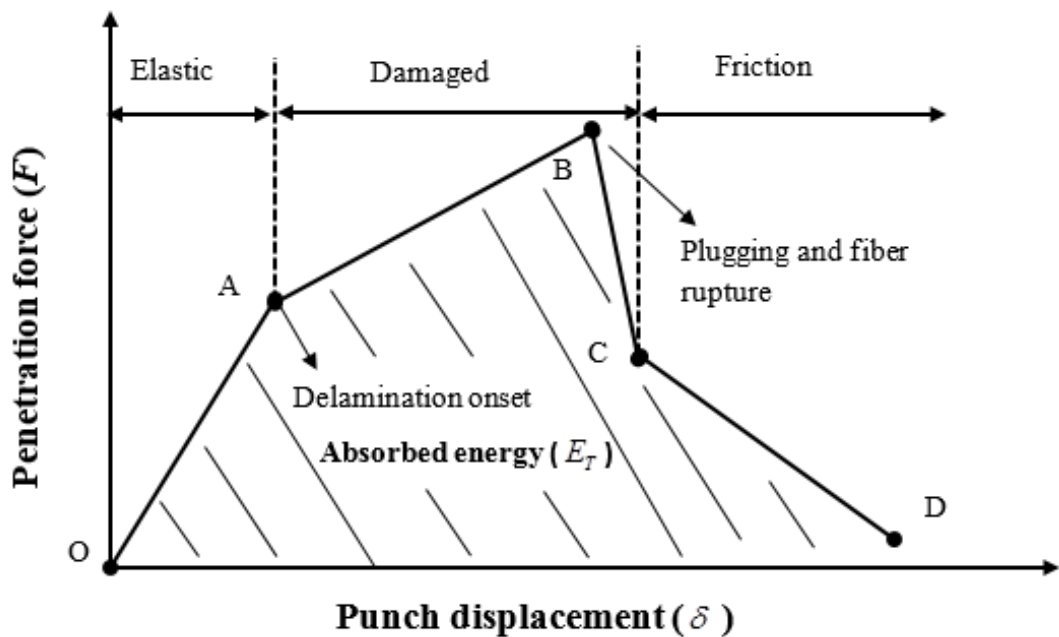
Figure 3.8 Schematics illustrations of a load-displacement curve for toughened matrix composites [98]

The absorbed energy in the composite laminates is represented by the area under the load- displacement curve OABCD as shown in Figure 3.8. The area under the load-displacement curve is the total energy absorbed by the composite laminates through the penetration process, and may be expressed as following equations, which consist of three stages of the damage mechanism.

$$E_E = \int_0^{\delta_A} F(\delta)d\delta \qquad (3.6)$$

49

$$E_D = \int_{\delta_A}^{\delta_C} F(\delta)d\delta \qquad\qquad (3.7)$$

$$E_F = \int_{\delta_C}^{\delta_D} F(\delta)d\delta \qquad\qquad (3.8)$$

Where, E_T, E_E, E_D and E_F are total strain energy, elastic energy, energy in damage region and frictional energy, respectively. The first stage of this area (OA) is the elastic strain energy, the second area (AB+BC) is the energy required for damage and complete plugging of the piece from the composite. Their values also correspond the work done during the QSPT, and can be expressed by integration in each section for total absorbed energy [123] required for penetration and perforation of the structure as given in equation 3.9.

$$E_T = E_E + E_D + E_F \qquad\qquad (3.9)$$

3.4 Procedures for QSI Experiments

Indentation tests were performed by a tensile testing machine (Shimadzu AGX) having load capacity of 300 kN (Figure 3.9 (a)). The apparatus of test frame used in QSI experiments is shown in Figure 3.9 (b). As can be seen in Figure 3.9, a thick section cover plate (20mm) with a circular hole in the middle, a thick section support plate (40mm) with a circular hole those same with cover plate, and a cylindrical projectile were used. During the designing of hybrid samples, twelve different composite laminates were produced with combinations of two and three different fibers. Samples were settled between two flat and steel molds having a circular cutout (D_S=76.2 mm), then subjected to an out of plane loading with a hemispherical end projectile (D_P=12.7 mm) in the middle of sample.

The test speed of the projectile was set to 1.25 mm/min. The extension and growth of the damage were identified by a constant punch displacement (10 mm) until the complete perforation of the sample. The ultimate failures were characterized by the development of fiber rupture initiating the multiple load drops as shown in Figure 3.10. It is clear that load increases linearly up to first load drop, resulting matrix cracking

(stage I), then follows the initiation of delamination resulting in reduction of stiffness (stage II) and finally fiber breakages with multiple load drops within the stage III [86].

In order to reach reliable results, five coupons for repeating each groups were experimentally tested, and their average values were recorded with standard deviations. The objective is to explore the failure modes through the hybrid and non-hybrid composite structures by simulating low velocity impact event. For this purpose, two and three different fibers having different mechanical properties were incorporated for characterization of hybridization effects. Their damage mechanisms were determined in terms of absorbed energy, and compared with non-hybrid composites.
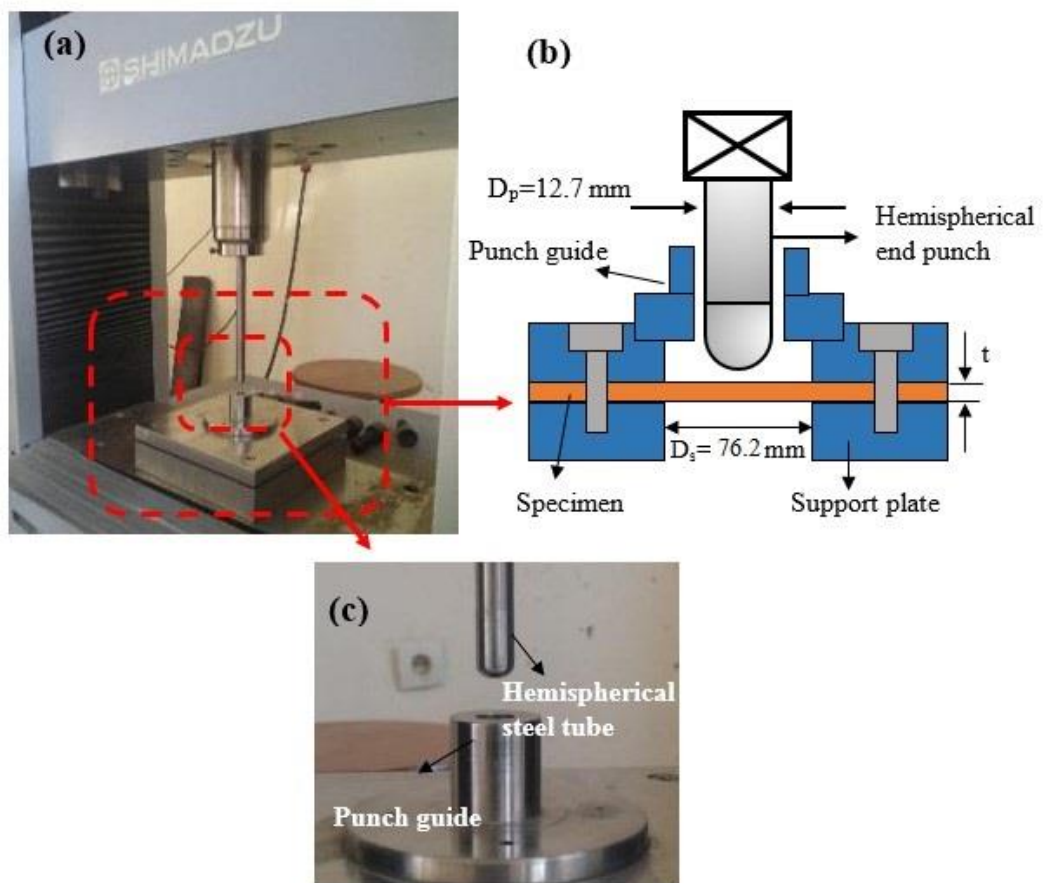
Figure 3.9 Damage mechanism for QSI. (a) Punch shear test fixture, (b) Schematic illustration of test fixture, (c) Hemispherical steel tube
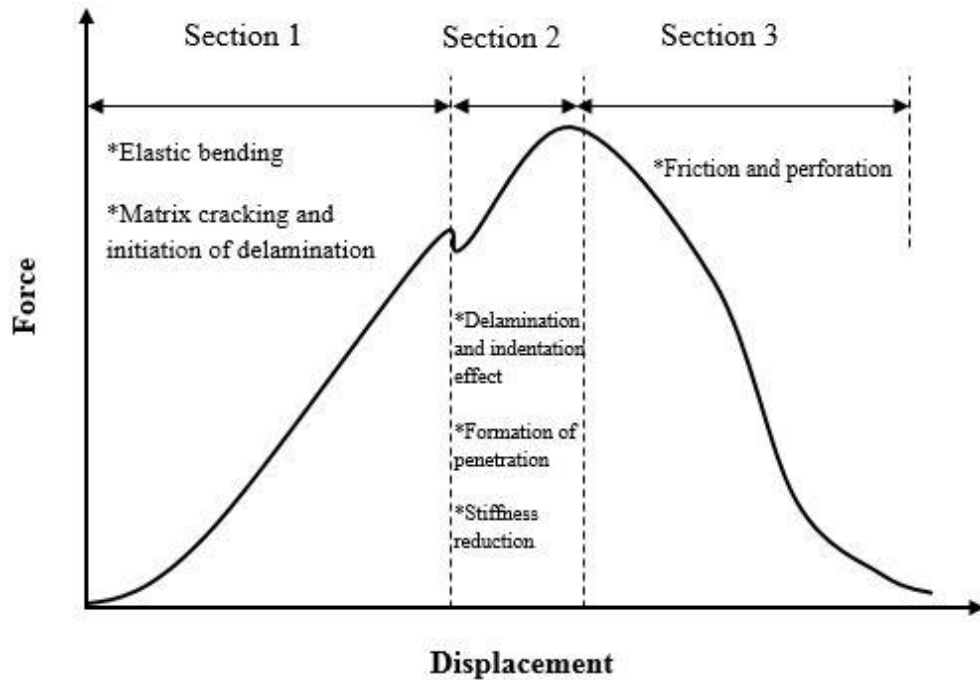
Figure 3.10 Schematic illustration of quasi-static indentation process

3.5 Procedures for LVI Experiments

The test coupons for impact tests were prepared from the laminates by cutting in the sizes of the 100x100 mm, having quasi-isotropic structure in accordance with ASTM D6264/D6264M [10] standard. In order to compare the hybridization effects, two different hybrid structures were designed and tested. First one is double fiber combinations by interplay hybridization of two different fibers, another is the triple fiber combinations by interplay hybridization of three different fibers.

Low velocity impact tests were performed by a guided drop weight tower in accordance with ASTM D7136/D7136M [74] standard (Figure 3.11). A breaking system was used in order to prevent multiple drops of impactor on the specimen, which could be further failure the samples. Two optic sensors, a flag connected to impactor, two pneumatic pistons, a solenoid valve, and a compressor were used in designing of impact machine. A winch with an electromagnet was used to lift the projectile in order to desired impact height and velocity.

During impact event, the force response of the structure was recorded by mounting a piezoelectric force sensor (ICP M202B ® quartz force ring) having maximum force

capacity of 44.48 kN under the impactor. A hemispherical tipped cylindrical shape of steel impactor with 12.7 mm diameter was used during the impact tests. The samples were clamped in the frame with 76.2 mm diameter of circular opening, which exposed to impact. The impact tests were carried out same conditions with impact energy of 30J, which resulting from impact velocity of 3.4 m/s with a total impactor weight of 5 kg. The actual velocity of total impactor was evaluated by optical sensors located just above 25 mm from the sample surface. To ensure reliability of the results, samples were impacted by three times and their average value of them was considered as result. A software (LABVIEW) was used in order to capture force signal from the sensor.
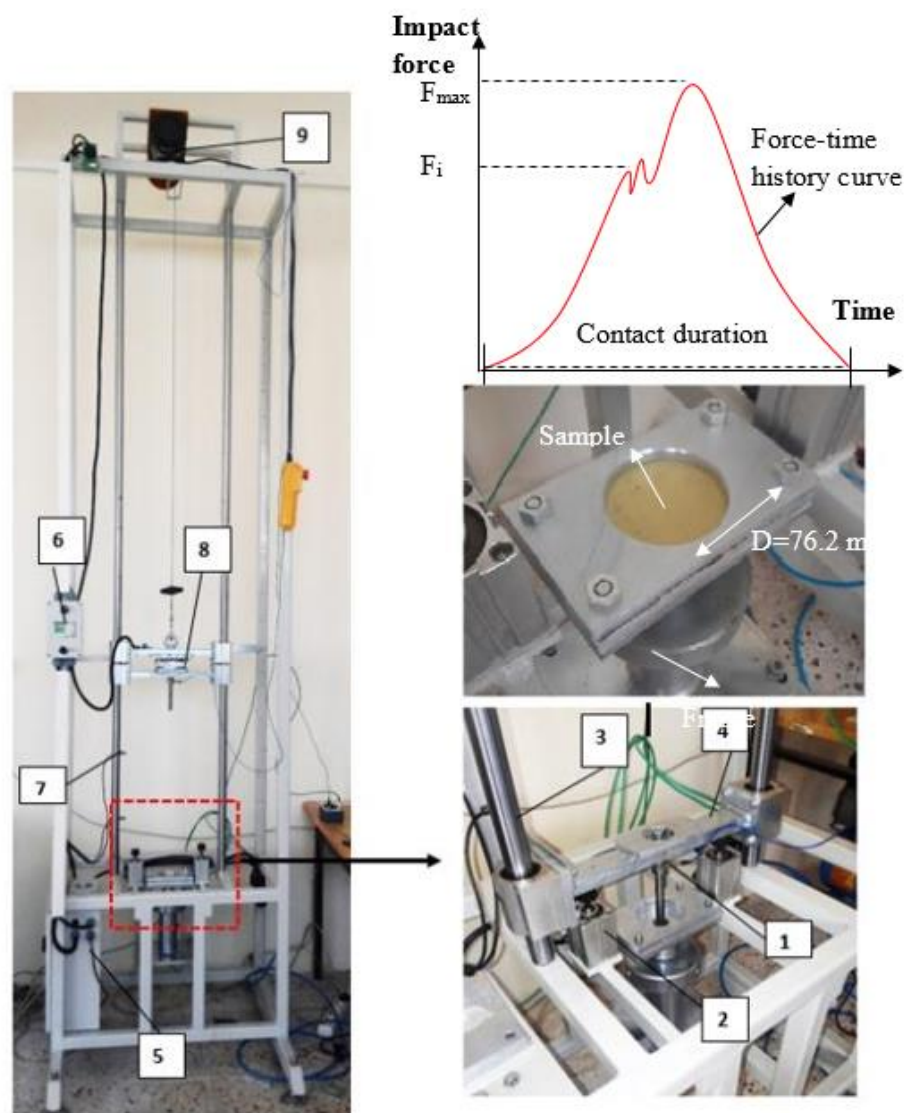
Figure 3.11 Drop weight test machine. (1) Load cell, (2) Rebound breaking system, (3) Guiding rods, (4) Impactor, (5) Control unit, (6) Velocity and time indicator, (7) Optical sensor, (8) Electro-magnet for clamping, (9) Lifting mechanism

The velocity, deformation, and absorbed energy values were obtained from the area under the force-displacement curves. The velocity-time versus force-time values during the impact change according to equation 3.6

$$v(t) = v_i + gt - \int_0^t \frac{F(t)}{m} dt \qquad (3.6)$$

Where t is the time, v is the velocity of impactor, g is the acceleration due to gravitation and m is the total mass of the impactor unit. If the impact device monitoring generates the impact force, the equation 3.7 has incorporated to represent the deformation of impactor from the initiation of impact event.

$$\delta(t) = v_i(t) + \frac{1}{2} gt^2 - \int_0^t (\int_0^t \frac{F(t)}{m} dt) dt \qquad (3.7)$$

By the use of equation 3.6 and 3.7, the absorbed energy has been calculated as given in equation 3.8

$$E_a(t) = \frac{m(v_i^2 - v(t)^2)}{2} + mg\delta(t) \qquad (3.8)$$

3.6 Hybrid Effect Calculations

The importance of hybrid effect has been gained great concern due to be able to arrange the some specific properties according to design requirements. By the hybridization of two or more different fibers, the structures may be designed as the high strength and stiffness while they exhibit low cost. A positive or negative hybrid effect will be occurred according to their common compositions by the rule of mixture [133].

Present study handles the hybrid effect incorporating rule of mixture (*RoM*). The values of RoM were evaluated not only the absorbed energy but also indentation force by using equation 3.9 and 3.10

$$E_{(RoM)} = \frac{1}{3}(E_C + E_K + E_G) \qquad (3.9)$$

$$F_{(RoM)} = \frac{1}{3}(F_C + F_K + F_G) \qquad (3.10)$$

Where E_C, E_K and E_G are absorbed energy values and F_C, F_K and F_G are the maximum resulting indentation load values through the indentation of full composites (CC, KK and GG laminates, respectively). $E_{(RoM)}$ and $F_{(RoM)}$ indicate rule of mixture values of full composites for absorbed energy and indentation load, respectively. Hybrid effect values were calculated from equation (3.11) and (3.12) by using equation (3.9) and (3.10).

$$\textit{Hybrid effect} \; (h_e) = \frac{E_h}{E_{(RoM)}} - 1 \qquad (3.11)$$

$$\textit{Hybrid effect} \; (h_e) = \frac{F_h}{F_{(RoM)}} - 1 \qquad (3.12)$$

Where he denotes the hybrid effect and it may be positive or negative. Absorbed energy and indentation force are shown as E_h and F_h, respectively. A positive or negative hybrid effect will be occurred according to equation 3.13.

$$
\begin{aligned}
&h_e > 1, \qquad \textit{Positive hybrid effect}, \\
&h_e < 1, \qquad \textit{Negative hybrid effect}
\end{aligned}
\qquad (3.13)
$$

CHAPTER 4

RESULTS AND DISCUSSIONS FOR QSPT EXPERIMENTS

4.1 Introduction.

In this section, the results of quasi-static penetration tests will be presented with discussions. It is also devoted to evaluate the hybrid effect of hybrid composites those influencing damage modes through the quasi-static penetration process.

4.2 QSPT results

The experimental progressive damage procedure was conducted on hybrid and non-hybrid composites under the quasi-static punch shear tests. Similar experimental studies were used by several researchers [97], [102] and [124]. Damage and failure mechanisms of composite laminates were identified for two different SPR ratios (SPR=2 and 5).

The effects of stacking sequence on damage process, absorption energy and failure mechanism of the hybrid composites were examined. The results of QSPT experiments are presented in Table 4.1, and the variations of PSS and absorbed energy (Ea) values are shown in Figure 4.3 and Figure 4.4, respectively. It is observed from Figure 4.3 (a) that PSS values of Kevlar/epoxy composites indicate the maximum value as compared with full carbon/epoxy and full glass/epoxy composites. The results of the QSPT results for hybrid samples were varied between the samples of full glass/epoxy and full Kevlar/epoxy.

When triple fiber combinations were compared, hybrid sample KCG exhibited the maximum penetration force and PSS values at the SPR= 2. However, the hybrid sample KGC showed maximum PSS and force at SPR=5. This can be explained by the flexural sensitivity of the fibers under the different support span ratios [125-126], and position of fibers in the lamina [127], which has significant effect on load to deformation characteristics of hybrid samples. Researchers [127-129] indicated that

the flexural strength was increased when glass layers were placed on the outer surfaces for carbon/glass hybrid configurations, and it is confirmed by the triple fiber combinations between GCK and CGK, and also GKC and CKG. When topmost lamina of the full carbon/epoxy or Kevlar/epoxy was replaced with a glass lamina, PSS values followed by the decreasing trend and similar results were found for hybrid carbon/glass laminates by [130].

Table 4.1 Comparison and variation of QSPT results

Sample	SPR=2, Dp=12.5mm				SPR=5, Dp=12.5mm			
	Pmax (kN)	Hc (mm)	PSS (MPa)	Ea (J)	Pmax (kN)	Hc (mm)	PSS (MPa)	Ea (J)
GGG	15.96	5.1	79.73	39.84	11.22	5.1	56.05	42.04
CCC	33.33	6.0	141.53	87.65	29.09	6.0	123.52	111.97
KKK	35.92	6.2	155.11	98.02	30.34	6.2	124.68	130.56
GCK	27.01	5.7	120.73	74.11	21.19	5.7	94.71	83.15
GKC	33.65	5.9	145.31	73.1	22.16	5.9	95.69	89.12
CGK	26.25	6.1	109.64	78.03	19.22	6.1	80.28	84.44
CKG	25.87	5.9	111.71	69.36	18.58	5.9	80.23	78.80
KCG	35.91	5.7	152.48	70.84	19.79	5.7	88.46	79.09
KGC	33.59	5.9	145.05	72.34	22.32	5.9	96.38	84.11
CKC	23.31	6.3	94.23	84.57	18.10	6.3	74.41	104.44
KCK	35.30	6.1	147.44	75.27	24.90	6.1	104.00	101.81
GCG	23.36	5.4	109.53	54.74	14.80	5.4	69.98	58.26
CGC	22.78	5.3	109.93	53.07	15.70	5.3	74.51	54.98
KGK	27.45	5.7	122.47	65.54	15.90	5.7	70.66	78.32
GKG	25.07	5.7	112.06	77.07	17.40	5.7	82.24	82.02
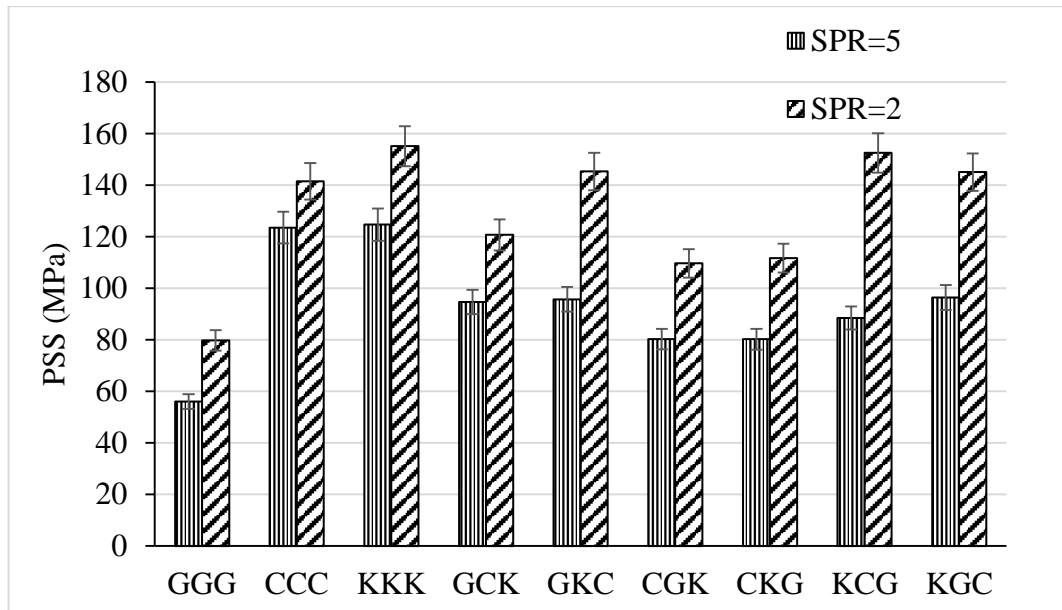
(a)
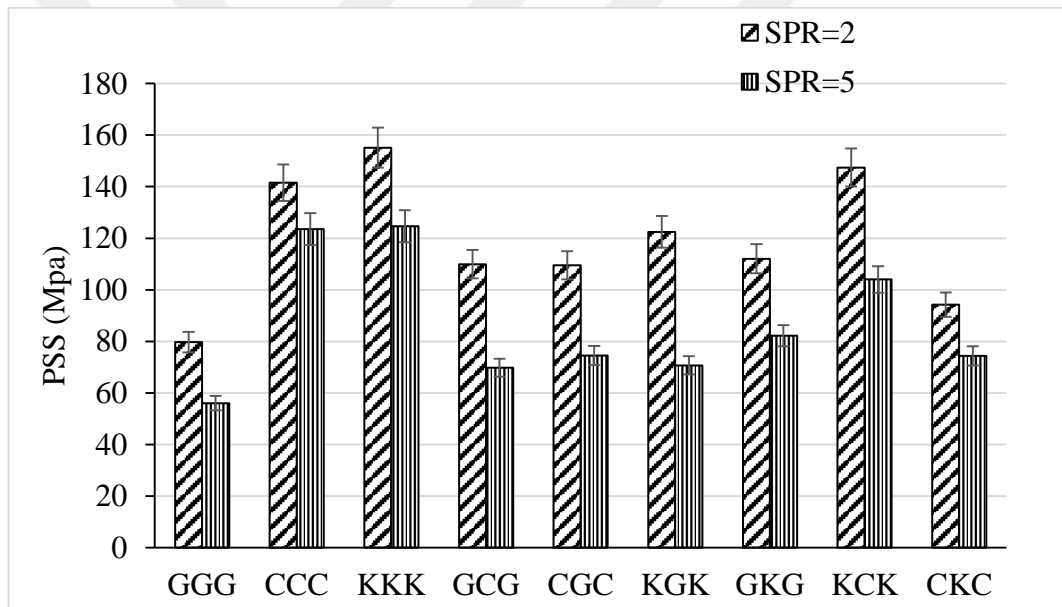
(b)

Figure 4.1 Punch shear stress distributions. (a) Triple fiber combinations, (b) Double fiber combinations

When double fiber combinations were compared, hybrid sample of KCK showed better penetration resistance and energy absorption capacity than other hybrid samples. The position of Kevlar fiber had significant effect on PSS values, and replacement of Kevlar fiber with glass or carbon fibers on the outer surfaces caused the reduction of PSS. However, replacement of carbon fiber with glass fiber on the topmost layers resulted in increase of PSS, which was also in agreement with [130]. When double fiber combinations were compared, hybrid sample of KCK showed better penetration

resistance and energy absorption capacity than other hybrid samples. The position of Kevlar fiber had significant effect on PSS values, and replacement of Kevlar fiber with glass or carbon fibers on the outer surfaces caused the reduction of PSS. However, replacement of carbon fiber with glass fiber on the topmost layers resulted in increase of PSS, which was also in agreement with [130].
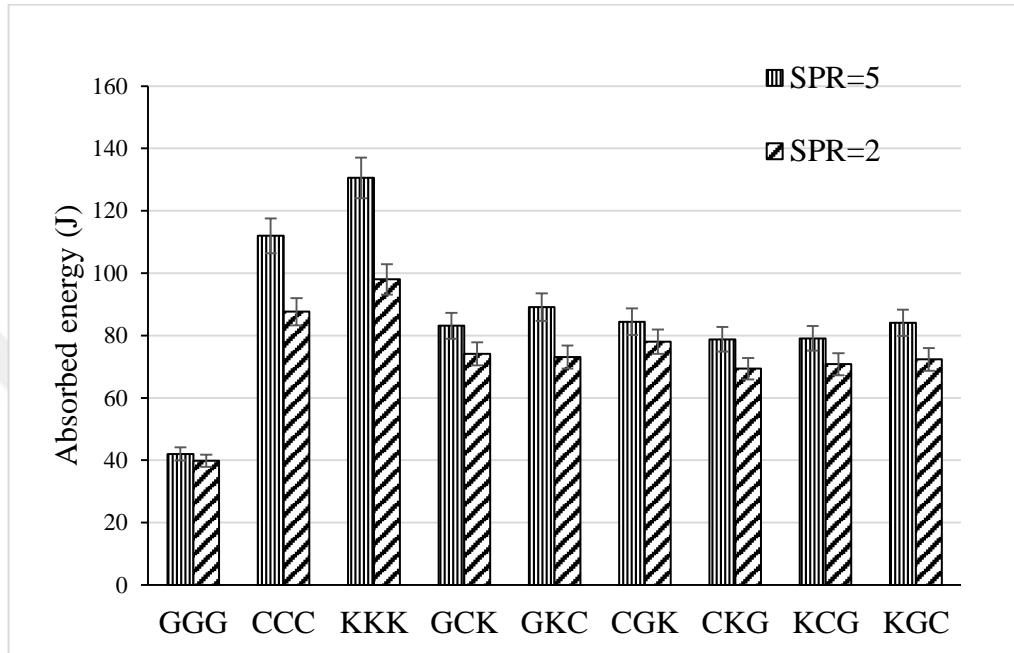
(a)
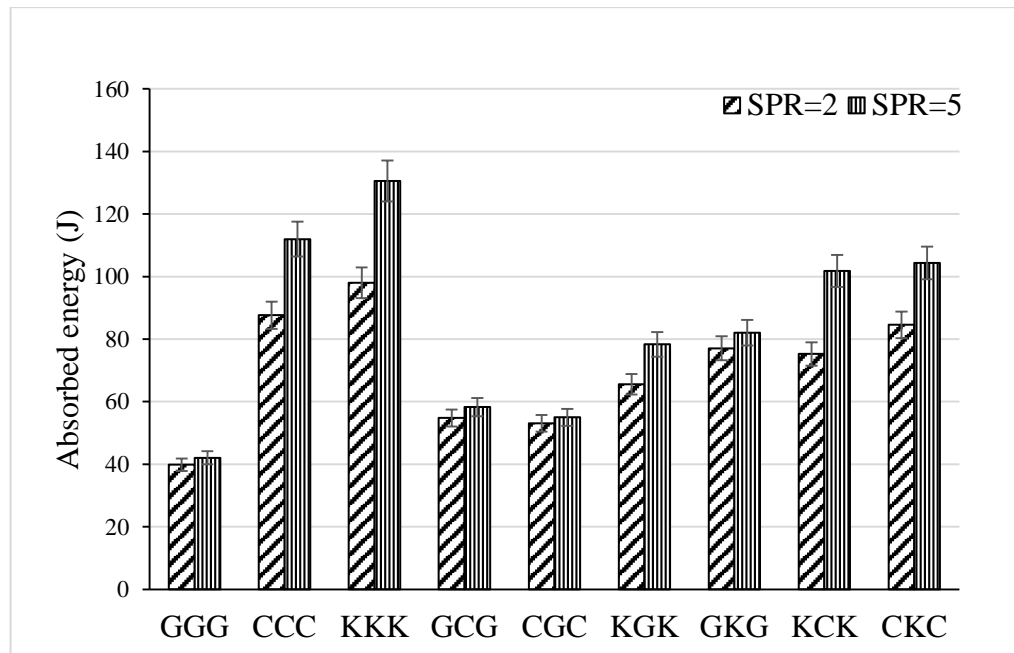
(b)

Figure 4.2 Absorbed energy until the maximum deformation. (a) Triple fiber combinations, (b) Double fiber combinations.

The variations of absorbed energy values from Figure 4.4 showed the increasing trend of penetration energy from GGG to KKK. The energy values obtained from load-displacement curves indicated that the sample of KKK exhibited maximum absorption energy at SPR=5 while sample of GGG showed the lowest values.

When hybrid composites were compared, the energy distributions showed the variations between GGG and KKK composite laminates. When double and triple fiber configurations are compared, it is observed that variations in double fiber configurations resulting from the stacking sequence effects are greater than those of triple fiber configurations. For double fiber configurations, substitution of KGK with GKG showed the 18.4 % divergence in terms of absorbed energy, while the maximum difference in triple fiber configurations was found about 11.3 % by substitution of CGK with CKG. This is attributed the existence of third fiber which balances between another two different fibers.

It is also noted that the absorbed energy increases with increase in SPR ratio. The differences in absorption energy values are not significantly observed in the hybrid configurations. This means that the absorption energy during the penetration progress is not sufficiently effected by the position of the fibers in the lamina. For triple fiber configurations, the sample of CGK exhibited maximum absorbed energy compared with other hybrid samples at SPR=2. However, the sample of GKC showed the maximum absorbed energy composite at SPR=5.

For double fiber configurations, KCK and CKC hybrid composites exhibited better performance in all hybrid composites at SPR=5. These variations were attributed to the flexural stiffness and transverse shear stress characteristics of the fibers [99]. For example, when the carbon fibers were placed in the topmost layers, they exhibited highest peak loads while resulting a sudden load drop after the plugging formation. Similarly, Jeng et al. [131] reported the damage modes of glass/epoxy composite laminates subjected to QSPT by hemispherical tipped indenters. It was asserted that the damage progress started by matrix cracking followed by an abrupt delamination, and resulted in a considerable decrease of load carrying capacity.

Penetration force to punch displacement curves of the hybrid and non-hybrid composites were obtained by a displacement controlled tensile test machine as shown in Figure 4.5 and Figure 4.6. As can be seen Figure 4.5 and Figure 4.6, the penetration

force increased linearly up to matrix cracking, then followed the damage progress until the initiation of plugging. The critical fiber rupture initiated the plugging and followed by a friction effect between punch and its contact area with sample. Similar results were reported by Deka [123], as indicated that the damage mechanisms of QSPT were dependent on the SPR values as a result of (a) transverse matrix cracking, (b) delamination and shear plug initiation, (c) delamination progress and complete shear plug formation, (d) push out of shear plug and (e) tensile fiber fracture and push out of shear plug. It is also clear from Figure 4.5 that force to deflection behaviors of full carbon/epoxy, Kevlar/epoxy and S-glass/epoxy composites showed the different trend of punch curves at SPR= 2 and 5. The trend of maximum load follows: KKK>CCC>GGG for each SPR value. These observations indicate that the hybridization of Kevlar and carbon fibers with glass fibers plays important role in failure and energy absorption of glass/epoxy composite laminates due to higher energy absorption capacity of Kevlar and carbon fibers.

Figure 4.6 and Figure 4.7 compare the variations of penetration forces for hybrid composite laminates having double and triple fiber configurations at SPR= 2 and 5. It is clear that the all of curves have followed by three different stages, that is, elastic deformation until the onset of delamination, damage region from onset of delamination to plugging and friction zone beyond the plugging.
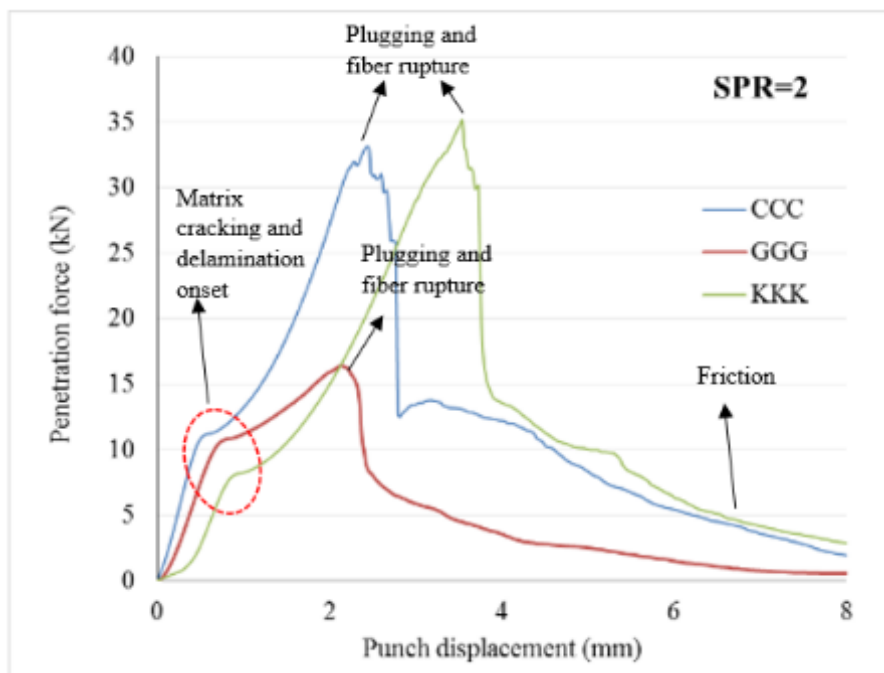
(a)
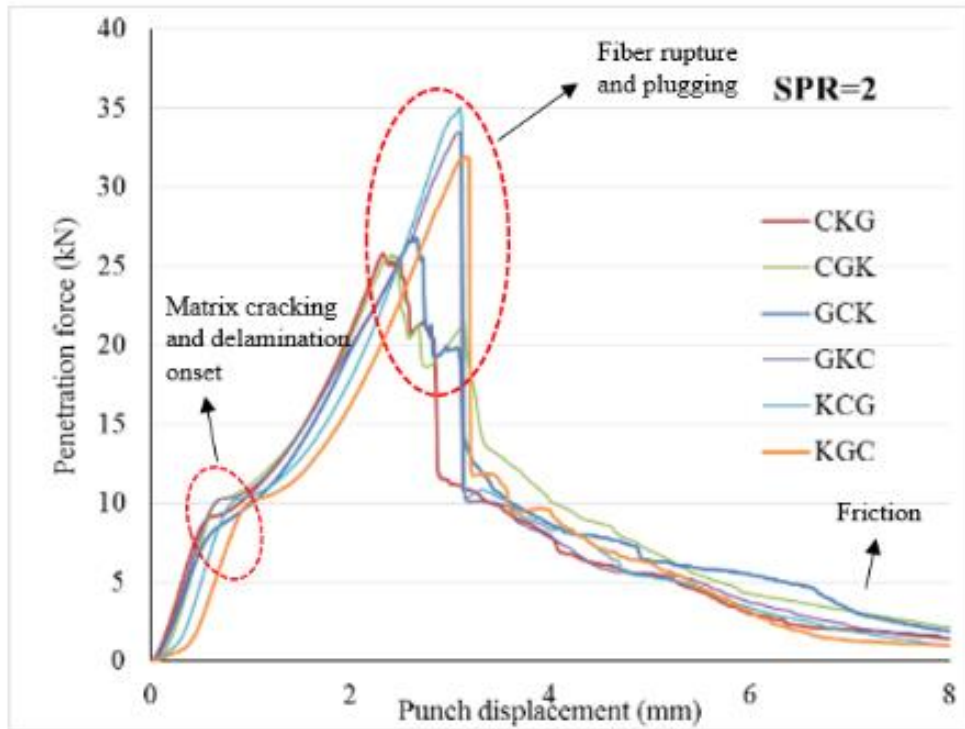
(b)

Figure 4.3 Variation of penetration force curves for triple fiber combinations at SPR=2. (a) Non-hybrid composites. (b) Hybrid composites
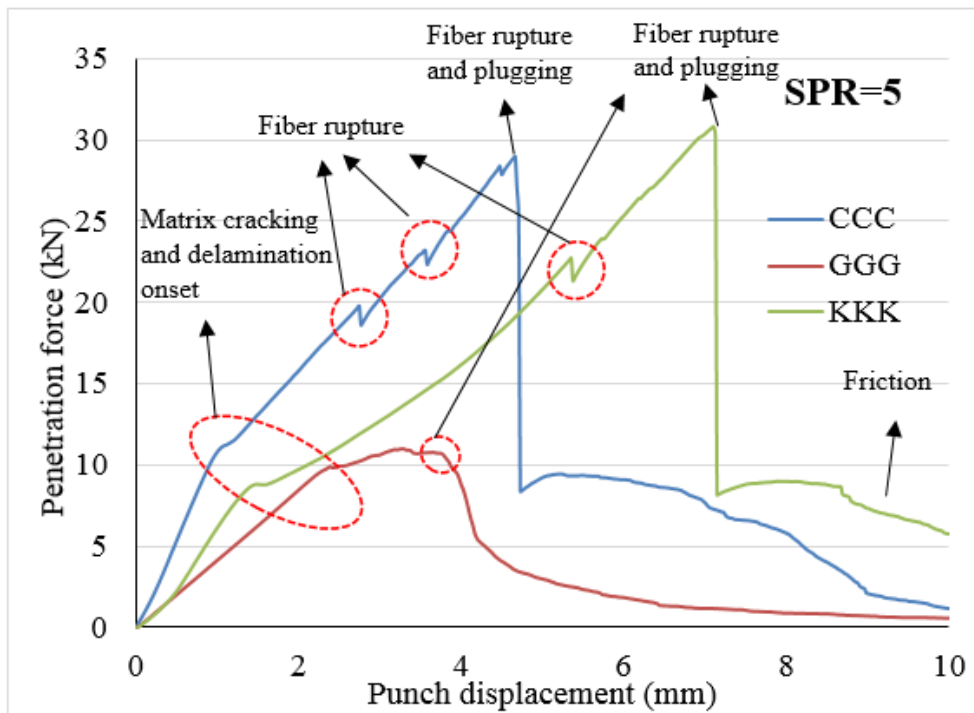
(a)
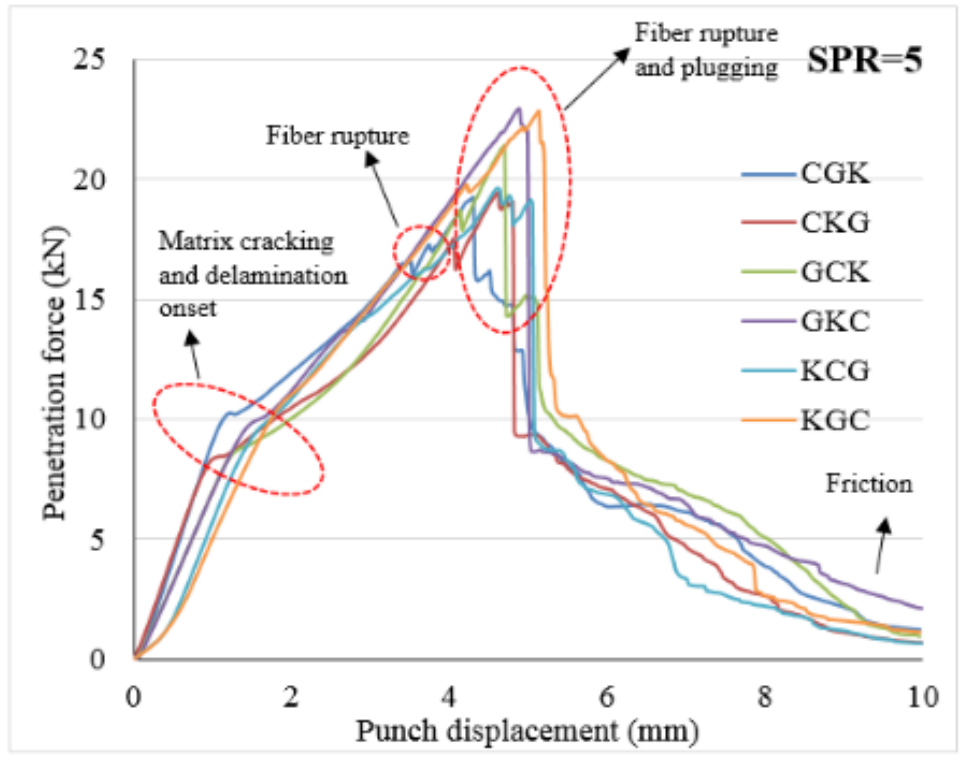
(b)

Figure 4.4 Variation of penetration force curves for triple fiber combinations at SPR=5. (a) Non-hybrid composites. (b) Hybrid composites
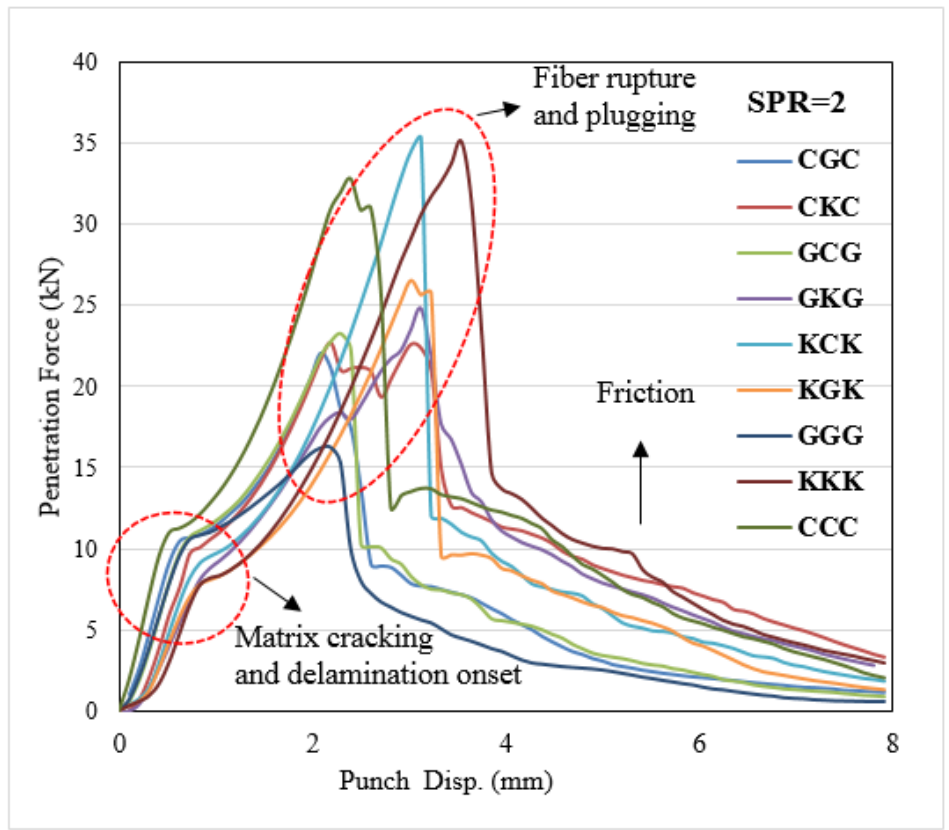
(a)
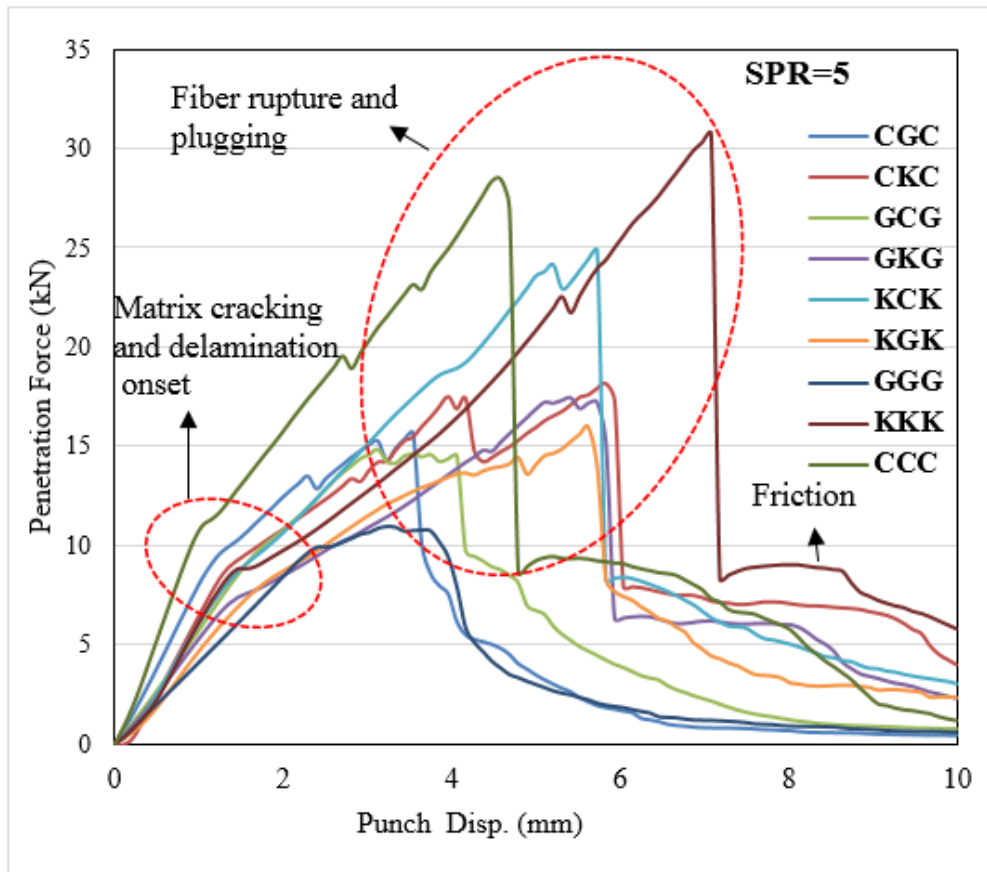
(b)
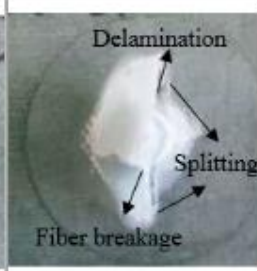
Figure 4.5 Variation of penetration force curves for double fiber combinations. (a) SPR=2, (b) SPR=5

During the damage process, the load increases up to maximum load has reached its critical value, then suddenly drops following by a plugging and perforation, finally this process initiates friction region until the long tail displacement of the punch [123]. For three different fiber hybridization, multiple load drops occurred in the CGK and CCC composite laminates at SPR=2 and 5, respectively. The curves at SPR=2 showed more smooth force-displacement behavior as compared with curves at SPR=5. This may be clarified by the poor toughness of the carbon fiber and position of it in the lamina.
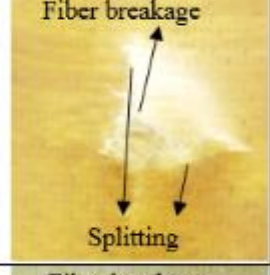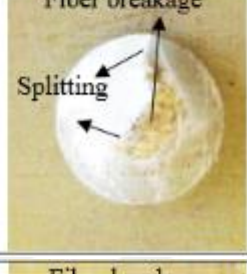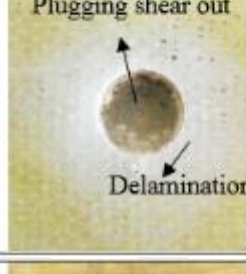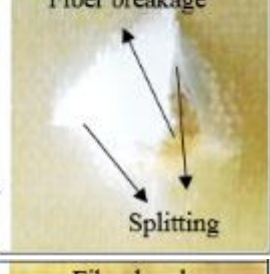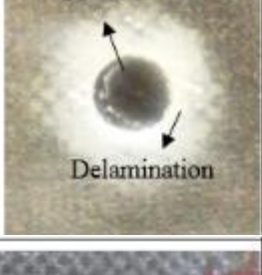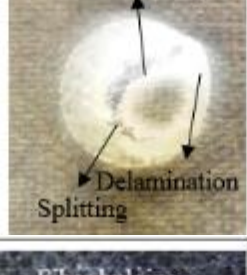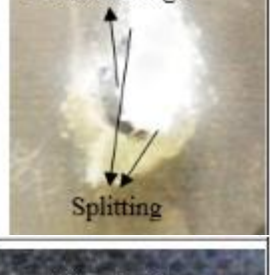
QSPT damage mechanisms of the hybrid and non-hybrid composites were characterized by taking the pictures of front and rear sides as shown in Table 4.2. During the QSPT in the composites, the increase of punch load until the long tail of friction stage was resulted in the damage mechanisms of fiber breakage, matrix cracking until the plug formation, then followed the shearing out of the plugging from the samples.

These observations showed that extend and spreads of the damage were significantly affected by the exposed support span area. For example, at SPR= 2 the transverse shear and compression stresses were dominant for initiation of plugging and fiber rupture, while at SPR=5 the tensile failures due to bending effects were dominant in the damage mechanisms.

Table 4.2 Front and back side views of the samples after the penetration tests

	SPR=2		SPR=5	
	Front side	Rear side	Front side	Rear side
GGG				
CCC				
KKK				
CKG				

CGC	Plugging shear out	Fiber breakage / Splitting and bulging	Plugging shear out	Fiber breakage / Splitting
KGK	Plugging shear out	Plugging shear out / Bulging / Splitting	Plugging shear out	Fiber breakage / Splitting
GKG	Plugging shear out / Delamination	Fiber breakage / Splitting	Plugging shear out / Delamination	Fiber breakage / Splitting
KCK	Plugging shear out / Delamination	Fiber breakage / Splitting		Fiber breakage / Splitting
GCG	Plugging shear out / Delamination	Fiber breakage / Delamination Splitting	Plugging shear out / Delamination	Fiber breakage / Splitting
CGK	Plugging shear out	Fiber bulging	Plugging shear out	Fiber breakage / Fiber splitting

The pictures of the samples showed that the damaged area at the rear surface of the GCK exhibited higher damaged area compared with other hybrid composites. This may be due to lower flexural strength and toughness of glass fibers located in the topmost layers. However, hybrid samples of KCG and KGC showed the smaller damage mechanisms in terms of fiber pull out and bending failures compared with other hybrid composites. The reason of this can be explained that the damage mechanism have occurred differently in the Kevlar, glass and carbon fibers due to their different overall stiffness and natural ductile properties.
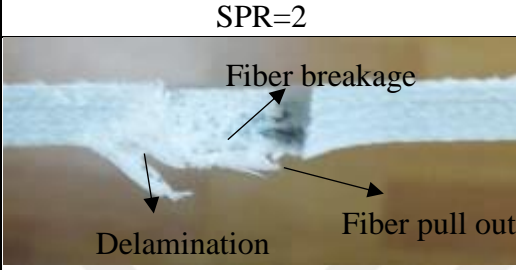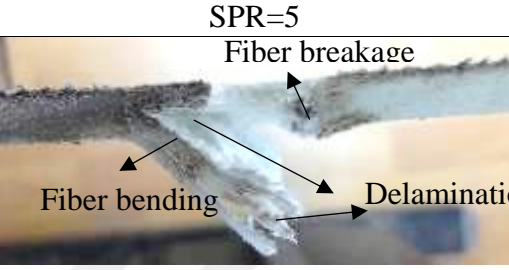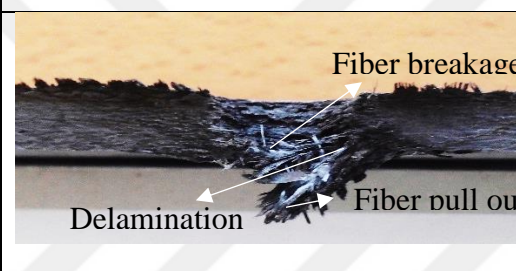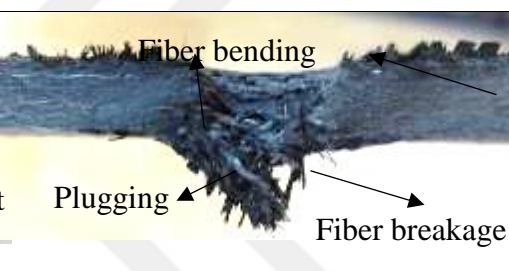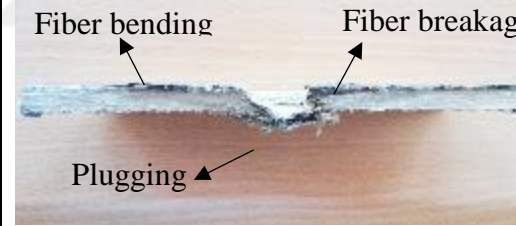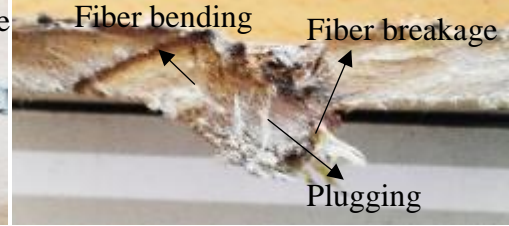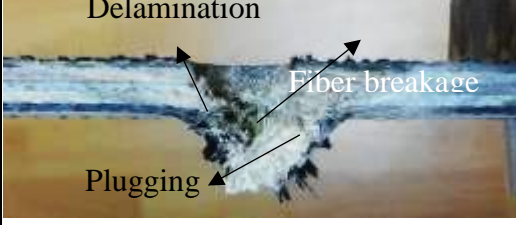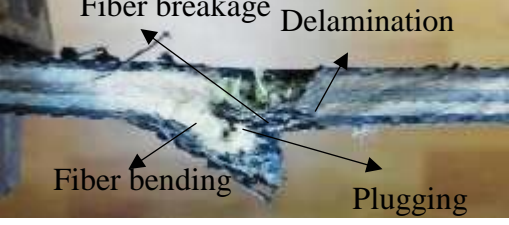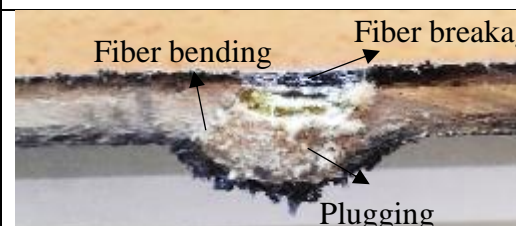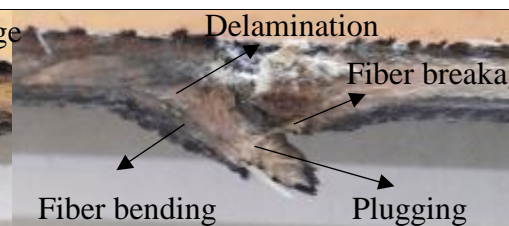
It is also noted that the outermost layers of the composite laminates played the most important role for improving damage and penetration resistance of hybrid composites. For example, when rear side of the fibers designed as Kevlar, the amount of delamination, splitting and fiber breakage was decreased. However, in the case of glass fibers were designed as outer layers, the failure mechanisms of fiber splitting and breakage exhibited the maximum degree when carbon and Kevlar were placed on outer layers.

After the penetration tests completed, the samples were cut along the half section of the damaged region using a saw for better understanding of damage assessment during the QSPT. The half-sectioned pictures of samples are given in Table 4.3 for SPR=2 and 5. It is observed that the initiation of the damage have followed by fiber breakage with abruptly load drop, and then the formation of shear plug and friction processes continued. The damage mechanisms of QSPT were recorded as matrix cracking, fiber breakage, fiber bending, and delamination. Due to the increasing bending and penetration, fiber breakages and delamination areas increased at rear side. At SPR=5, the resulting degree of fiber ruptures due to bending effect in the rear side was greater

than those of delamination at SPR=2. Dominantly, shear out based fiber breakages were resulted in around the striker.

When all of composite laminates were compared, sample of GGG provided the higher delamination at SPR= 5. In particular, the plug formation and shear out from the samples were clearly visible in hybrid composites.

Table 4.3 Half sectioned sides of the samples after the penetration tests
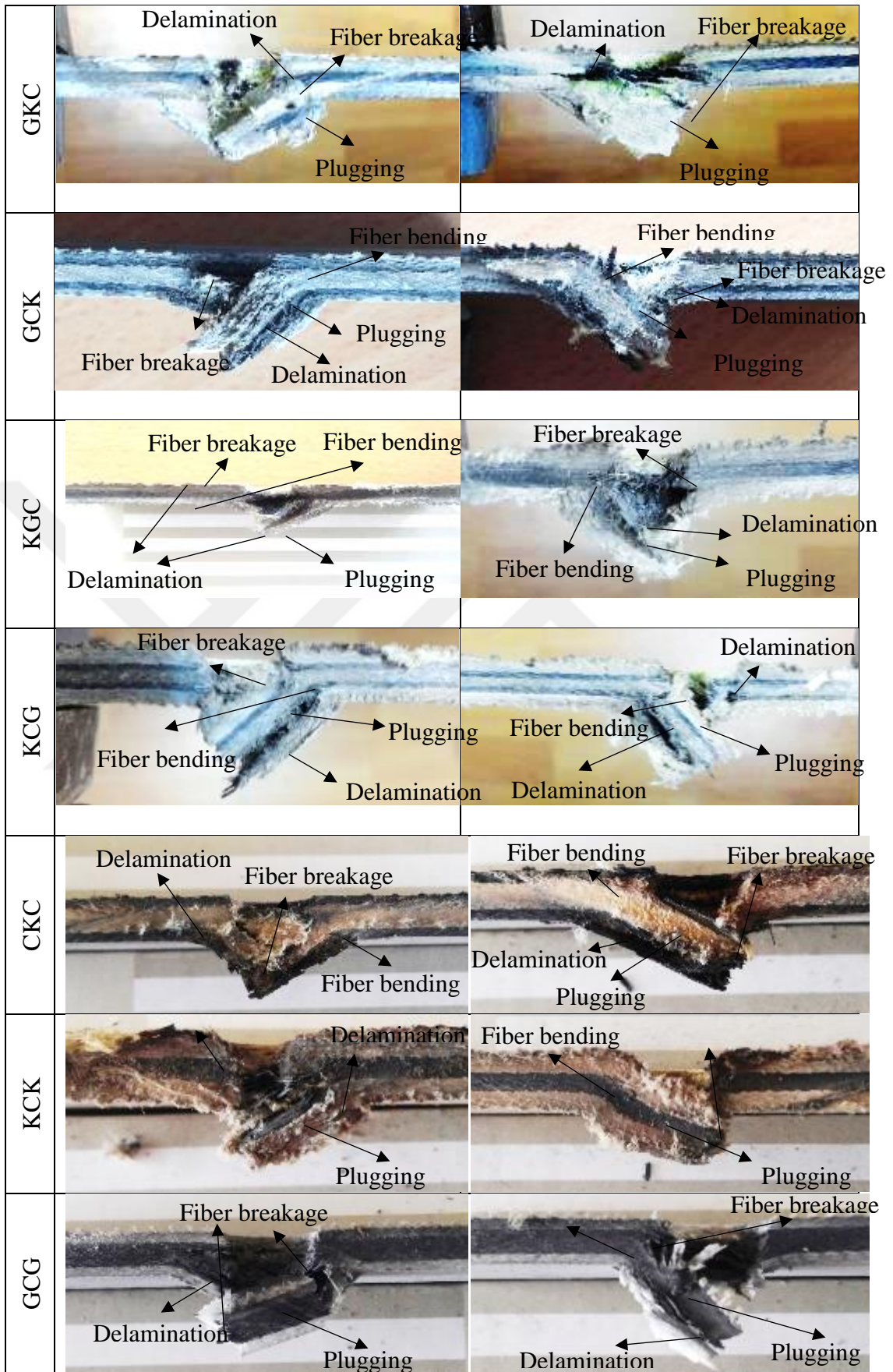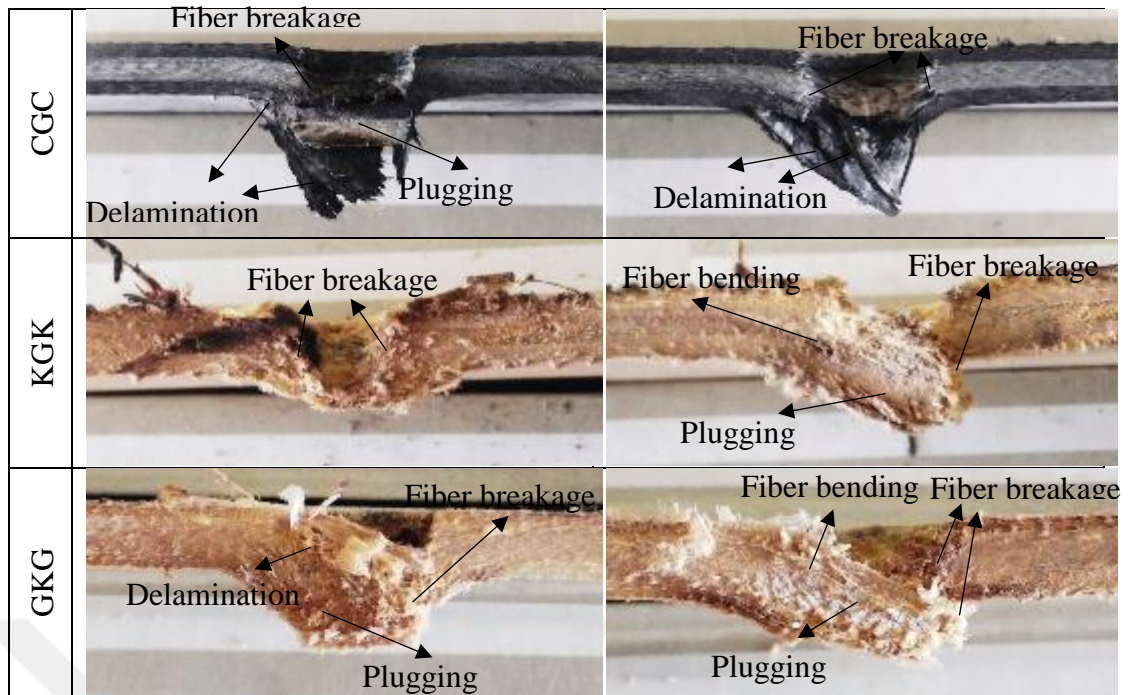
It is also observed that the formation of delamination between layers gradually have increased in the bottom layers. During the QSPT, the fibers in the bottom sides were dominantly failed by tension forces induced flexural bending since the cutting action of the punch was severely reduced by plugging in front of it [132]. Based on these results, the cross sectional pictures of samples showed that the extension and propagation of delamination between fibers in the bottom side were severely increased due to the bending effects in fibers.

In hybrid composites, when glass fibers placed in the outermost layers, a significant delamination and fiber pull out were observed due to lower tensile strength and brittle nature of glass fibers as well as poor transverse stress between glass layers. In particular, damage mechanism of fiber pull out was dominant at SPR=5 in the case of Kevlar fibers were placed at the inner layers. Due to the effect of SPR (2 and 5), a significant amount of failures was observed depending on bending and shear effects around the punch. For example, the cross section view of KCG at SPR=5 showed a significant delamination failure between Kevlar and carbon interfaces when compared with SPR=2. As presented in Table 4.3, the plug formations of hybrid samples are different at SPR= 2 and 5 through the QSPT process. For example, plug formations in the hybrid samples of CGC, GCG, GKC, KCK were clearly visible at SPR=2 compared with SPR=5.

Hybrid effect values of the samples were obtained as presented in Table 4.4 and their variations are illustrated in Figure 4.6. The results from Table 4.4 and Figure 4.6 showed that the sample of CKC exhibited the highest positive hybrid effect for SPR=2 and SPR=5, while the sample of CGC showed the highest negative hybrid effect.
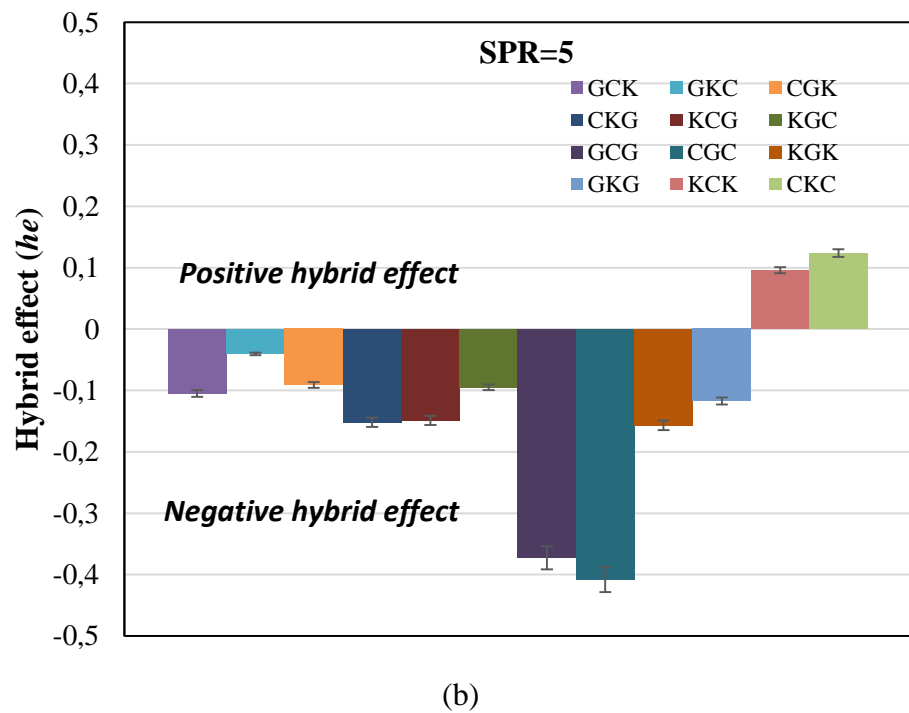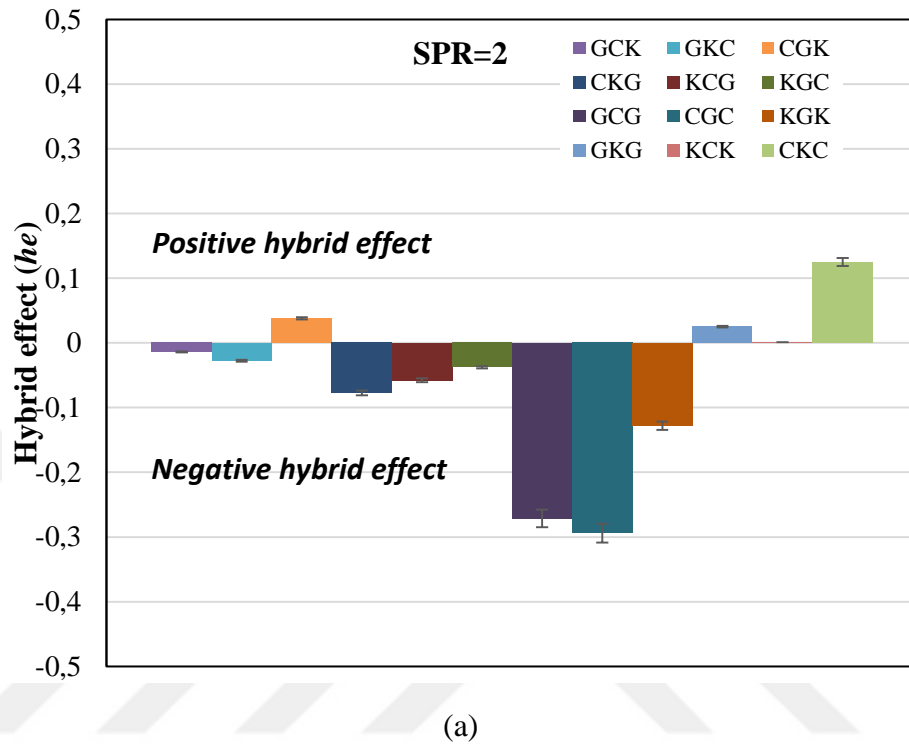

(a)

(b)

Figure 4.6 Hybrid effect variations of the samples by means of RoM. (a) SPR=2, (b) SPR=5

Table 4.4 Hybrid effect values for SPR=2

Hybrid sample	SPR=2	SPR=5
GCK	-0.014	-0.014
GKC	-0.028	-0.028
CGK	0.038	0.038
CKG	-0.077	-0.077
KCG	-0.058	-0.058
KGC	-0.038	-0.038
GCG	-0.271	-0.271
CGC	-0.294	-0.294
KGK	-0.128	-0.157
GKG	0.025	-0.117
KCK	0.001	0.096
CKC	0.125	0.124
E_{RoM} (J)	**75.17**	**92.89**

CHAPTER 5

RESULTS AND DISCUSSIONS FOR QSI EXPERIMENTS

5.1 Double Fiber Configurations

Figure 5.1 illustrates the load-displacement behavior of the hybrid samples with double configurations. It is clear that all curves behaved similar trend in terms of indentation load. Initially, load increases linearly up to the first load drop (knee point). In this section, laminates dominantly exposed to elastic bending under the out of plane loads by indenter. In particular, tensile properties of the fibers placed on the backside of the samples were displayed an important role for enhancement of maximum load.

In the second section named as damages section, initiation of delamination resulted the reduction in stiffness of the laminates. In this section, multiple load drops due to fiber ruptures may be observed up to the maximum load reached. In the last section, complete perforation and penetration events were then followed in the composite samples. Jeng et al. [131] showed the damage sequence within the composite laminates, indicating that load carrying capacity was considerably decreased in the damaged section after the first load drop.

The area under the load-displacement curve yields the absorbed energy during the indentation process and this area was directly obtained from the tensile test machine. Absorbed energy values (E) and corresponding maximum indentation forces (F_{max}) with displacements were presented in Table 5.1. It is observed from Table 5.1 that the sample of CC showed the maximum indentation force when compared with samples of KK and GG. The variations of absorbed energy and indentation forces of the hybrid samples were distributed between results of GG and CC except hybrid sample of CK. It is also observed that indentation force and absorbed energy values of full carbon/epoxy were greater than sample of full Kevlar epoxy by about 9.5 % and 15 %, respectively. When hybrid combinations were compared, hybrid samples of CK and

KC showed the maximum force and absorbed energy under the indentation force and constant punch displacement. This can be explained by the position of Kevlar and carbon fibers, which are placed on outer layers, resulting in better tensile strength and energy absorption capacity compared with glass fibers.
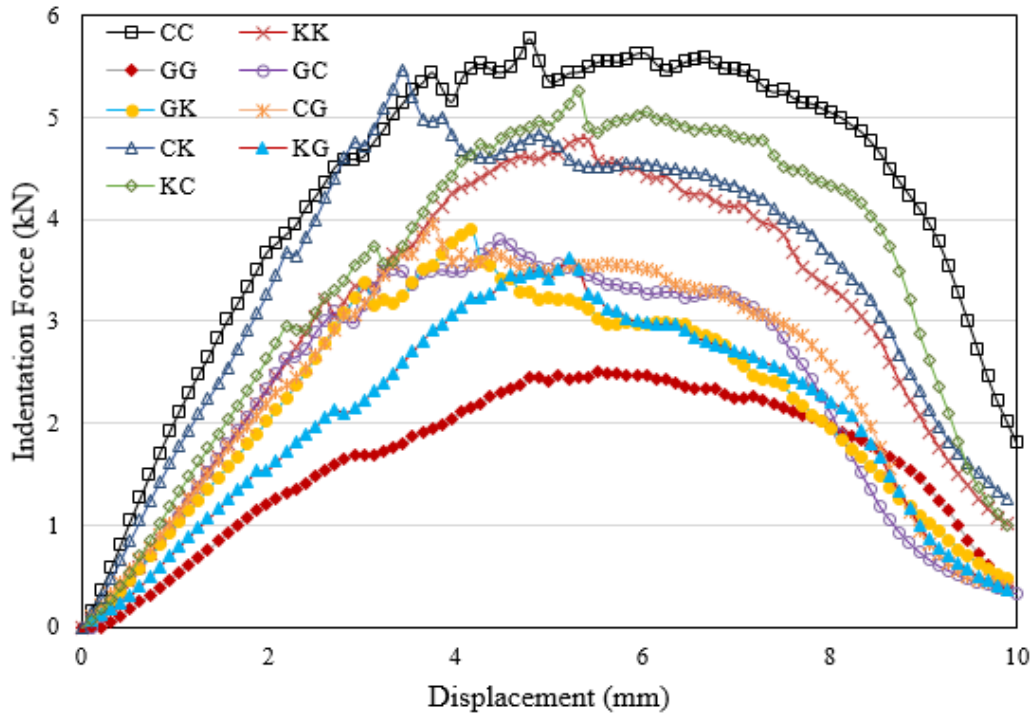

Figure 5.1 Indentation load to displacement curves for double fiber configurations

Table 5.1 Indentation results for double fiber configurations

Sample	F_{max} (kN)	E(J)	Max. disp. at max load (mm)
CC	5.67±1.67	38.24±2.24	4.80±0.11
KK	5.13±1.25	32.40±2.86	4.79±0.16
GG	2.66±0.92	16.95±2.21	5.57±0.19
GC	3.87±0.84	24.42±1.15	4.54±0.22
GK	3.85±0.59	22.91±2.11	4.12±0.15
CG	3.99±0.68	25.63±2.29	3.80±0.21
CK	5.91±0.91	35.15±1.28	3.48±0.27
KG	3.70±0.67	21.29±1.66	5.25±0.26
KC	5.34±0.88	34.12±2.01	5.36±0.12

Based on results, several researchers [102, 134-135] found that the influence of fiber fabric ply position played an important role on impact resistance of hybrid composite laminates. It is indicated that the fibers placed in the outer skin of the laminates played an important role for load carrying, failure mechanism and energy absorption capacity associated with impact resistance.

When glass layers were placed at indented side, the replacement of carbon fibers with Kevlar fibers at the rear side of the laminate did not cause a significant effect on indentation force and absorbed energy. The maximum increase in indentation force and absorbed energy was observed by about 48 % and % 40 respectively when carbon fibers were located at the indented side while replacing glass fibers with Kevlar fibers.
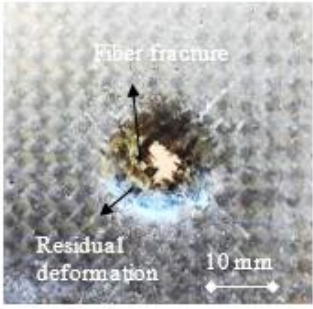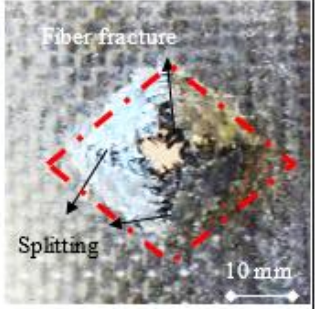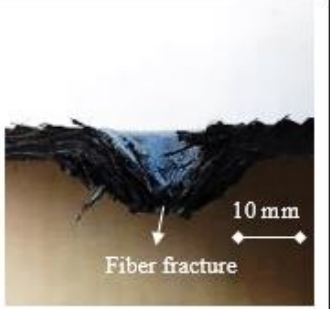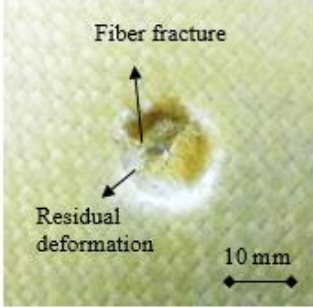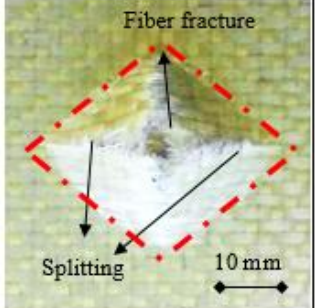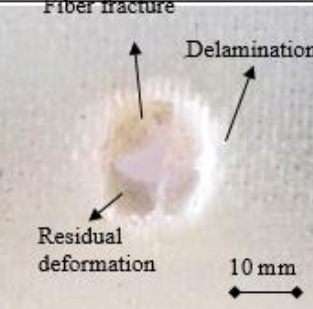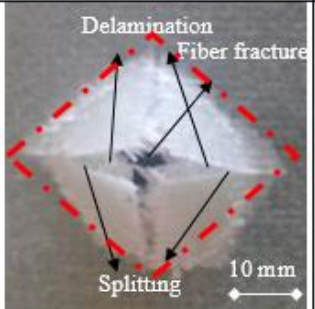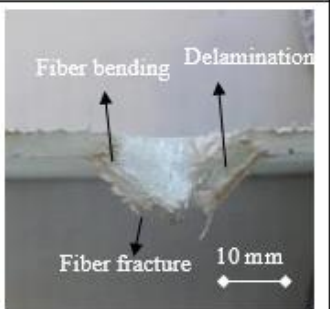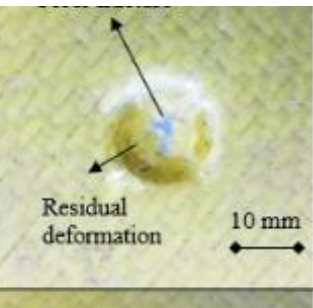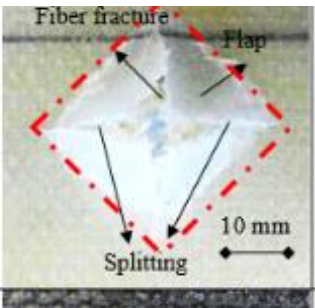
The sample of GG showed the lowest absorbed energy, having 47.6 % and 55.6 % lower values than samples of KK and CC, respectively. Sample of CK exhibited the highest indentation force as compared with other hybrid and full composites, while showing 8.7 % lower absorbed energy compared with sample of CC. This can be attributed to the synergistic effects between produced hybrid samples [136-137]. Synergistic effect can be explained that any interacting two or more materials produce an effect that are greater than sum of their constituent's effects.

One should be also noted that the change of the fiber position in the laminate did not significantly affect the indentation behavior of the samples. In general, the maximum load and absorbed energy values of the hybrid samples were recorded in similar and nearly same except the samples of KC and CK.
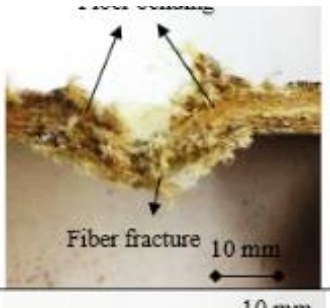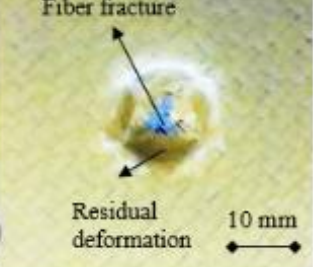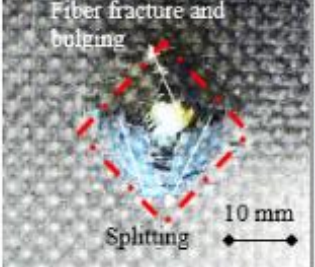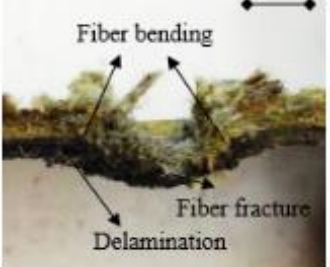
The failure mechanisms of the hybrid composite samples reinforced with two different fibers were visualized by observing indented and non-indented sides. In addition, the specimen was half sectioned in order to visualize the damage sequence in the lateral side of the samples. Findings of these observations are presented in Table 5.2.

As a result of these observations, load increases up to the first load drop by the matrix cracking only, then delamination between layers and initiation of fiber breakages were followed, finally friction and perforation were followed after the abrupt load drop at maximum load. In friction section, fiber splitting and bulging can be clearly seen at the rear side of the samples.

Table 5.2 Front and rear side views of the samples after the indentation tests (For double fiber configurations)
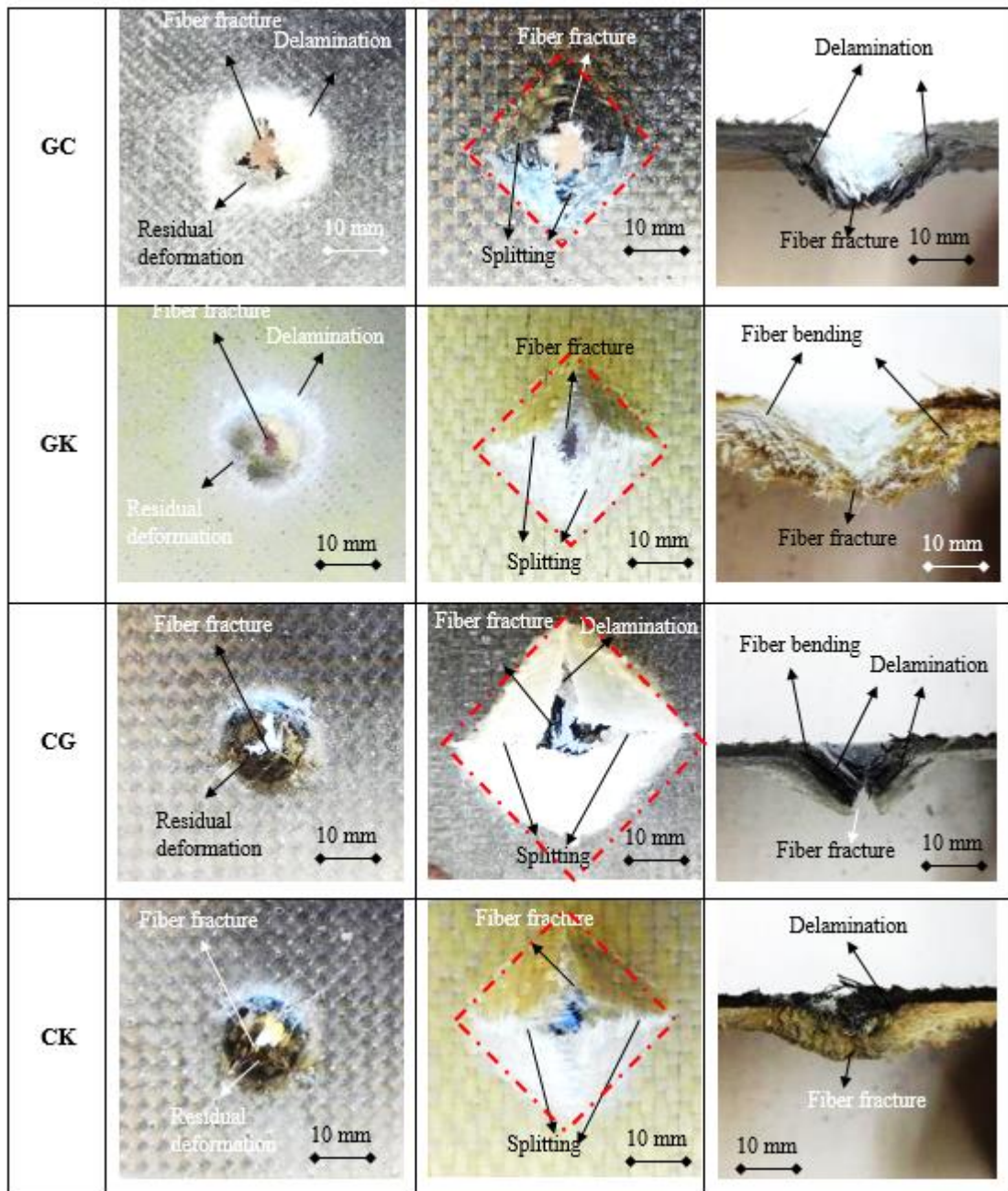
The reduction of specimen stiffness has resulted the delamination initiation and delamination propagation. It is revealed that the position of fibers designed rear side of the laminates played an important role for damage mechanism of the samples. For instance, if the rear and outer side of the samples were stacked as the glass fibers, the degree and growth of the failures were clearly higher than other surfaces (Kevlar and carbon). This effect was attributed to lower stiffness and brittle nature of glass fiber. However, the carbon and Kevlar fiber surfaces at the rear sides showed the relatively lower amount of damage in terms of splitting and delamination compared with glass

fiber surfaces. This can be attributed by the fact that high tensile strength of carbon and good toughness and tensile properties of Kevlar fibers showing better impact resistance and damage tolerances.

5.2 Triple Fiber Configurations

Figure 5.2 shows the indentation load to displacement behavior of the hybrid composites reinforced with three different fibers. For triple fiber configurations, absorbed energy values and corresponding maximum indentation forces with displacements were presented in Table 5.3. As compared with the sample of GG, the sample of CC showed the 53 % and 55 % higher values in terms of indentation force and absorbed energy, respectively.

As shown in Figure 5.2, , similar indentation force- displacement curves were obtained for triple fiber configurations as compared with those of double fiber configurations. It can be ensured that the incorporation of the third fiber as an interphase material provided the more smooth curves with balanced load and absorbed energy showing lower divergence between two another fibers. The damage mechanisms of the samples showed that severe fiber breakages and delaminations at the exterior layers were observed depending on the fibers placed at the rear side, significantly effecting the energy dissipation properties in the composite samples.

From Table 5.3, for triple fiber configurations, hybrid samples showed a similar indentation force responses and results were distributed between the samples of GG and CC. In hybrid samples, GKC hybrid configuration provided the highest absorbed energy and load carrying capacity compared with others, showing an increase of maximum indentation force and absorbed energy by about 75 % according to sample of GG. This can be attributed the position of carbon fibers having high tensile strength and elastic properties which is placed in the tension side. The replacement of the fibers caused approximately ±12% deviations by means of absorbed energy, while the indentation force deviations were about ±12%.

When glass surface at indented side, the replacement of carbon fiber with Kevlar fiber caused an increase in indentation load and absorbed energy about 8.8 % and 10 %, respectively. When Kevlar surface at indented side, the replacement of glass fiber with

carbon fiber resulted in decrease of indentation load and absorbed energy by about 10.9 % and % 5.5, respectively.
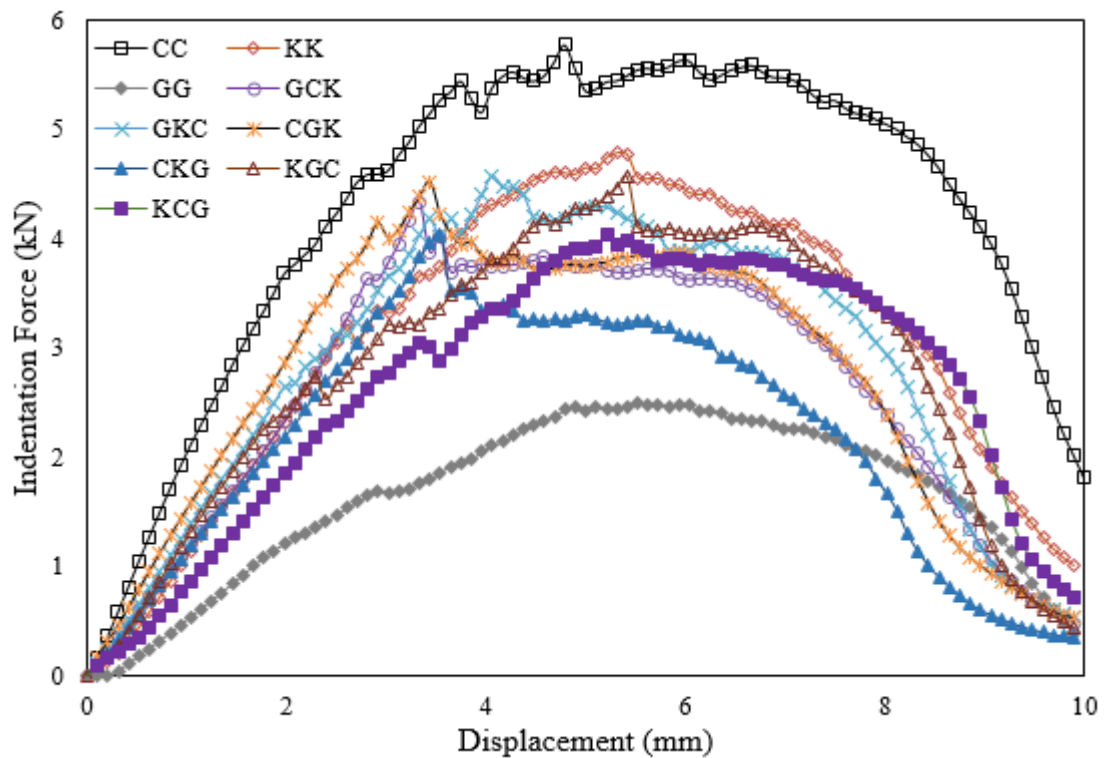
Figure 5.2 Indentation load to displacement curves for triple fiber configurations
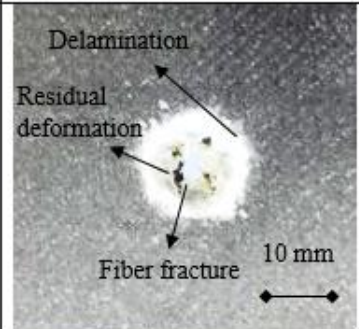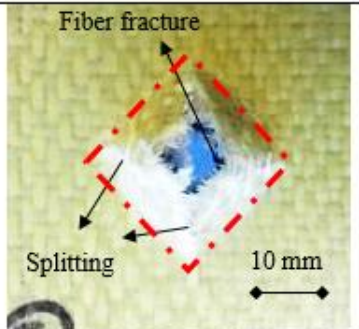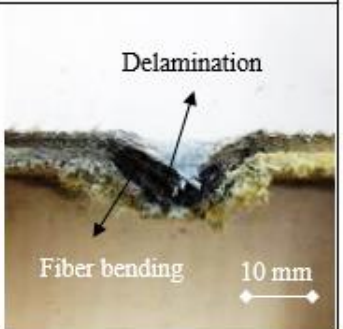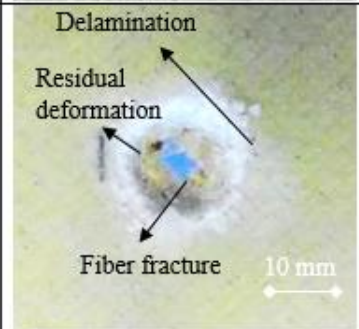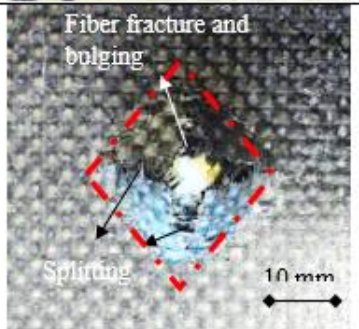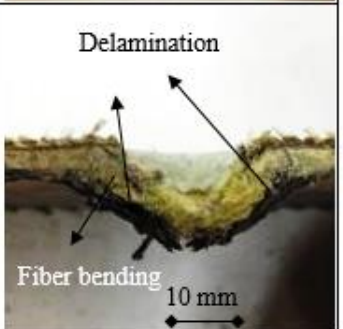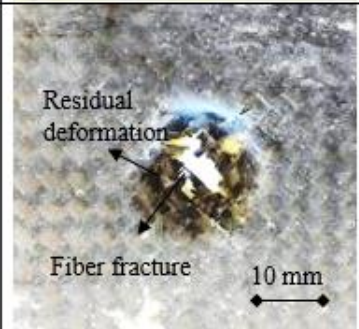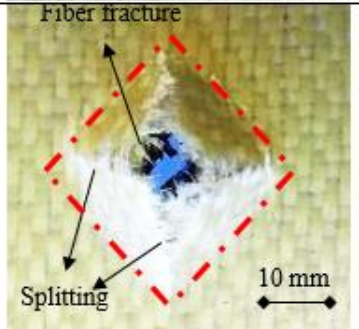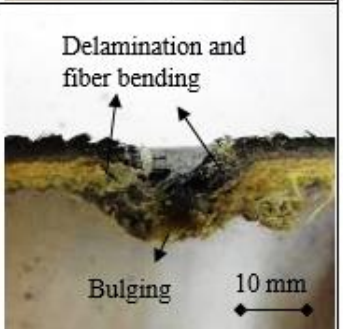
Table 5.3 Indentation results for triple fiber configurations

Sample	F_{max} (kN)	E(J)	Max. disp. at max load (mm)
CC	5.67±0.02	38.24±3.13	4.80±0.12
KK	5.13±0.24	32.40±1.72	4.79±0.14
GG	2.66±0.12	16.95±0.53	5.57±0.19
GCK	4.28±0.17	26.31±0.44	3.41±0.15
GKC	4.66±0.07	28.92±0.85	4.08±0.11
CGK	4.27±0.18	26.80±0.77	3.44±0.10
CKG	4.30±0.19	22.24±0.52	3.54±0.09
KGC	4.57±0.01	26.96±0.62	5.42±0.17
KCG	4.07±0.01	25.48±1.34	5.25±0.18

However, no reasonable variations in indentation force were observed in the case of carbon layers placed at indented side while replacing glass and Kevlar fibers. It is noted from here that flexural properties and stacking sequence of the fibers are the major parameters, which are effecting the load-deflection and energy absorption capacity of the hybrid composites [125, 130]. Meanwhile, the residual dent depth after QSI tests indicated that the sample of KCG revealed the highest value compared with others.

Failure and fractured surfaces on the front, back and cross sections of the samples were visualized in order to observe the extension and development of damage event as presented in Table 5.4.

Table 5.4 Damaged sections of the samples (For triple fiber configurations)
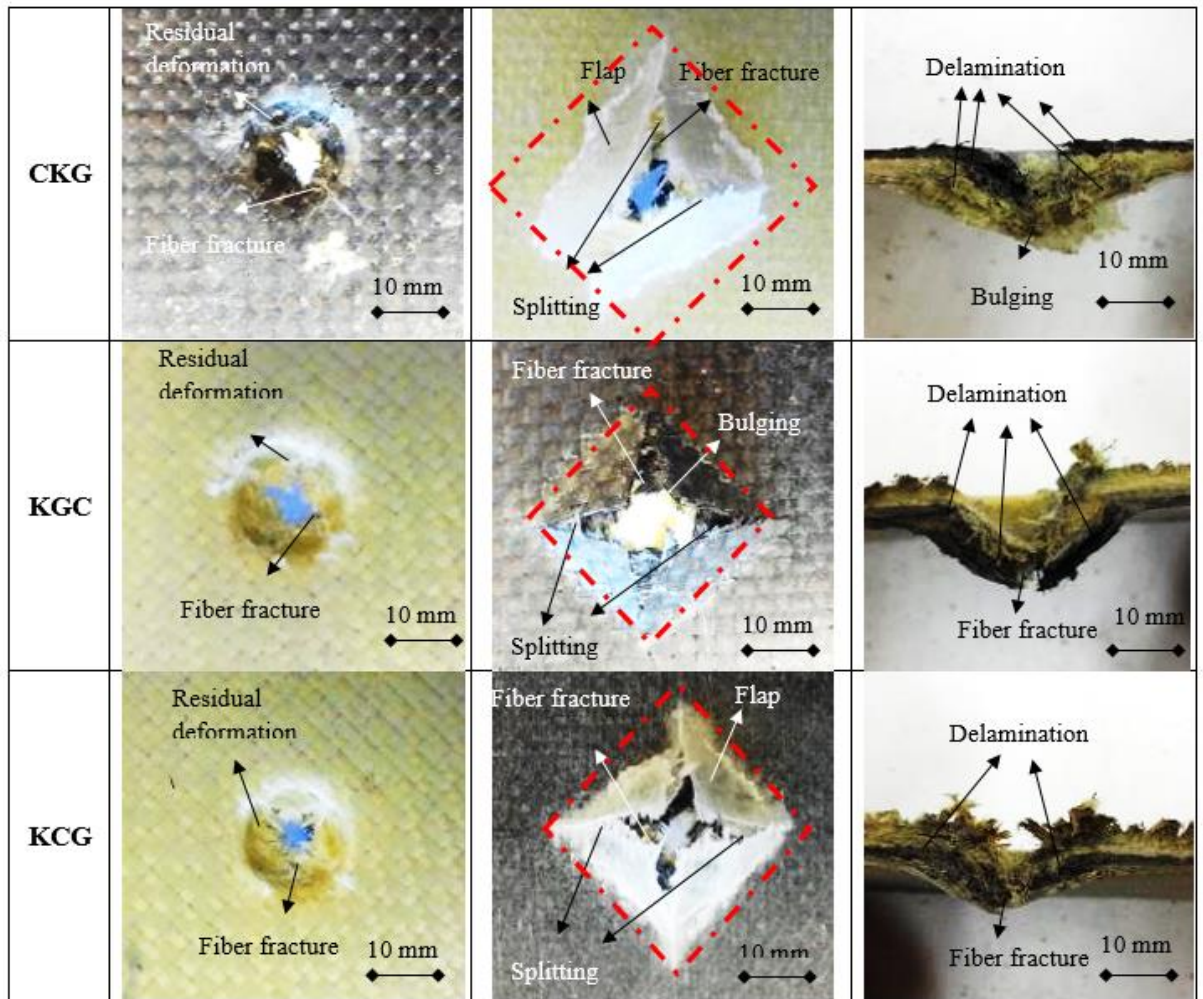
It is clear from Table 5.4 that the S-glass fiber face sheets placed in the rear sides showed the maximum amount of delamination resulting in long tail of fiber splittings along fiber directions as compared with carbon and Kevlar face sheets, while carbon fiber face sheets at the rear sides exhibited the lowest amount of delaminations. In particular, delamination and splittings on the rear surfaces of the Kevlar face sheets were lowest compared with others. This is explained by the mechanical properties and position of fibers in the lamina. For example, glass fibers showed a brittle nature and lower tensile strength due to bending effect, while Kevlar fibers showed the lowest flexural strength with highest deformation and carbon fibers exhibited the highest tensile strength and energy absorption capacity. In addition, matrix cracking, fiber-matrix debonding and the fractured fibers near the localized area were clearly observed failure mechanisms by scanning electroscope machine (SEM) as shown in Figure 5.3.
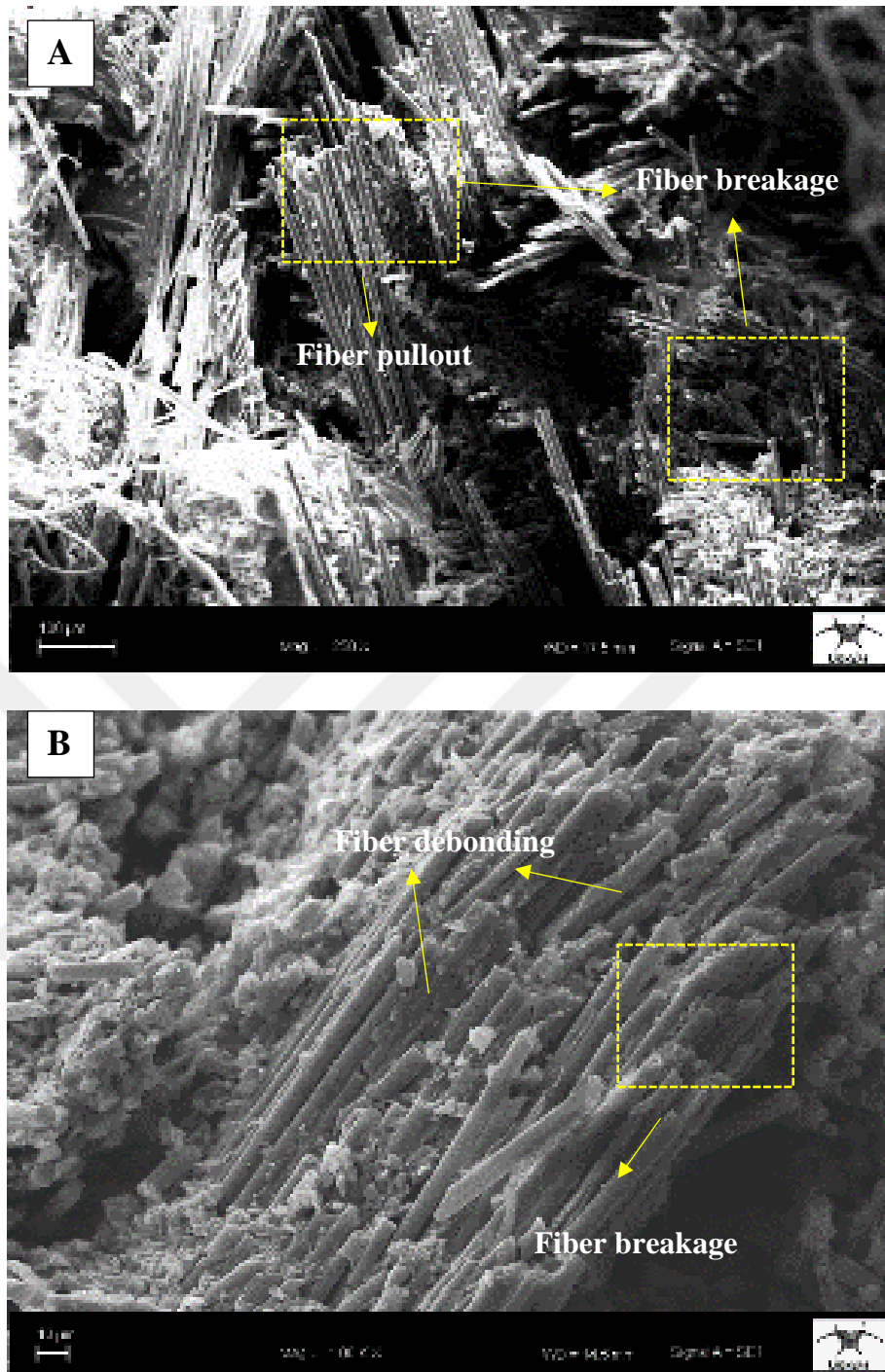
Figure 5.3 SEM image of hybrid sample CK near the fracture area. (a) 250X, (b) 1000X

The values of hybrid effect were presented in Table 5.5 and Table 5.6, and their variations were illustrated as shown in Figure 5.4. The results from Table 5.5 and Figure 5.4 (a) showed that the CK and KC revealed the positive hybrid effect for indentation load and absorbed energy, while the KG showed the maximum negative hybridization effects.

When triple fiber configurations were compared from Table 5.6 and Figure 4(b), GKC, and KGC configurations exhibited a positive hybrid effect, which is attributed the stacking sequence of the fibers in the lamina effecting the force and displacement behavior of the structure. When carbon fibers placed at the rear side and S-glass fibers placed at the front side, the carbon fibers restricted the global deformation of the laminate due to high tensile strength and stiffness of the carbon fibers resulting the enhancement of the load carrying and damage resistance capability of the laminate.

Table 5.5 Hybrid effect values for double fiber configurations

Hybrid sample	he(F)	he(E)
GC	-0.138	-0.164
GK	-0.143	-0.215
CG	-0.110	-0.122
CK	0.317	0.204
KG	-0.176	-0.271
KC	0.189	0.169
RoM	$F_{RoM}(kN)=4.49$	$E_{RoM}(J)=29.2$

Table 5.6 Hybrid effect values for triple fiber configurations

Hybrid sample	he(F)	he(E)
GCK	-0.046	-0.099
GKC	0.039	-0.009
CGK	-0.046	-0.082
CKG	-0.041	-0.238
KGC	0.017	-0.077
KCG	-0.093	-0.127
RoM	$F_{RoM}(kN)=4.49$	$E_{RoM}(J)=29.2$
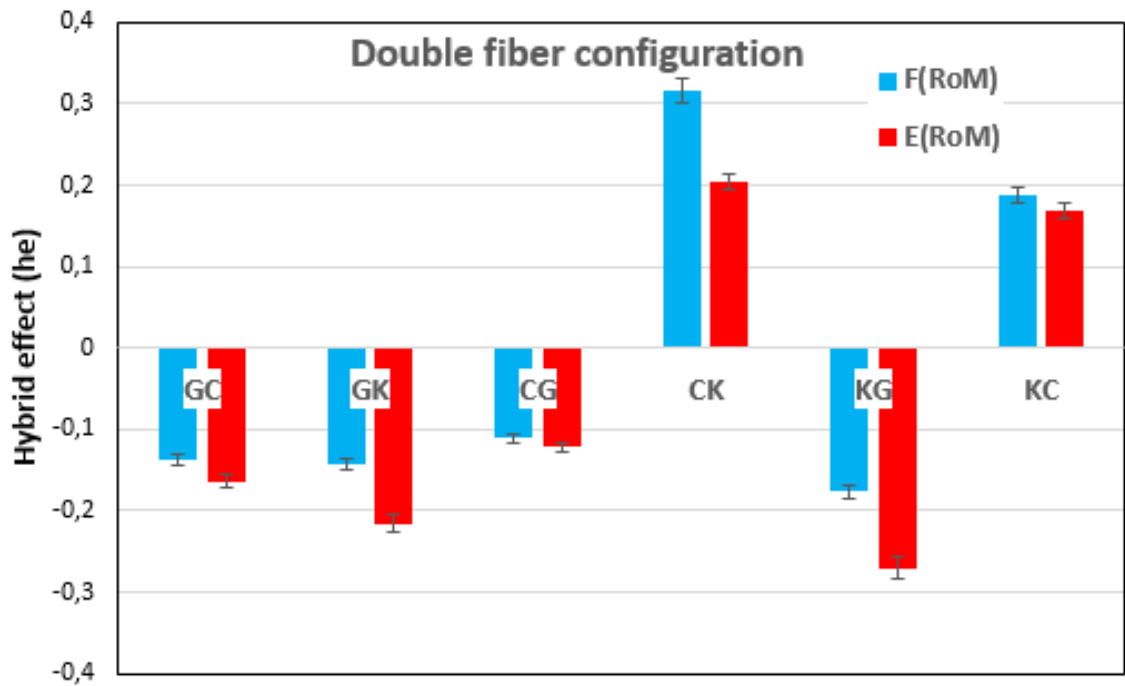
(a)
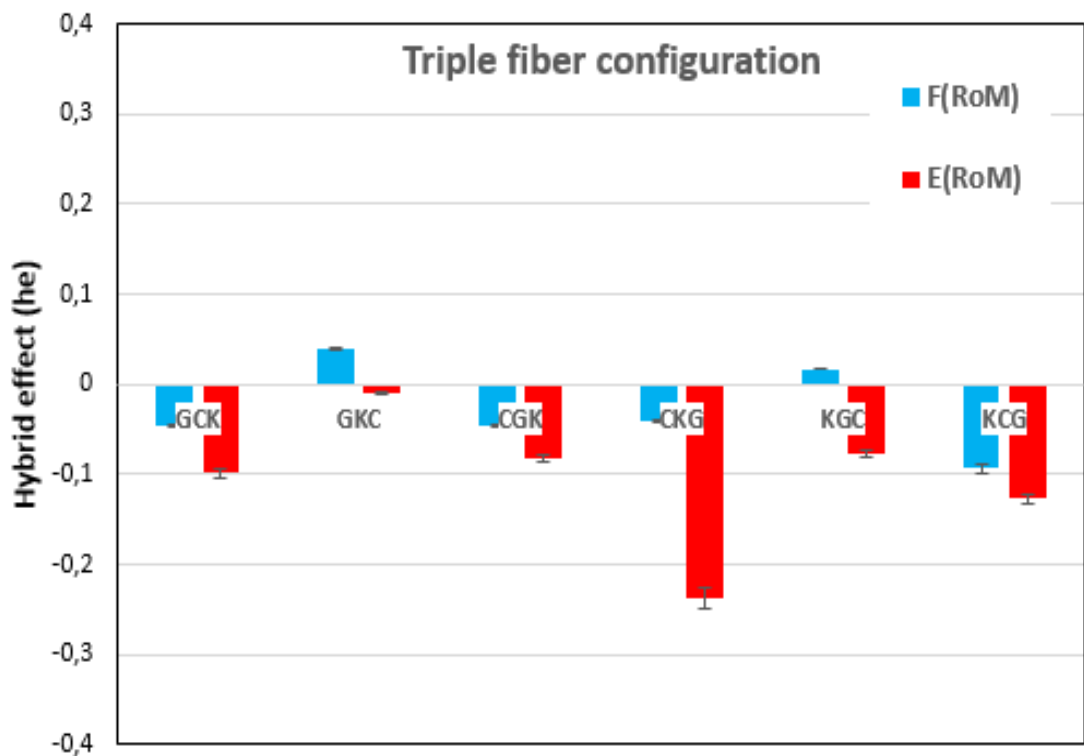
(b)

Figure 5.4 Variation relative indentation according to non-hybrid composite samples. (a) Indentation force, (b) Absorbed energy

CHAPTER 6

RESULTS AND DISCUSSIONS FOR LVI EXPERIMENTS

6.1 Introduction

In this section, the results of low velocity impact tests will be presented with discussions. Low velocity impact behavior of hybrid samples will be investigated showing hybridization effects in terms of laminate stacking sequence those influencing damage modes through the LVI process

The chapter has been divided into three parts according to fiber configurations, namely, full composites, double fiber configurations and triple fiber configurations. The impact behavior of laminated hybrid composites was evaluated by an instrumented drop weight impact machine at 15 and 30 J. The failure modes and corresponding to force-deflection behavior of the samples were presented by comparing front and rear side of the surface damages. Key important parameters like peak load, absorbed energy, and load-displacement were evaluated by using the data acquisition system. Stacking configuration effect was handled in terms of hybrid effect with reference to the rule of mixture.

6.2 Full Composite Samples

In order to compare impact behavior of hybrid samples, the behavior of full composites (glass/epoxy, carbon/epoxy, and Kevlar/epoxy) should be examined separately due to different rigidity and stiffness properties of fibers. For this reason, full laminate samples were tested initially, and then compared with hybrid samples. Figure 6.1 illustrates the force-time and force-displacement histories of the full composite samples and their maximum force and deformation values were presented in Table 6.1. The absorbed energy stored in the samples was evaluated under the load-displacement curves by using numerical integration method. The load-deflection histories of full composites showed the three situations at 30 J, namely, perforation with sample of GG, partial penetration and rebounding with sample of CC, and penetration with

86

sample of KK. However, all samples have shown the load recovery and rebound at 15 J (Figure 6.1 (b)).
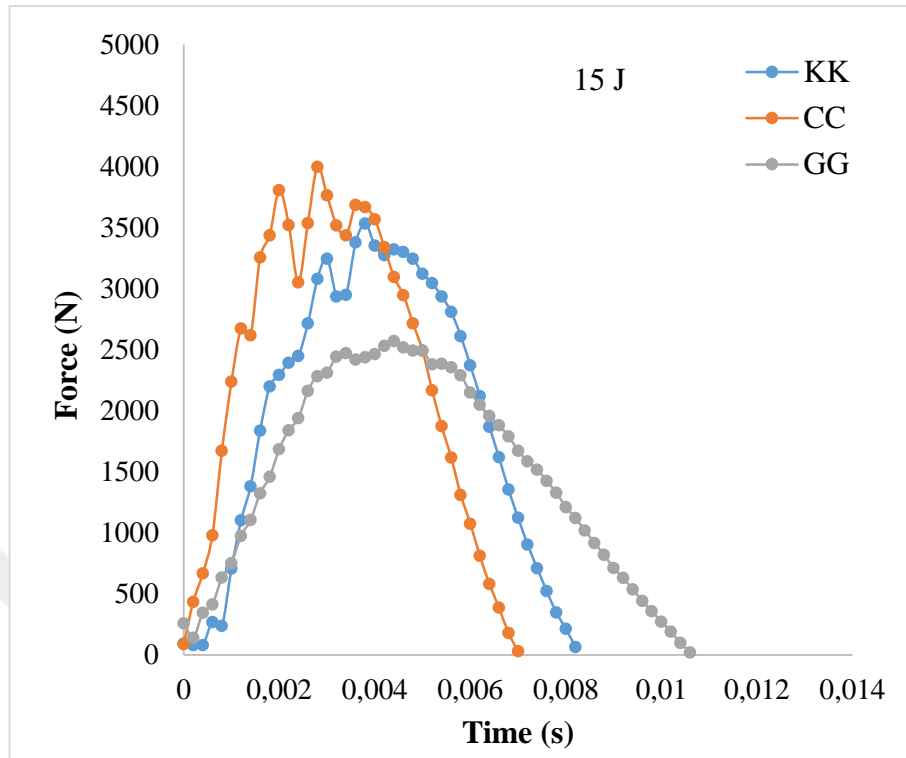
(a)
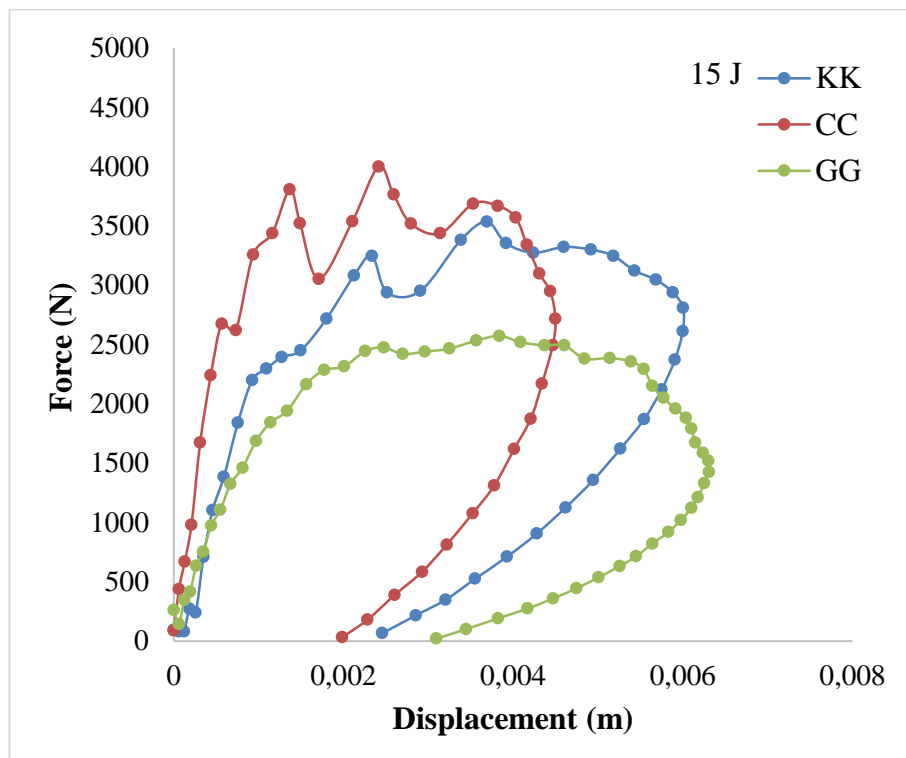
(b)
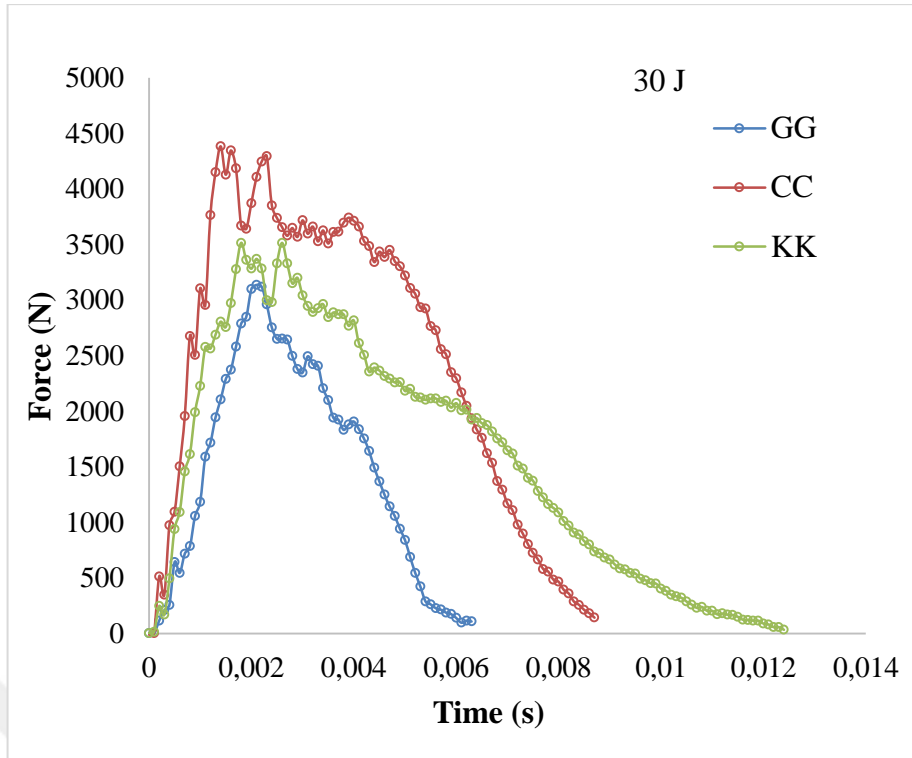
(c)
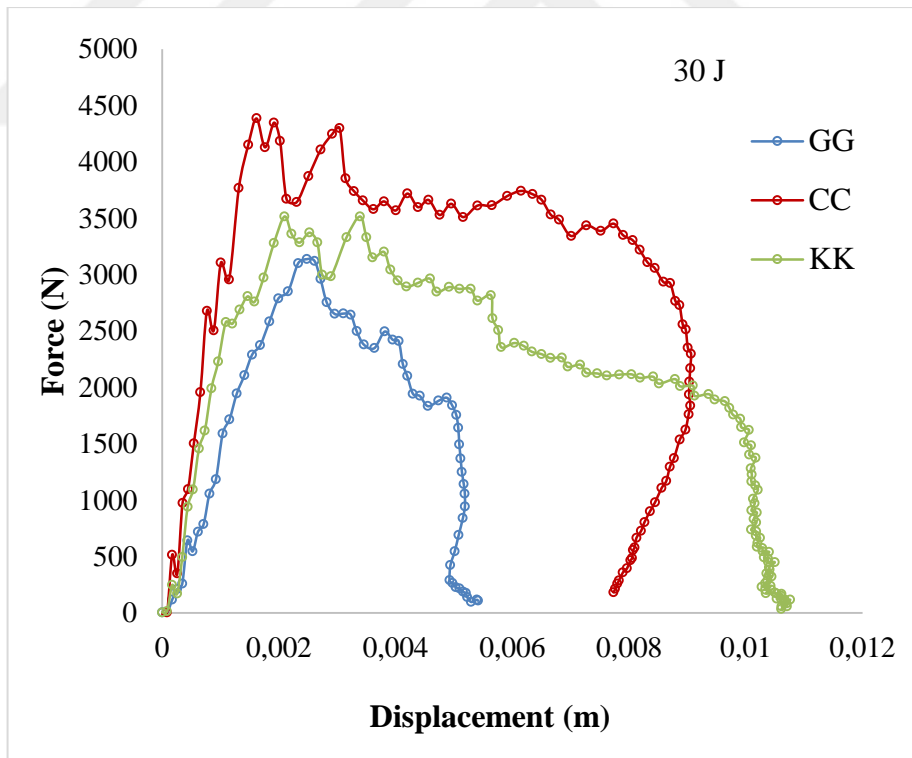
(d)

Figure 6.1 Force- deflection histories of the full composites. (a) Force-time at 15 J, (b) Force-displacement at 15 J, (c) Force-time at 30 J, (d) Force-displacement at 30 J

Table 6.1 Load and absorbed energy values of full composites

	Laminate	Fmax(KN)	Ea(J)	d(mm)
15 J	GG	2.57	7.8	3.1
	CC	3.99	8.6	1.9
	KK	3.53	9.6	2.4
30 J	GG	3.13	19.82	5.6
	CC	4.38	28.21	6.6
	KK	3.51	24.78	7.1

It is clear from Figure 6.1 and Table 6.1 that sample of GG showed the lowest impact strength by means of peak load and absorbed energy, resulting short tail of impactor displacement at 30 J. In addition, impact duration was occurred within the shorter time compared with samples of CC and KK. However, the trend of impact duration followed as: GG>KK>CC at 15 J. Damaged surfaces of the full composites are illustrated in Figure 6.2 at 15 and 30 J. When failure mechanisms in these samples are visualized as seen in Figure 6.2, the major failures were revealed as delamination, matrix cracking, multiple fiber ruptures. The sample of GG showed the complete perforation at 30 J and penetration at 15 J with a dramatic matrix cracking on the impacted surface. The sample of CC exhibited the highest impact resistance with rebounding of the impactor. Although peak load of CC is greater than sample of KK, the absorbed energy values of these samples were close to each other due to the high toughness of the Kevlar fibers resulting long tail of deformations under the impact loading. In contrast to sample of CC, KK exhibited the penetration failure after the impact showing the long splittings along the fiber directions at the rear side for both impact energies.
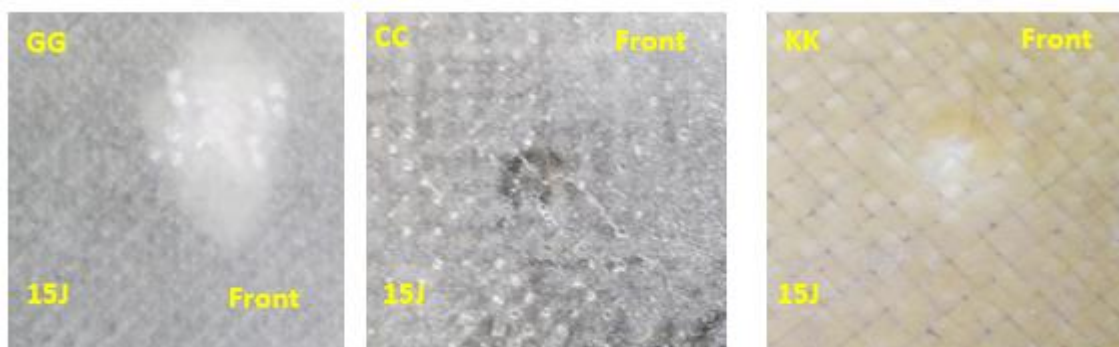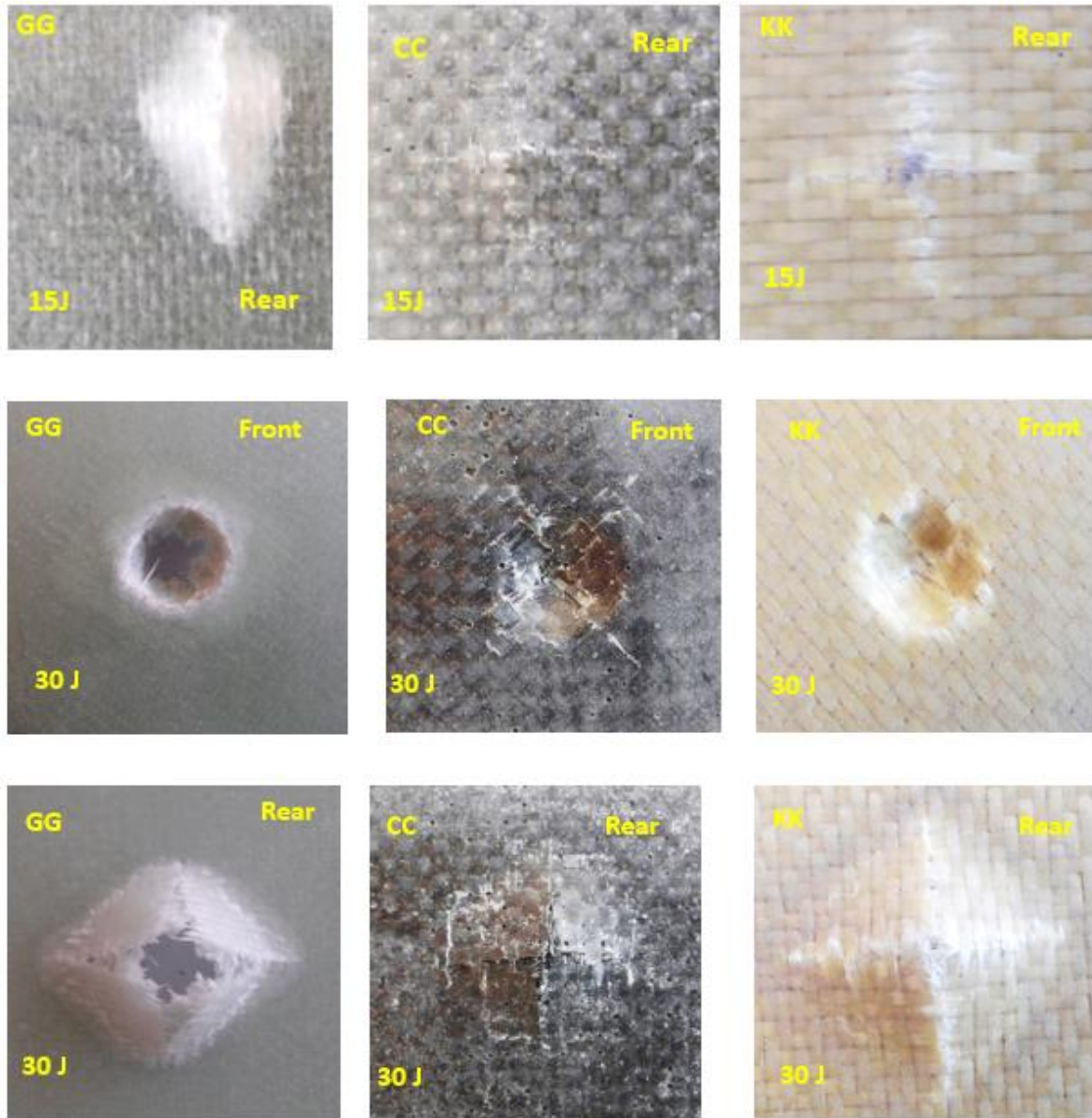
Figure 6.2 Failure surfaces of the full composites after the impact tests

6.3 Double Fiber Configurations

Typical load- time and load–displacement curves of the impact tests associated with the double fiber configurations are plotted in Figure 6.3 and their resulting peak load and overall absorbed energy values are presented in Table 6.2. It is clear from Figure 6.3 that all of the curves showed a similar and nonlinear behavior during the impact event. Initially, load increased up to the first load drop just before the peak load. In this region, the samples were subjected to elastic bending by the out of plane indenter load. In particular, tensile properties of the fibers placed on the backside of the samples were displayed an important role for enhancement of maximum load. After the first

90

load drop, the formation of damage was followed by delamination and matrix cracking until the maximum load has reached, and followed by the complete penetration and perforation of the samples. Similarly, Jeng et al. [131] asserted that the damage progress started by matrix cracking followed by an abrupt delamination, and resulted in a considerable decrease of load carrying capacity.

Force-time histories were compared as seen in Figure 6.3. All curves of the samples nearly exhibited the same behavior up to peak load, and then followed the decreasing trend resulting final failure of the structure with a constant value. The fracture surfaces of the samples were illustrated as shown in Figure 6.4.

At impact energy of 30 J, it is clear that samples of GK, GC, and CG exceeded the perforation limit showing long tail of impactor displacement, while samples of KC, KG, and CK were in the penetration threshold after the impact tests. At impact energy of 15 J, samples have shown the indentation resulting a residual deformation at the impacted side.
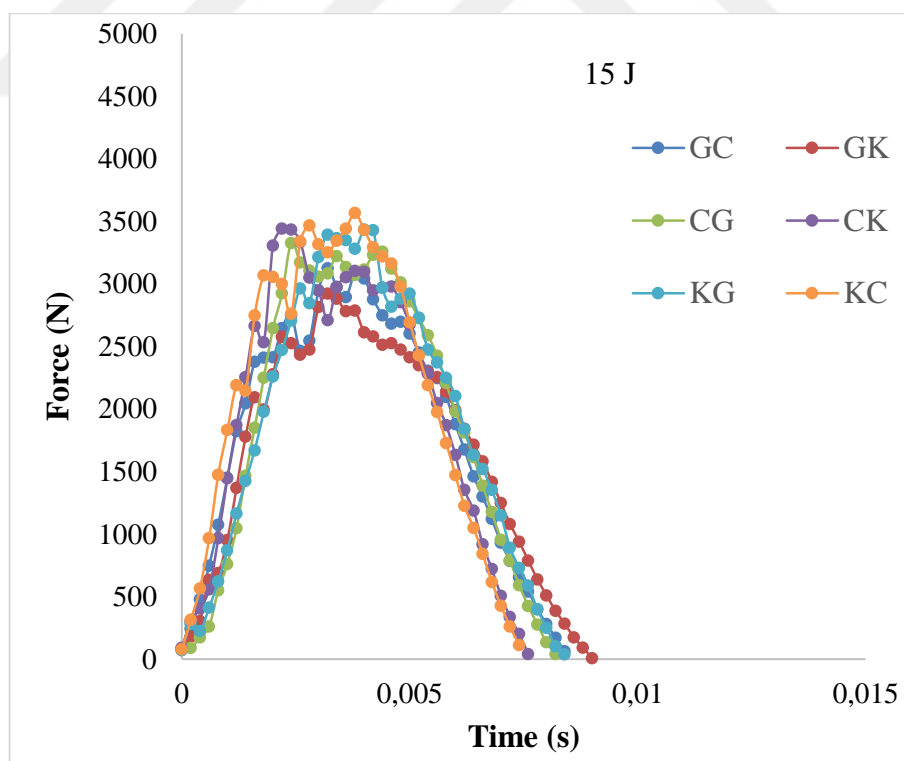
(a)
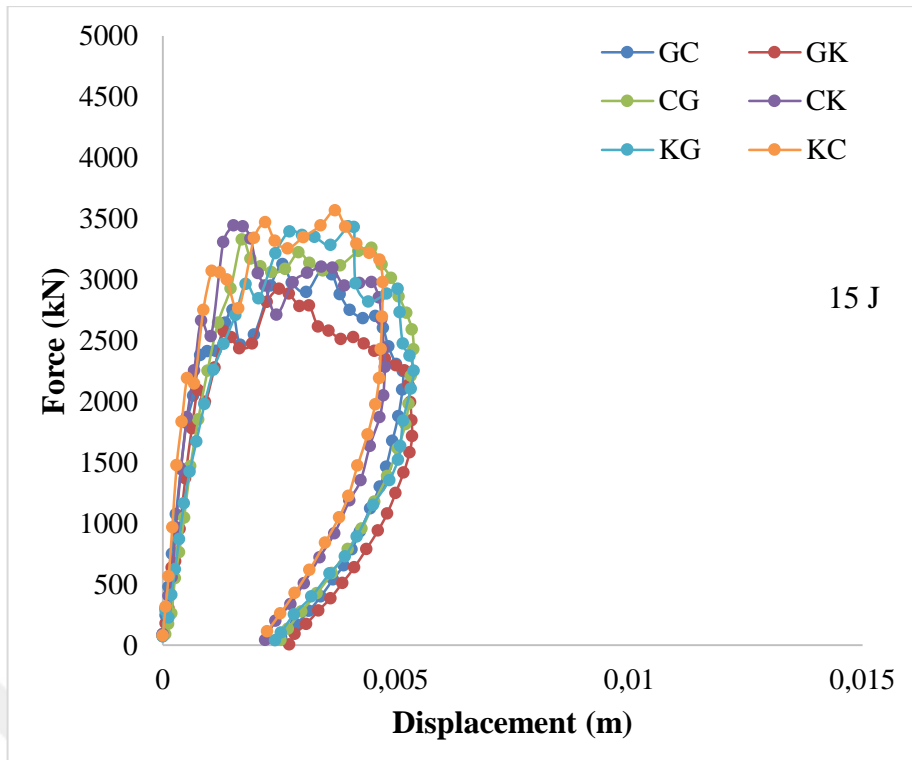
(b)
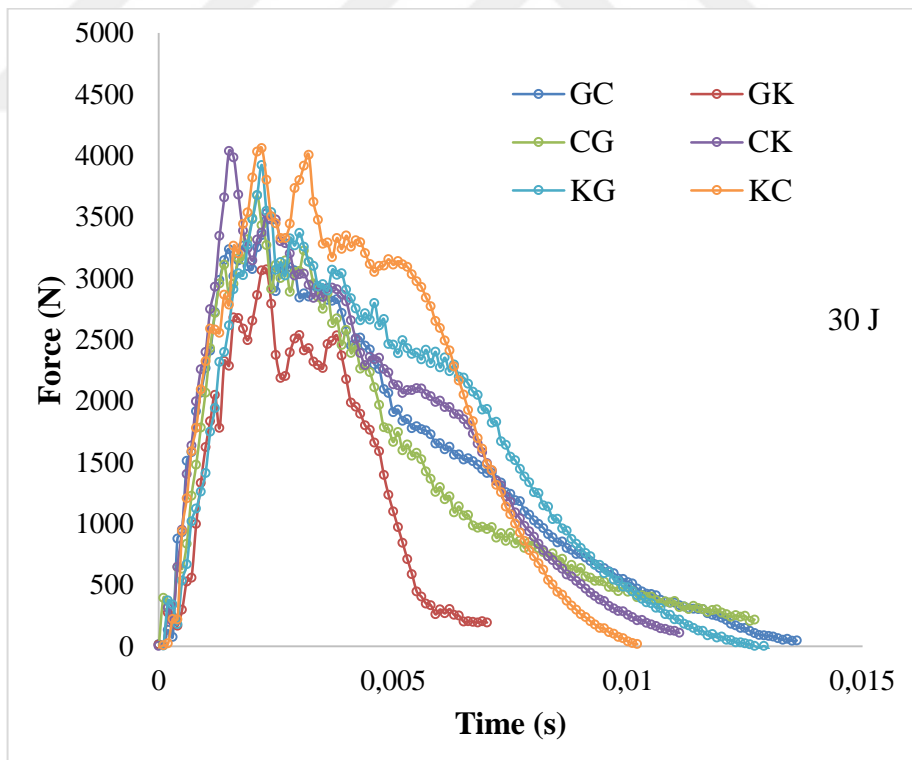
(c)

(d)

Figure 6.3 Force histories of the double fiber configurations. (a) Force-time at 15 J, (b) Force-displacement at 15 J, (a) Force-time at 30 J, (b) Force-displacement at 30 J

Table 6.2 Load and absorbed energy values of double fiber configurations for double fiber configurations

	Laminate	Fmax(kN)	Ea(J)	d(mm)
15 J	GC	3.12	7.81	2.5
	GK	2.92	7.52	2.6
	CG	3.32	7.96	2.2
	CK	3.44	8.29	2.3
	KG	3.43	7.98	2.4
	KC	3.56	9.6	2.5
30 J	GC	3.47	22.91	11.40
	GK	3.07	19.85	6.22
	CG	3.67	23.17	12.35
	CK	4.03	25.15	9.75
	KG	3.92	27.04	10.45
	KC	4.06	28.15	8.61

For double configurations as shown in Figure 6.3 and Figure 6.4, the impact performance of the KC was greater than those of other samples at 15 and 30 J, showing the lower fiber splitting and breakage at rear side. The results also revealed that the impact surface and rear side of fibers played a significant role for both impact and damage mechanism of the hybrid samples. For example, when glass layers were placed at rear side, the replacement of glass fibers with Kevlar fibers caused a significant delamination and fiber splittings with a final penetration of the laminate. However, the replacement of the Kevlar fiber with glass fiber (glass at impacted surface and Kevlar at non-impacted surface) resulted poor impact resistance, which is attributed by the position of fibers in the lamina, indicating the different deflection and flexural sensitivity during the impact event [130].
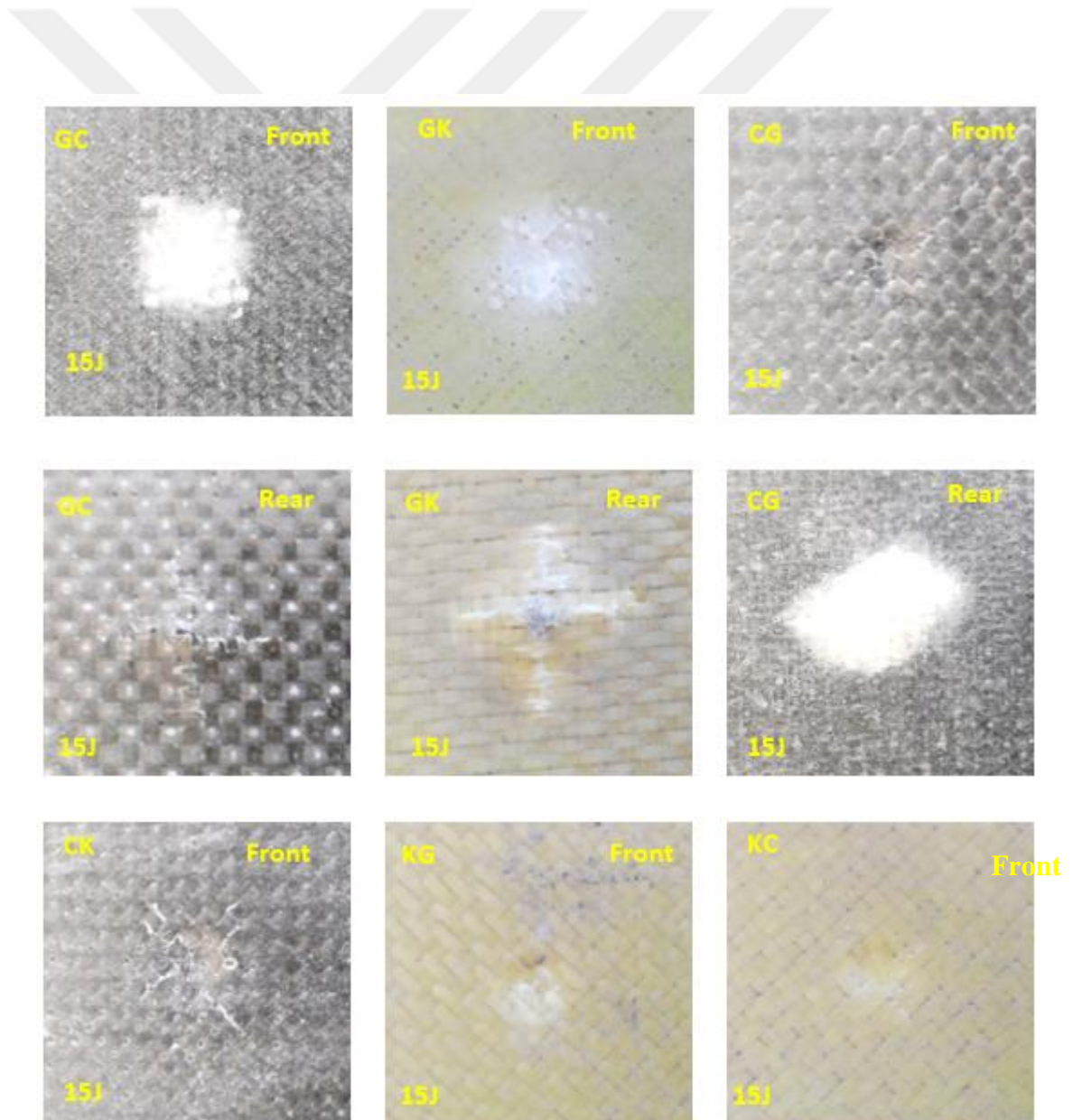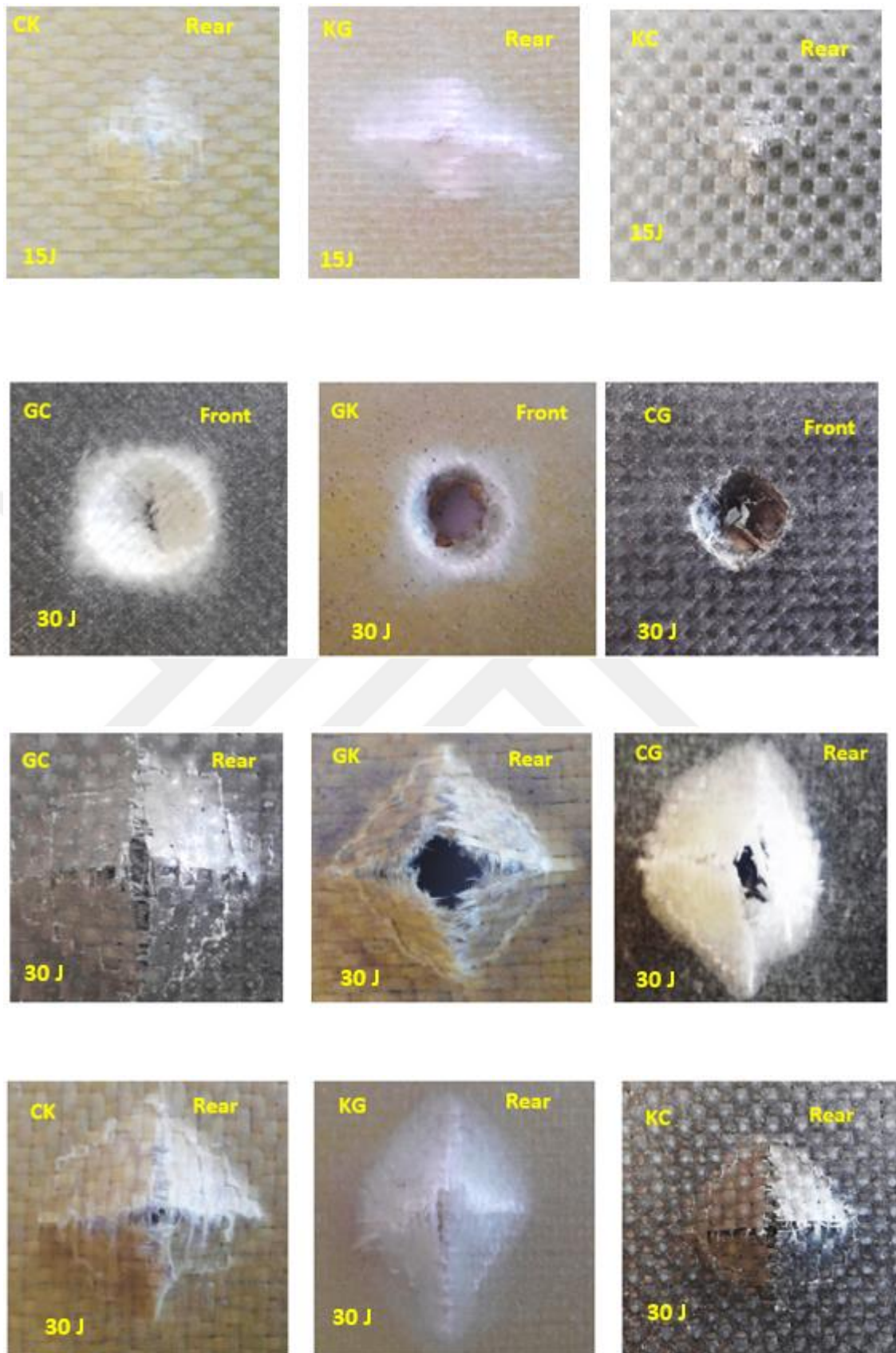
Figure 6.4 Failure surfaces of the double fiber configurations after the impact tests

6.4 Triple Fiber Configurations

Figure 6.5 illustrates the load-time and deflection histories for triple fiber configurations during the impact tests and their peak load and entire absorbed energy values are presented in Table 6.3. The corresponding failure surfaces are provided in Figure 6.6. To obtain further insight for stacking sequence effects, it may be useful to incorporate third fiber, which balances between two different fibers, and showing the advantages in terms of damage mechanisms in the hybrid samples. The results suggested that incorporation of third fiber revealed the similar damage mechanisms and load histories in the samples. The sample of KCG showed the highest peak load. However, sample of GKC showed the higher absorbed energy compared with other samples. This means that hybrid sample behaves different impact resistance and failure modes when they are designed as asymmetric structure. It is also noted that sample of CKG has the lowest peak load and absorbed energy. This is attributed the poor tensile properties of glass fibers placed at rear side and brittle nature of carbon fibers subjected to compressive loads created by impactor. Several researchers [125-129] indicated that the flexural strength was increased when glass layers were placed on the outer surfaces for carbon/glass hybrid configurations, and it is confirmed by triple fiber combinations between GCK and GKC.
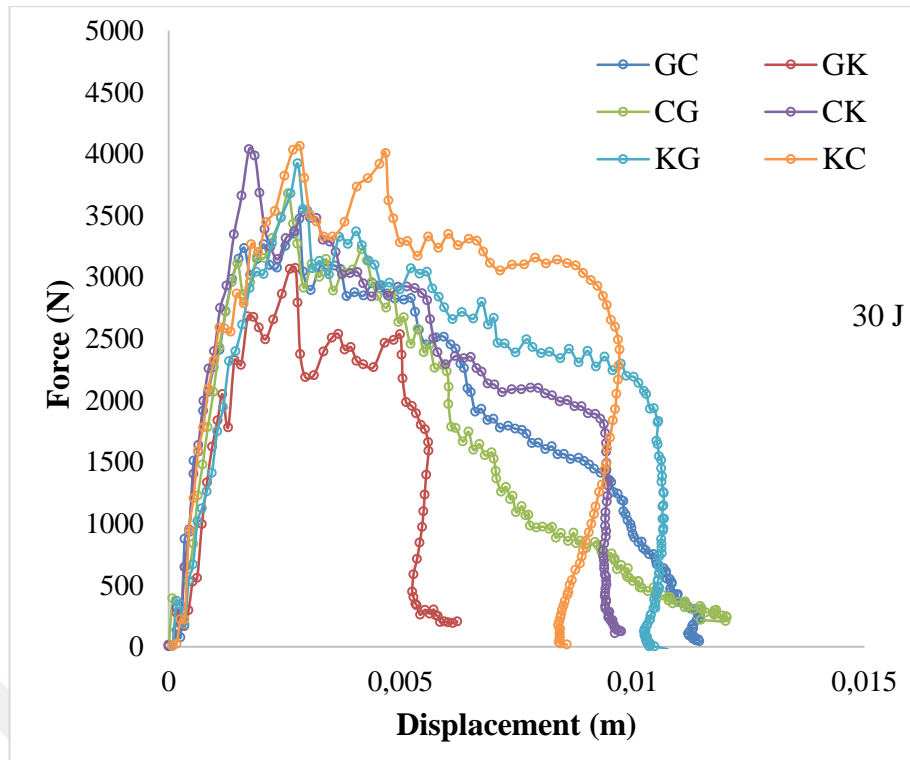

(a)

96
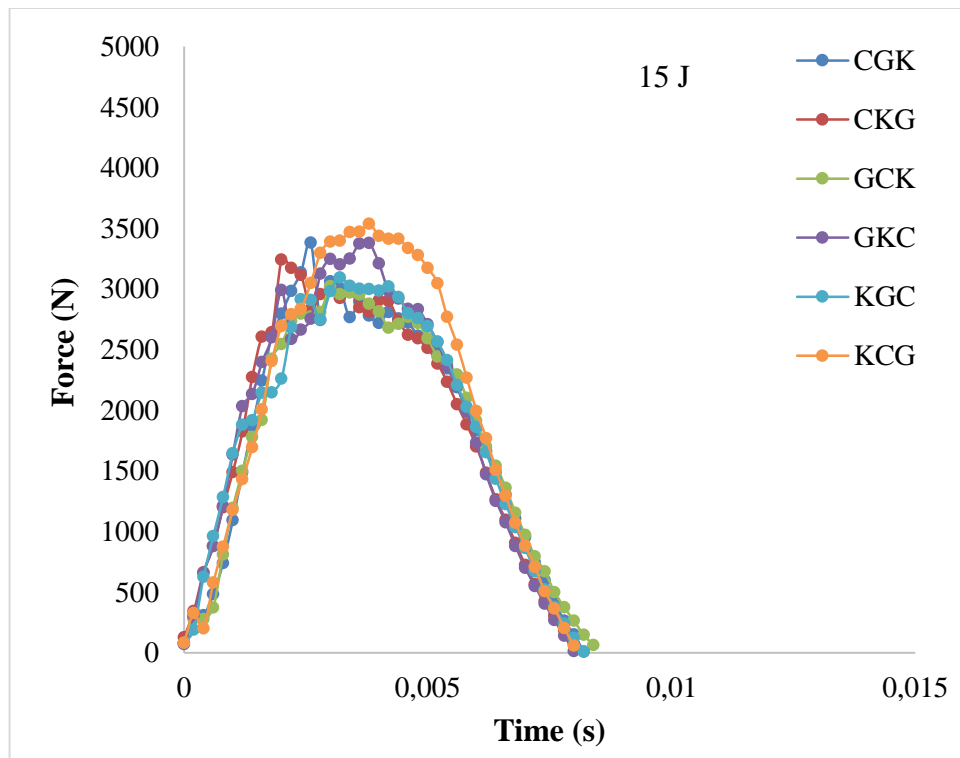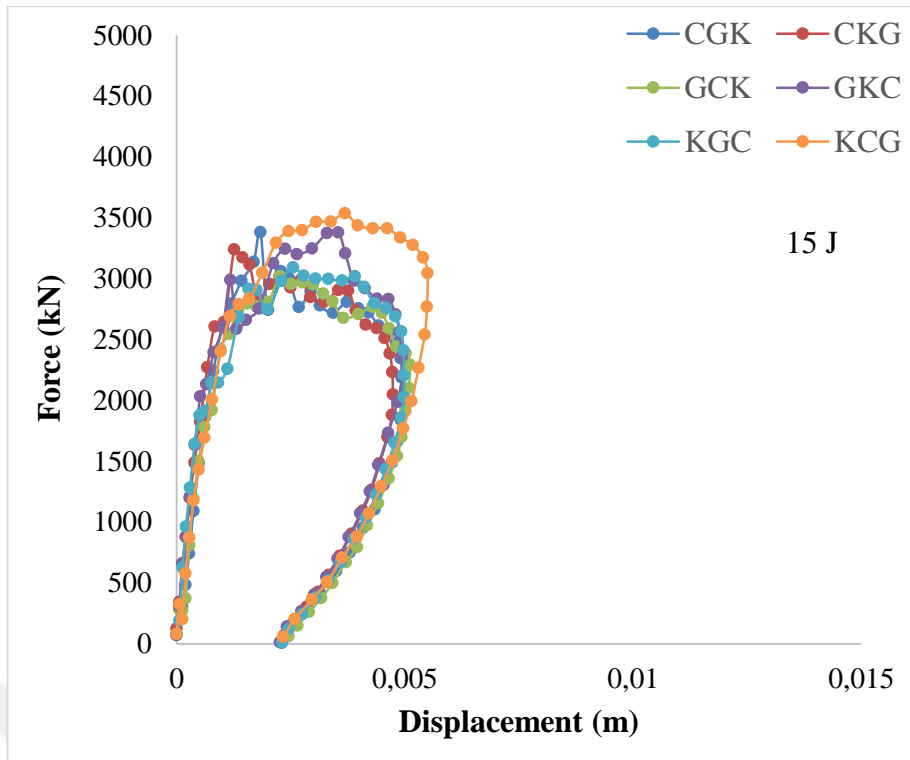
(b)
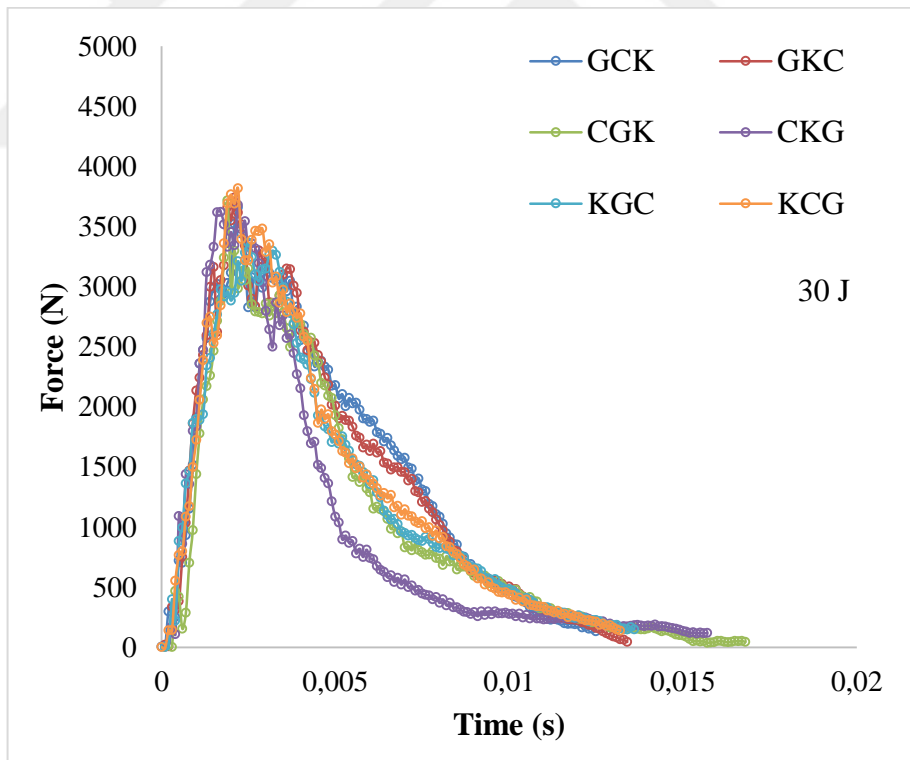
(c)
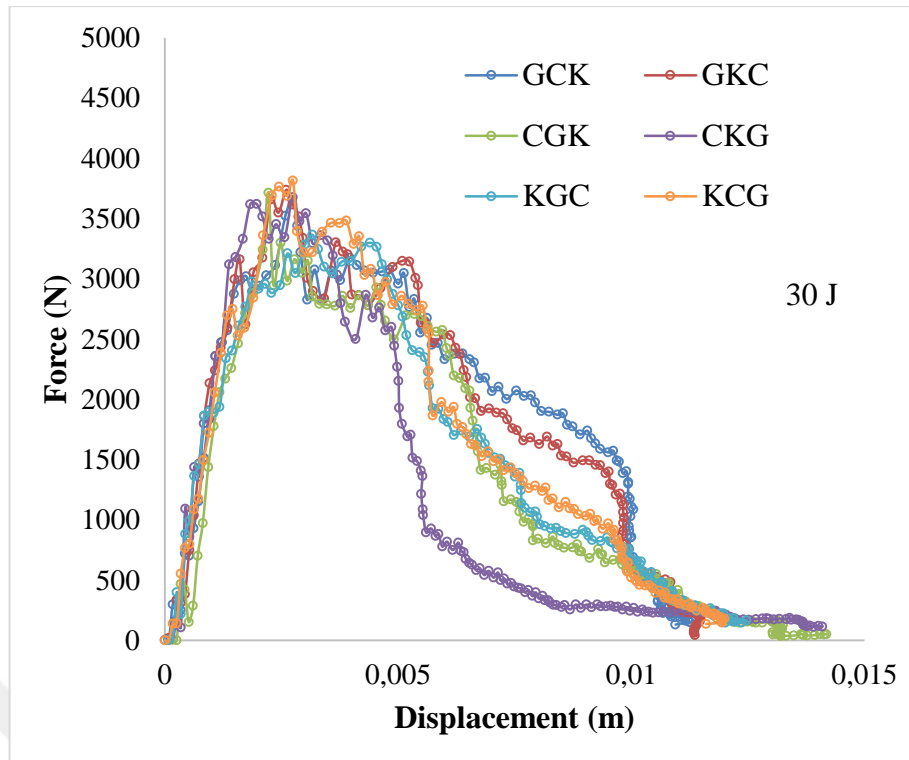
(d)

Figure 6.5 Force histories of the triple fiber configurations. (a) Force-time at 15 J, (b) Force-displacement at 15 J, (c) Force-time at 30 J, (d) Force-displacement at 30 J

Table 6.3 Load and absorbed energy values of double fiber configurations

	Laminate	Fmax(kN)	Ea(J)	d(mm)
15 J	GCK	3.02	8.11	2.7
	GKC	3.37	8.42	2.5
	CGK	3.38	8.55	2.5
	CKG	3.24	7.52	2.3
	KGC	3.09	8.01	2.6
	KCG	3.53	9.82	2.8
30 J	GCK	3.65	22.44	11.40
	GKC	3.73	24.42	11.60
	CGK	3.71	22.26	13.60
	CKG	3.33	20.54	12.80
	KGC	3.67	20.52	12.30
	KCG	3.81	21.51	12.20

Failure surfaces of the triple fiber configurations from Figure 6.6 indicated that all samples resulted in penetration failure after the impact tests. In the case of glass layers at rear side, delamination and amount of failure in the glass layers were clearly visible and greater than those of other fibers placed at rear side (CKG and KCG). In addition, when samples were impacted at glass side, delamination as impacted region was limited due to localized and concentrated force of the impactor which leads to dissipate the impact energy to the interior laminates revealing the pine three and conical shape along the impactor movement. This effect can be clearly seen by comparing damaged area between impacted and non-impacted surfaces.
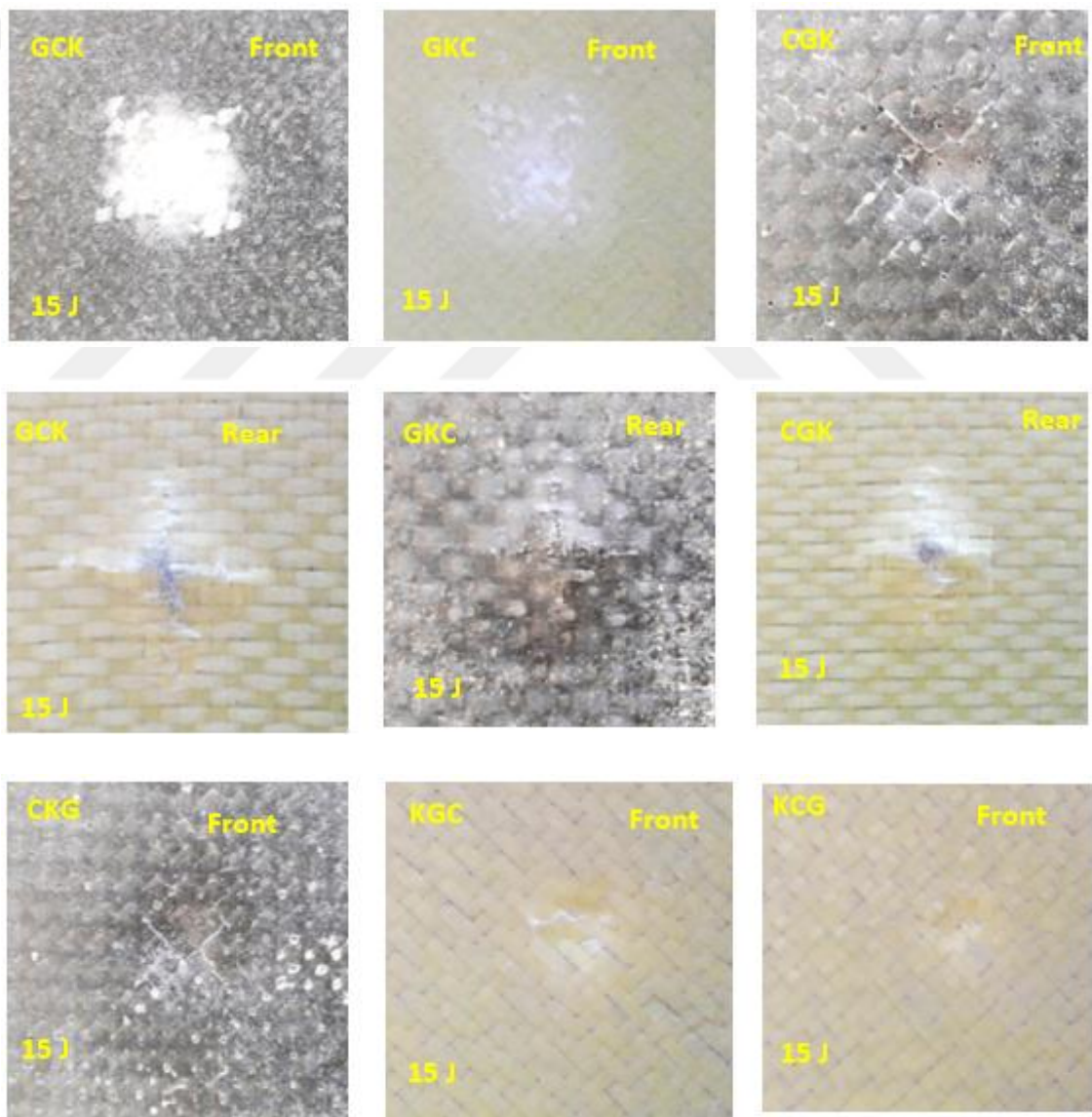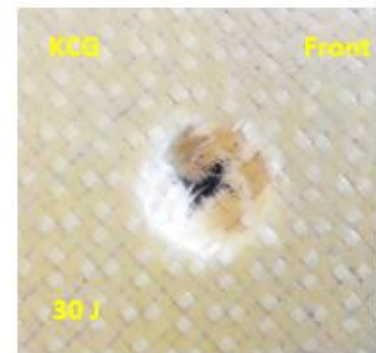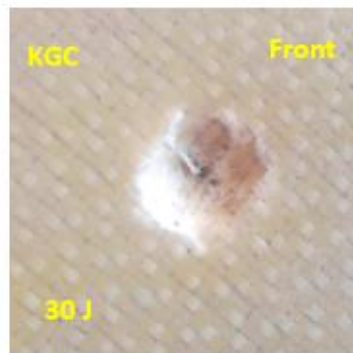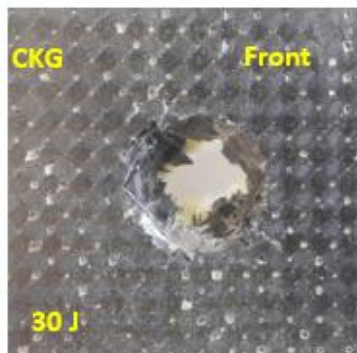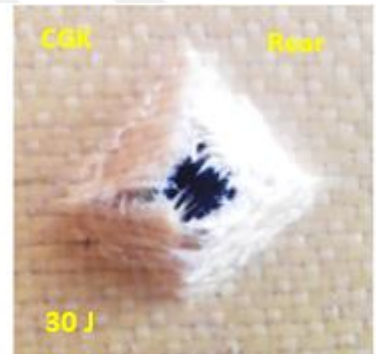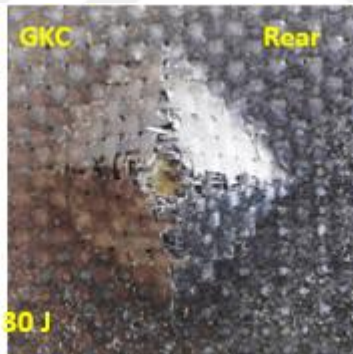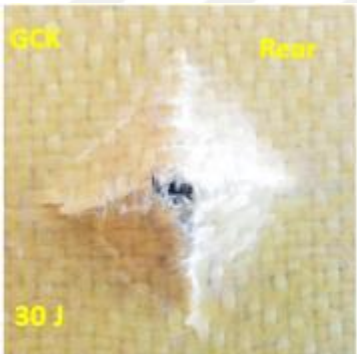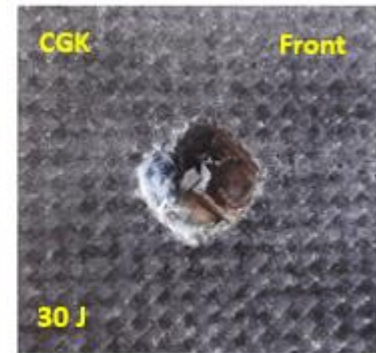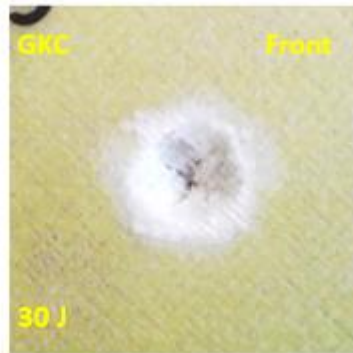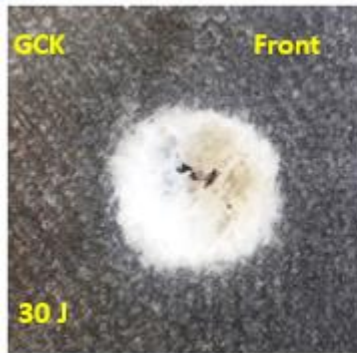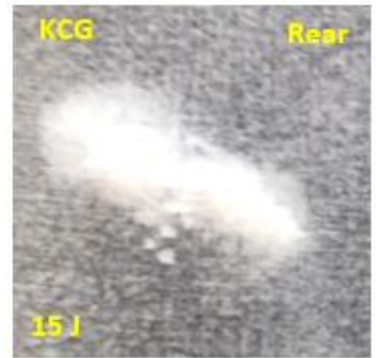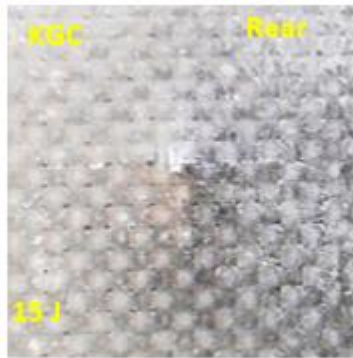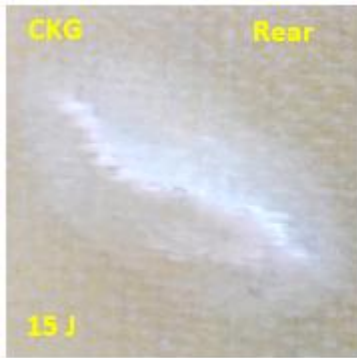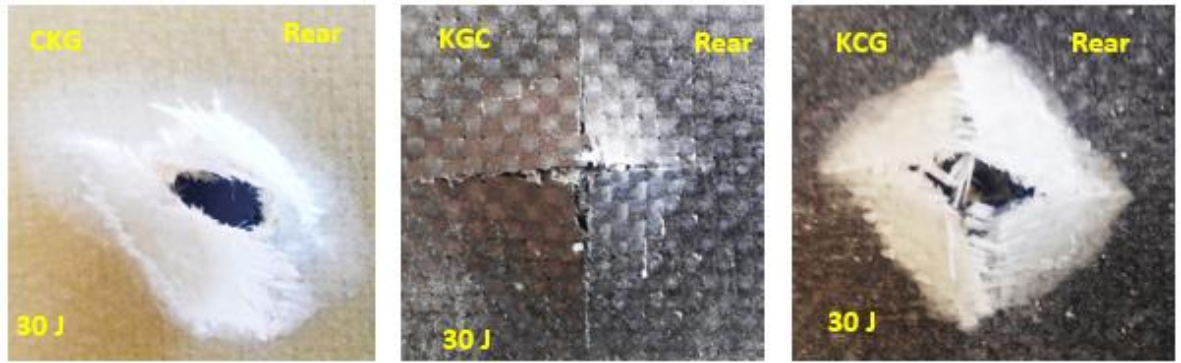
Figure 6.6 Failure surfaces of the triple fiber configurations after the impact tests

The SEM images in Figure 6.7 illustrate the several inter-ply damage modes between interphase of carbon and Kevlar layers. It is clear from Figure 6.7 that damages were composed of matrix cracking, debonding between matrix and fiber and multiple fiber breakages at tension side.
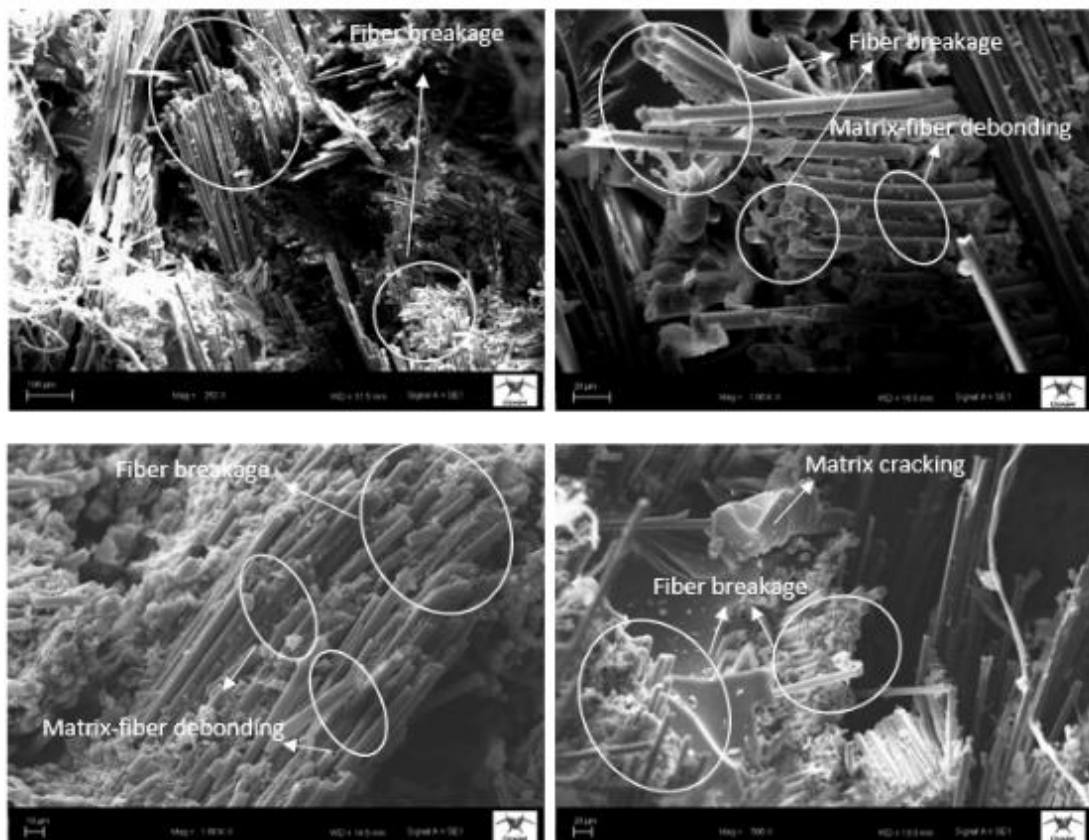
Figure 6.7 Typical SEM images after the impact tests for Carbon/Kevlar (CK) hybrid sample

Hybrid effect values of the samples are illustrated at 30 J as shown in Figure 6.8. The results from Figure 6.8 (a) showed that the samples of CK, KG and KC exhibited the positive hybrid effect for indentation load and absorbed energy, while the sample of GK showed the highest negative hybrid effect.
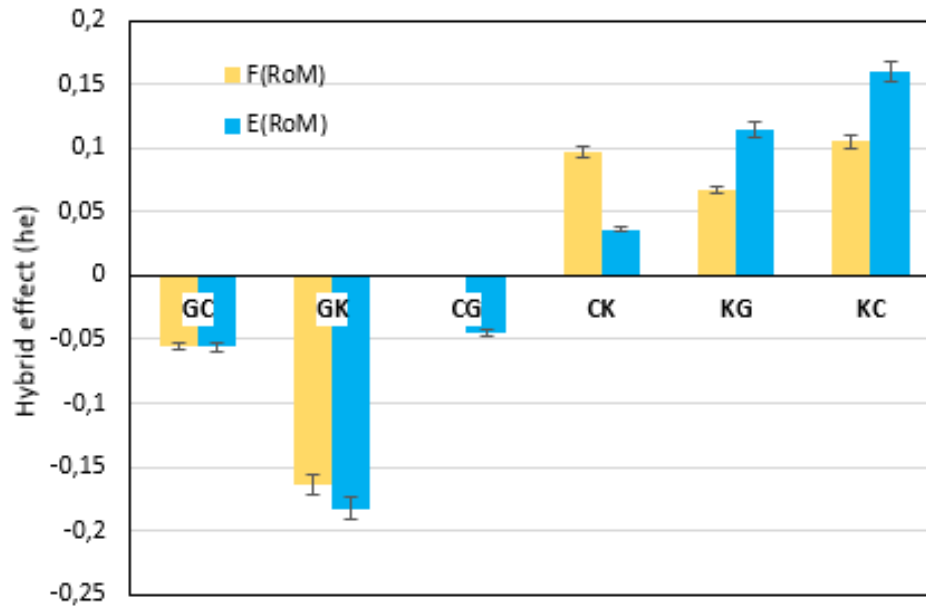
(a)
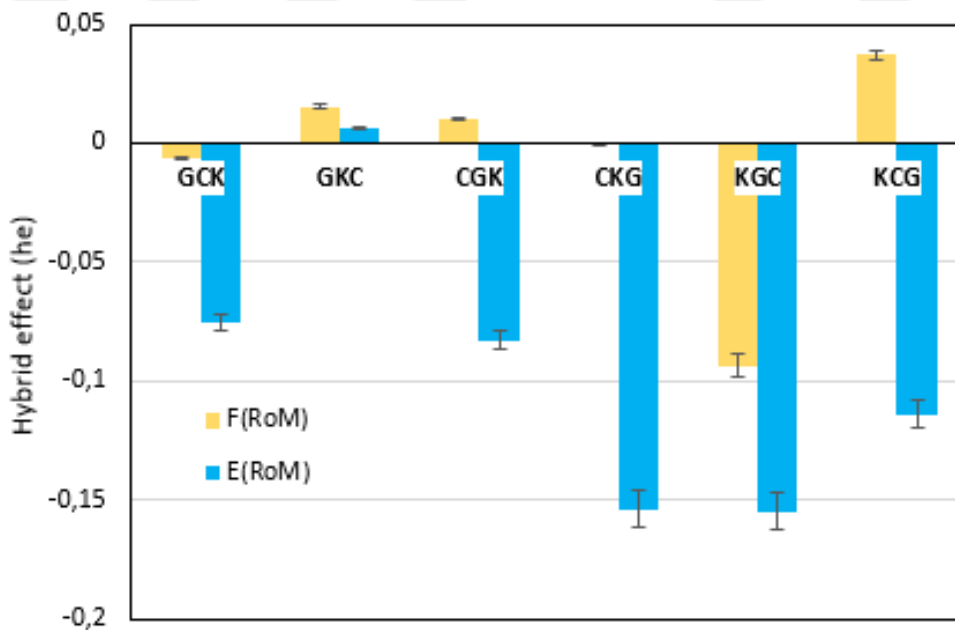
(b)

Figure 6.8 Variation of hybrid effect values according to non-hybrid composite samples. (a) Double fiber configuration, (b) Triple fiber configuration

When triple fiber configurations were compared from Figure 6.8 (b), samples of GKC showed the positive hybrid effect that is attributed to the fact that position of fibers in the lamina is effecting force and displacement behavior of the structure. Samples of CGK and KCG showed similar behavior resulting a positive hybrid effect by means of peak force as well as resulting negative hybrid effect by means of absorbed energy. This may be also attributed to the result of stacking sequence effect and impacted side of the laminates due to asymmetric structure.

When carbon fibers placed at the rear side and S-glass fibers placed at the front side, the carbon fibers restricted the global deformation of the laminate due to high strength and stiffness of the carbon fibers resulting the enhancement of the load carrying and damage resistance capability of the laminate. Similar results were observed with Kevlar/S-glass hybrid configurations, hybrid samples showed higher impact resistance when Kevlar fiber was placed at the impacted side. This is attributed the flexible layers placed at the impacted side were performed larger deformations, showing good energy absorption capacity [84, 88]

6.5 Comparison the Similarity of QSI and LVI Results

In this section, it is aimed to compare the results from QSI and LVI for employing the validity of QSI experiments to characterize feasibility whether it represents the low velocity impact process. The maximum resulting force and absorbed energy values obtained with QSI and LVI tests were represented in Figure 6.9, Figure 6.10, and Figure 6.11, respectively.
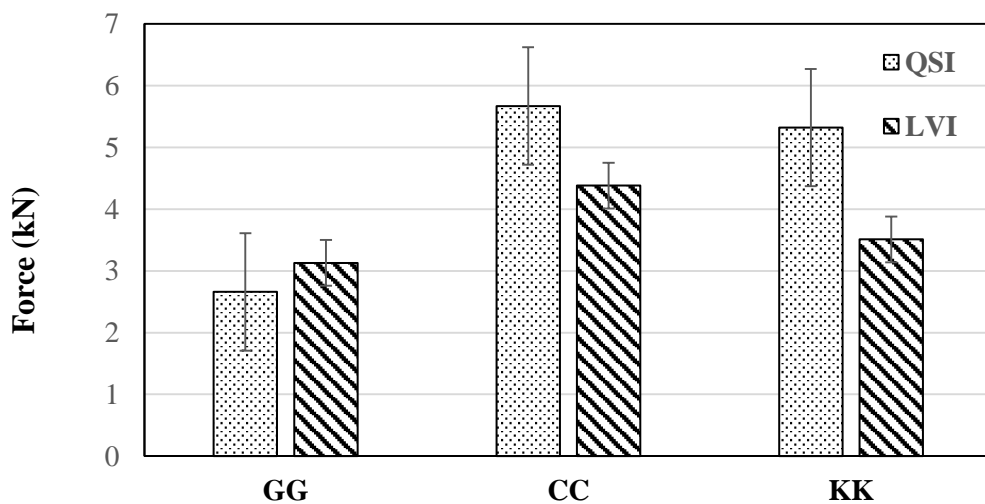
(a)
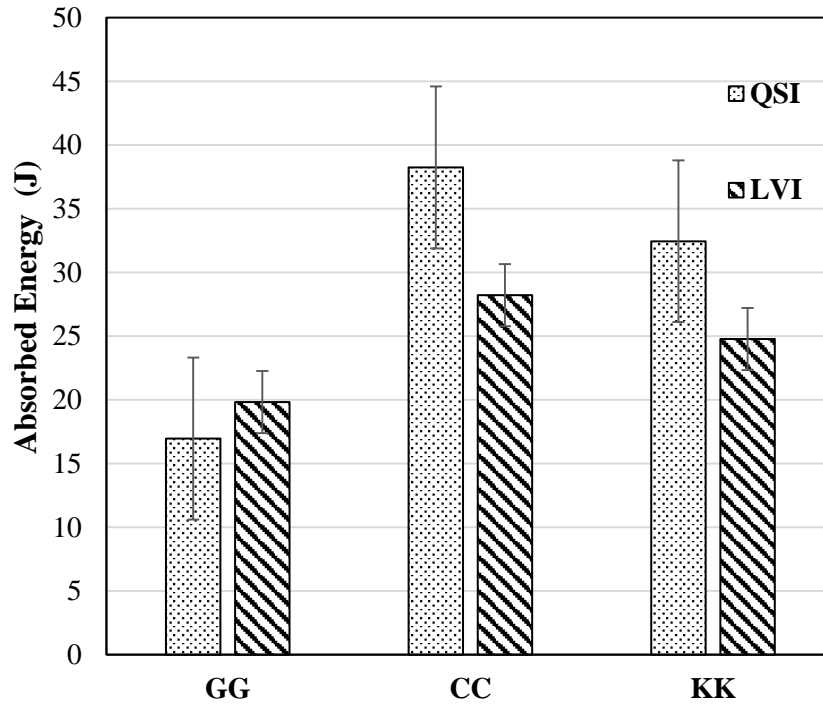
(b)

Figure 6.9 Comparison of QSI and LVI for full composites. (a) Force, (b) Absorbed energy
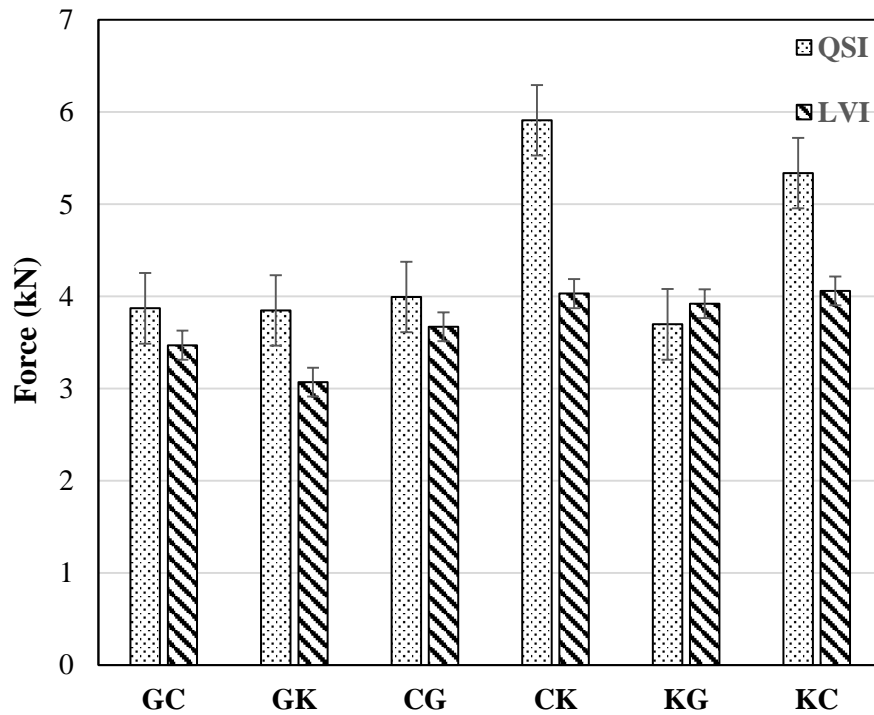
(a)
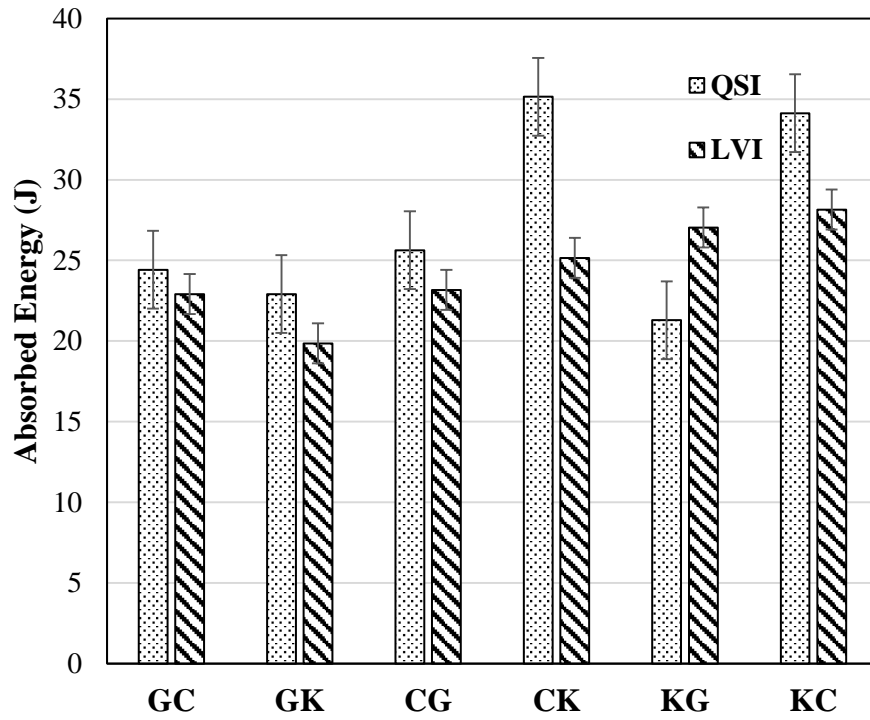
(b)

Figure 6.10 Comparison of QSI and LVI for double fiber configurations. (a) Force, (b) Absorbed energy
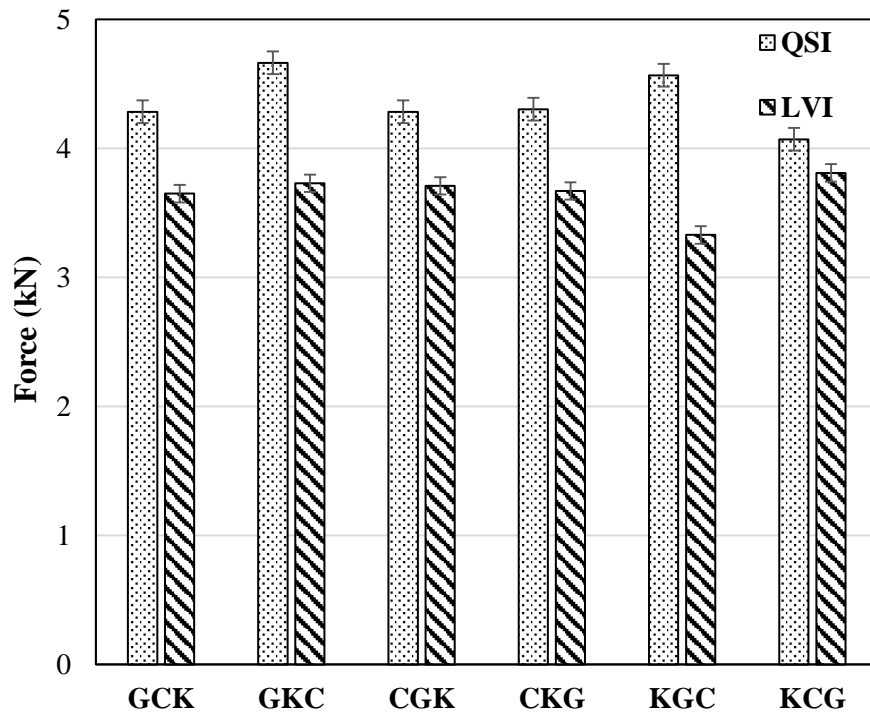
(a)
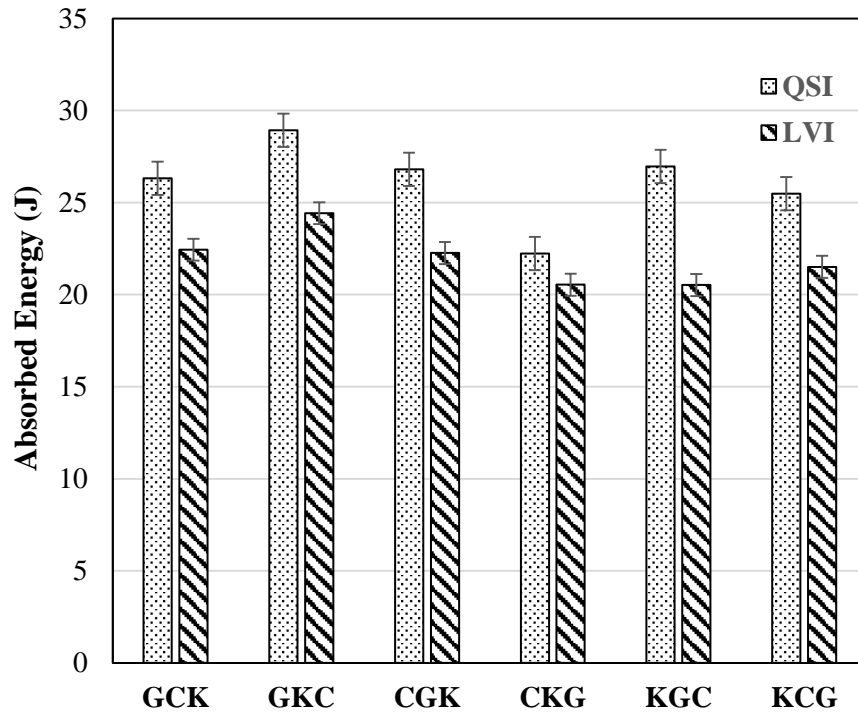
(b)

Figure 6.11 Comparison of QSI and LVI for triple fiber configurations. (a) Force, (b) Absorbed energy

For the same material and boundary conditions of LVI and QSI tests, the results of QSI experiments were obtained with constant punch displacement (10 mm) resulting final perforation of the samples, and compared with the results of LVI experiments under the constant impact energy of 30 J.

It is clear that the trend in the force variation is same in both tests. However, indentation force and ebsorbed energy values obtained with QSI were generally greater than results of LVI tests. This difference can be acceptable for the reason of inherent difference between LVI and QSI measurements. According to results, it is noted that QSI tests provided more information and reliable results about damage event during the low velocity impact process. Generally, it can be also concluded from the overall study that an agreement between QSI and LVI results was found in terms of maximum load and absorbed energy [11, 32, 106-111]. The similarity of QSI and LVI experiments has also been studied in terms of damage characterizations, showing the applicability of the QSI tests to represent the low velocity impact events in the most cases. In this way, it is possible to reduce research costs with obtaining high accurately and efficiently data collecting.

CHAPTER 7

CONCLUSION

A series of QSPT tests were experimentally conducted to evaluate the energy absorption capacity and penetration resistance of woven laminated hybrid composites reinforced with two and three different combinations of woven carbon, Kevlar and glass fibers. Failure characteristics of composite samples during the QSPT were also identified with different fiber configurations at SPR=2 and 5. The main conclusions from this study can be summarized as follows:

- Penetration resistance of composite laminates varies as a function of support span ratio,

- The main failure mechanisms were recorded as fiber fracture due to transverse shear and tensile loading, matrix plasticity and cracking, delamination between layers, fiber pullout, fiber bending and plugging shear out,

- At SPR=5, penetration tests reveals the long tail of extended splits on the back side when glass fiber is placed in the outermost layers,

- The trend of energy absorption capacity of the fibers is followed as: Kevlar>carbon>S-glass,

- Penetration force, punch shear stress and maximum absorption energy values have been increased as support span ratio (SPR) increases,

- At SPR= 2, complete perforation energy capacity of all Kevlar/epoxy (KFRP) is 11 % and 146 % higher than those full carbon/epoxy and full S-glass/epoxy, respectively,

- According to absorbed energy values, sample of CKC exhibited the highest positive hybrid effect, while the sample of CGC showed the highest negative hybrid effect,

- Punch shear stress and absorbed energy values are not sufficiently affected by stacking sequence of the fibers in the lamina at SPR=2,

- Fibers placed in the outer layers plays important role for energy absorption capacity and damage mechanism of the structure.

The indentation behavior of hybrid composite laminates was investigated for two different cases: Double fiber configurations and triple fiber configurations. The influence of hybridizations was explored with different stacking configurations under the constant dent depth of the indenter. The failure modes and spreading of damage in the hybrid composite structures were determined by observing front and back surfaces. Based on results, following conclusions from this study can be summarized.

- Hybridization of two or three different fibers significantly affected the indentation responses (force and absorbed energy) with respect to non-hybrid composites,

- The main failure mechanisms were recorded as fiber fracture due to flexural bending and tensile loading, matrix plasticity and cracking, delamination between layers, debonding and fiber bending,

- S-glass reinforced composite laminates showed the poor indentation resistance and damage characteristics which could be increased by the hybridization of Carbon and Kevlar layers,

- The trend of maximum energy absorption and load carrying capacity of fibers is followed as: Carbon>Kevlar>S-glass,

- Full Carbon/epoxy has shown 15 % and 55 % higher complete perforation energy than those full Kevlar/epoxy and full S-glass/epoxy, respectively,

- When double fiber combinations were compared, hybrid samples of CK and KC exhibited the maximum penetration force and absorbed energy.

- When triple fiber configurations were compared, sample of GKC exhibited maximum indentation force and absorbed energy compared with other hybrid

- Composites, showing an increase of maximum indentation force and absorbed energy by about 75 % according to sample GG.

- The results suggest that it is possible to get desired composite laminates which are similar to Carbon/epoxy laminates by the hybridization of cheaper S-glass fibers

The low velocity impact behavior of hybrid composite laminates was investigated for two different cases: (1) double fiber configurations and (2) triple fiber configurations. The influence of hybridizations was explored with different stacking configurations under the constant impact energies of 15 J and 30 J. Failure modes and spreading of damage in the hybrid composites were identified by observing front and back surfaces. Based on results, following conclusions from this study can be summarized.

- Hybridization of two or three different fibers significantly affect the failure and impact resistance of the composite samples,

- The main failure mechanisms are recorded as fiber fracture due to flexural bending and tensile loading, matrix plasticity and cracking, delamination between layers, debonding and fiber bending,

- S-glass reinforced composite laminates showed the poor impact resistance and tolerances, and also having long splitting and large delaminations when rear side of the hybrid samples were designed as glass fiber and this could be increased by the hybridization of Carbon and Kevlar layers,

- In the view of hybrid effect, samples of CK, KG, and KC exhibited the positive hybrid effect for indentation load and absorbed energy, while the sample of GK showed the highest negative hybrid effect.

- For triple fiber configurations, samples of CGK and KCG behaved the same effect showing the positive hybrid effect by means of peak force while resulting negative hybrid effect by means of absorbed energy.

- When QSI and LVI results were compared, trend in the force variation is same in both QSI and LVI tests. However, indentation force and absorbed energy values obtained with QSI were generally greater than results of LVI tests,

- QSI tests provided more information and reliable results about damage event during the low velocity impact process.

CHAPTER 8

FUTURE WORKS

Following aspects can be considered to extend this study:

- Impact behavior of hybrid composites can be investigated with incorporation of micro and nano scale particles,
- Different fibers with different stacking sequences can be treated to study impact and damage tolerances of the hybrid composites,
- Thermal and aging effects can also be studied for different hybrid configurations.

REFERENCES

[1]   Berthelot, JM. (1999). Mechanics of Composite Materials and Structures, Springer, New York.

[2]   Sanjay, K. (2002). Mazumdar. Composites Manufacturing Materials, Product, and Process Engineering. CRC Press LLC, United States of America.

[3]   http://www.euroaviasevilla.es/compositesymposium/why_composites.php

[4]   Balasubramanian, M. (2014). Composite materials and processing. CRC PressTaylor & Francis Group, Boca Raton.

[5]   Harris, B. (1999). Engineering Composite Materials. The Institute of Materials, London.

[6]   Reid, S.R., Zhou, G. (2000). Impact behavior of fiber-reinforced composite materials and structures. Wood head Publishing Ltd and CRC Press LLC; 1-125, Boca Raton FL 33431, USA.

[7]   Abrate, S. (1998). The Dynamics of Impact on Composite Structures. Key Engineering Materials, 141-143: 671-694.

[8]   Hoskin, B.C., Baker, A.A. (1986). Composite Materials for Aircraft Structures. AIAA education series, American institute of aeronautics and astronautics, , Inc., New York,

[9]   ASTM Standard D6264-8 (1999). ASTM Book of Standards, 15.03.

[10]   ASTM D6264/D6264M (2012). Standard Test Method for Measuring the Damage Resistance of a Fiber-Reinforced Polymer-Matrix Composite to a Concentrated Quasi-Static Indentation Force,

[11]   Nettles, A.T., Douglas, M.J. (2000). A Comparison of Quasi-Static Indentation to Low-Velocity Impact. NASA / TP--210481, Hanover.

[12]   Hosseinzadeh, R., Shokrieh, M.M., Lessard, L. (2006). Damage behavior of fiber reinforced composite plates subjected to drop weight impacts. Composites Science and Technology, **66**, 61−68.

[13] Agrawal, S., Singh, K.K., Sarkar, P.K. (2014). Impact damage on fibre-reinforced polymer matrix composite – A review. Journal of Composite Materials; **48**, 317-332.

[14] Atas, C. (2007). An experimental investigation on the impact response of fiberGlass/aluminum composites. Journal of reinforced plastics and composites, **26**, 1479-1491.

[15] Ji, C., Sun, B., Qiu, Y, Gu, B. (2007). Impact Damage of 3D orthogonal woven composite circular plates. Applied composite materials, **14**, 343–362.

[16] Fan, J., Cantwell, W.J., Guan, Z.W. (2011). The low-velocity impact response of fiber-metal laminates. Journal of reinforced plastics and composites, **30,** 26–35.

[17] Caprino, G., Spataro, G., Luong, S.D. (2004). Low-velocity impact behaviour of fibreglass–aluminium laminates. Composites: Part A, **35**, 605–616.

[18] Mathivanan, N.R., Jerald, J. (2010). Experimental investigation of low-velocity impact characteristics of woven Glass fiber epoxy matrix composite laminates of EP3 grade. Materials and design, **31,** 4553–4560.

[19] Mili, F., Necib, B. (2001). Impact behavior of cross-ply laminated composite plates under low velocities. Composite Structures, **51**, 237-244.

[20] Shyr, T.W., Pan, Y.H. (2003). Impact resistance and damage characteristics of composite laminates. Composite Structures, **62**, 193–203.

[21] Atas, C., Akgun., A, Dagdelen., O, Icten, B.M., Sarikanat, M. (2011). An experimental investigation on the low velocity impact response of composite plates repaired by VARIM and hand lay-up processes. Composite Structures, **93,** 1178–1186.

[22] Zainuddin, S., Arefin T., Fahim A., Hosur, M.V., Tyson, J.D., Kumar, A., Trovillion J., Jeelani, S. (2014). Recovery and improvement in low-velocity impact properties of e-Glass/epoxy composites through novel self-healing technique. Composite Structures, **108**, 277–286.

[23] Baucom, J.N., Zikry, M.A., Rajendran, A.M. (2006). Low-velocity impact damage accumulation in woven S2-Glass composite systems. Composites Science and Technology, **66**, 1229–1238.

[24] Icten, B.M., Kıral, B.G., Deniz, M.E. (2013). Impactor diameter effect on low velocity impact response of woven Glass epoxy composite plates. Composites: Part B, **50,** 325–332.

[25] Santos, M.J., Santos, J.B., Amaro, A.M., Neto, M.A. (2013). Low velocity impact damage evaluation in fiber Glass composite plates using PZT sensors. Composites: Part B, **55,** 269–276.

[26] Belingardi, G., Vadori, R.. (2002). Low velocity impact tests of laminate Glass-fiber-epoxy matrix composite material plates. International Journal of Impact Engineering, **27,** 213–229.

[27] Davies, G.O.A, Hitchings, D. (1996). Impact damage and residual strengths of woven fabric Glass/polyester laminates. Composites Part A, **27**, 1147-1156.

[28] Ghelli, D., Minak, G. (2011). Low velocity impact and compression after impact tests on thin Carbon/epoxy laminates. Composites: Part B, **42,** 2067–2079.

[29] Rı´o, T.G., Zaera, R., Barbero, E., Navarro, C. (2005). Damage in CFRPs due to low velocity impact at low temperature. Composites: Part B, **36,** 41–50.

[30] Quaresimin, M., Ricotta, M., Martello, L., Mian, S. (2013). Energy absorption in composite laminates under impact loading. Composites: Part B, **44,** 133–140.

[31] Pegoretti, A., Cristelli, I., Migliaresi, C. (2008). Experimental optimization of the impact energy absorption of epoxy–Carbon laminates through controlled delamination. Composites Science and Technology, **68,** 2653–2662.

[32] Bull, D.J., Scott, A.E., Spearing, S.M., Sinclair, I. (2014). The influence of toughening-particles in CFRPs on low velocity impact damage resistance performance. Composites: Part A, **58,** 47–55.

[33] Hosur, M.V., Jain, K., Chowdhury, K., Jeelani, S, Bhat, M.R., Murthy, C.R.L. (2007). Low-velocity impact response of Carbon/epoxy laminates subjected to cold–dry and cold–moist conditioning. Composite Structures, **79,** 300–311.

[34] Tiberkak, R., Bachene, M., Rechak, S., Necib., B. (2008). Damage prediction in composite plates subjected to low velocity impact. Composite Structures, **83**, 73–82.

[35] Zabala, H., Aretxabaleta, L., Castillo, G., Urien, J., Aurrekoetxea, J. (2014). Impact velocity effect on the delamination of woven Carbon–epoxy plates subjected to low-velocity equienergetic impact loads. Composites Science and Technology, **94**, 48–53.

[36] Qiu, A., Fu, K., Lin, W., Zhao, C., Tang, Y. (2014). Modelling low-speed drop-weight impact on composite laminates. Materials and Design, **60,** 520–531.

[37] Belingardi, G., Vadori, R. (2003). Influence of the laminate thickness in low velocity impact behavior of composite material plate. Composite Structures, **61,** 27–38.

[38] Moura, M.F.S.F, Marques, A.T. (2002). Prediction of low velocity impact damage in Carbon-epoxy laminates. Composites: Part A, **33,** 361-368.

[39] William, D.C, David, G.R. (2014). Materials Science and Engineering, Wiley, 9th Edition SI Version.

[40] Singh, T.J, Samanta, S. (2015). Characterization of Kevlar Fiber and Its Composites: A Review. Materials Today: Proceedings, **2**, 1381 – 1387.

[41] Das, S., Shaw, J.A, Pal, A. (2015). Determination of inter-yarn friction and its effect on ballistic response of para-aramid woven fabric under low velocity impact. Composite Structures, **120**, 129–140.

[42] Bandaru, A.K, Chavan, V.V, Ahmad, S., Alagirusamy, R. (2016). Ballistic impact response of Kevlar® reinforced thermoplastic composite armors. International Journal of Impact Engineering, **89**, 1–13.

[43] Kumar, S., Gupta, D.S, Singh, I., Sharma, A. (2010). Behavior of kevlar/epoxy composite plates under ballistic impact. Journal of Reinforced Plastics and Composites, **29**, 2048-2064.

[44] Yang, L., Yan, Y., Kuang, N. (2013). Experimental and numerical investigation of Aramid fiber reinforced laminates subjected to low velocity impact. Polymer Testing, **32,** 1163–1173.

[45] Taraghi, I., Fereidoon, A., Taheri-Behrooz, F. (2014). Low-velocity impact response of woven Kevlar/epoxy laminated composites reinforced with multi-walled Carbon nanotubes at ambient and low temperatures. Materials and Design, **53**, 152–158.

[46] Reis, P.N.B., Ferreira, J.A.M., Zhang, Z.Y., Benameur, T., Richardson, M.O.W. (2013). Impact response of Kevlar composites with nano clay enhanced epoxy matrix. Composites: Part B, **46,** 7–14.

[47] Mishra, R., Behera, B.K., Militky., J. (2014). Impact simulation of three-dimensional woven Kevlar-epoxy composites. Journal of Industrial Textiles, **45**, 978-994.

[48] Zukas, J.A. Impact Dynamics. (1992). Malabar, Florida: Krieger Publishing Company.

[49] Nunna, S., Chandra, P.R., Shrivastava, S., Jalan, A.K. (2012). A review on mechanical behavior of natural fiber based hybrid composites. Journal of Reinforced Plastics and Composites, **31**,759–769,

[50] Larsson, F. (1997). Damage tolerance of a stitched carbon/epoxy laminate. Compos Part A, **28,** 923–934.

[51] Abrate, S. Impact on laminated composites: recent advances. (1994). Appl. Mech. Rev., **47**, 517–544.

[52] Cantwell, WJ, Morton, J. (1991). The impact resistance of composite materials– a review. Composites, **22**, 347–362.

[53] Sadasivam, B., Mallick, P.K. (2002). Impact damage resistance of random fiber reinforced automotive composites. Journal of Thermoplastics Composite Materials, **15**, 181–191.

[54] Wyrick, D.A, Adams, D.F. (1988). Damage sustained by a carbon/epoxy composite material subjected to repeated impact. Composites, **19,** 19–27.

[55] Abrate, S. (1998). Impact on composite structures. Cambridge (UK): Cambridge University Press.

[56] Atas, C., Liu, D. (2008). Impact response of woven composites with small weaving angles. International Journal of Impact Engineering, **35,** 80–97.

[57] Hosur, M.V., Karim, M.R., Jeelani, S. (2003). Experimental investigations on the response of stitched/unstitched woven S2-glass/SC15 epoxy composites under single and repeated low velocity impact loading. Composite Structures, **62**, 89–102.

[58] Kaw, A.K. (2006) Mechanics of Composite Materials, Taylor & Francis Group, LLC.

[59] Bunsell, A.R., Renard, J. (2005). Fundamentals of Fibre Reinforced Composite Materials, Taylor & Francis.

[60] Harris, B. (1999). Engineering Composite Materials, Maney Materials Science.

[61] Vejen, N, Pyrz, R. (2001). Transverse crack growth in glass/epoxy composites with exactly positioned long fibres. Part I: Experiments. Compos Part B: Engineering, **32**, 557-64.

[62] Caprino, G. (1984). Residual strength prediction of impacted CFRP laminates. Journal of Composite Materials, **18,** 508-18.

[63] Shyr, T.W., Pan, Y.H. (2003). Impact resistance and damage characteristics of composite laminates. Composite Structures, **62**, 193–203.

[64] Gellert, E.P, Cimpoeru, S.J, Woodward, R.L. (2000). A study of the effect of target thickness on the ballistic perforation of glass–fiber-reinforced plastic composites. International Journal of Impact Engineering, **24**, 445–56.

[65] Morais, W.A, Monteiro, S.N, D'Almeida J.R.M. (2005). Effect of the laminate thickness on the composite strength to repeated low energy impacts. Composite Structures, **70**, 223–228.

[66] Belingardi, G., Vadori, R. (2003). Influence of the laminate thickness in low velocity impact behavior of composite material plate. Composite Structures, **61**, 27–38.

[67] Sevkat, E., Liaw, B., Delale, F. (2013). Drop-weight impact response of hybrid composites impacted by impactor of various geometries. Materials and Design, **52**, 67–77.

[68] Sarasini, F., Tirillo J., Valente, M., Valente, T, Cioffi, S., Iannace, S., Sorrentino, L. (2013). Effect of basalt fiber hybridization on the impact behavior under low impact velocity of glass/basalt woven fabric/epoxy resin composites. Composites: Part A, **47**, 109–123.

[69] Bandaru, A.K., Vetiyatil, L., Ahmad, S. (2015). The effect of hybridization on the ballistic impact behavior of hybrid composite armors. Composites Part B, **76**, 300-319.

[70] Naik, N.K, Ramasimha, R., Arya, H., Prabhu, S.V., Shama Rao, N. (2001). Impact Response and damage tolerance characteristics of glass– carbon/epoxy hybrid composite plates. Composites Part B, **32**, 565–74.

[71] Sevkat, E., Liaw, B., Delale, F. (2013). Drop-weight impact response of hybrid composites impacted by impactor of various geometries. Materials and Design, **52,** 67–77.

[72] Sevkat, E., Liaw, B., Delale, F. (2012). Ballistic performance of hybrid and non-hybrid composite plates. Journal of Strain Analysis, **47**, 453–470.

[73] González, E.V., Maimí, P., Sainz, J.R., Cruz, P., Camanho, P.P. (2014). Effects of inter-ply hybridization on the damage resistance and tolerance of composite laminates. Composite Structures, **108,** 319–331.

[74] Hosur, M.V., Adbullah, M., Jeelani, S. (2005). Studies on the low-velocity impact response of woven hybrid composites. Composite Structures, **67,** 253–262.

[75] Evci, C., Gülgeç, M. (2012). An experimental investigation on the impact response of composite materials. International Journal of Impact Engineering, **43,** 40-51.

[76] Sarasini, F., Tirillò, J., Valente, M., Ferrante, L., Cioffi, S., Iannace, S. (2013). Hybrid composites based on Aramid and Basalt woven fabrics: Impact damage modes and residual flexural properties. Materials and Design, **49**, 290–302.

[77] Sarasini, F., Tirillò, J., Valente, M., Ferrante, L., Valente, T., Cioffi, S., Iannace, S, Sorrentino, L. (2013). Effect of Basalt fiber hybridization on the impact behavior under low impact velocity of Glass/Basalt woven fabric/epoxy resin composites. Composites: Part A, **47**, 109–123.

[78] Sarasini, F., Tirillò, J., Ferrante, L., Valente, M., Valente, T., Lampani, L., Gaudenzi, P., Cioffi, S., Iannace, S., Sorrentino, L. (2014). Drop-weight impact behaviour of woven hybrid Basalt–Carbon/epoxy composites. Composites: Part B, **59,** 204–220.

[79] Wang, X., Hu, B., Feng, Y., Liang, F., Mo, J, Xiong, J., Qiu, Y. (2008). Low velocity impact properties of 3D woven Basalt/Aramid hybrid composites. Composites Science and Technology, **68**, 444–450.

[80] ASTM D: 7136 (2005). Standard Test Method for Measuring the Damage Resistance of a Fiber-Reinforced Polymer Matrix Composite to a Drop-Weight Impact Event.

[81] Sayer, M. (2009). Hibrit kompozitlerin darbe davranişlarinin incelenmesi. PhD Thesis in Mechanical Engineering, Dokuz Eylül University, Izmir/Turkey.

[82] Sayer, M., Bektas, N.B., Sayman, O. (2010). An experimental investigation on the impact behavior of hybrid composite plates. Composite Structures, **92,** 1256–1262.

[83] Sayer, M., Bektas, N.B, Demir, E., Çallioğlu, H. (2012). The effect of temperatures on hybrid composite laminates under impact loading. Composites: Part B, **43**, 2152–2160.

[84] Park, R., Jang, J. (1998). The effects of hybridization on the mechanical performance of aramid/polyethylene intraply fabric composites. Composites Science and Technology, **58**, 1621–1628.

[85] Tjong, S.C., Xu, S.A., Mai, Y.W. (2003). Impact fracture toughness of short glass fiber reinforced polyimide 6, 6 hybrid composites containing elastomer

particles using essential work of fracture concept. Materials Science and Engineering A, **347**, 338–345.

[86] Abisset, E., Daghia, F., Sun, X.C., Wisnom, M.R., Hallett, S.R. (2016). Interaction of inter- and intralaminar damage in scaled quasi-static indentation tests: Part 1 – Experiments. Composite Structures, **136**, 712–726.

[87] Sreekala, M.S., George, J., Kumaran, M.G., Thomas, S. (2002). The mechanical performance of hybrid phenol-formaldehyde-based composites reinforced with glass and oil palm fibres. Composites Science and Technology, **62**, 339–353.

[88] Erklig, A., Bulut, M. (2016). Experimental investigation on tensile and Charpy impact behavior of Kevlar/S-glass/epoxy hybrid composite laminates. Journal of Polymer Engineering, DOI 10.1515/polyeng-2015-0538.

[89] Bozkurt, O.Y, Erklig, A, Bulut, M. (2016). Hybridization Effects on Charpy Impact Behavior of Basalt/Aramid Fiber Reinforced Hybrid Composite Laminates. Polymer Composites, DOI 10.1002/pc.23957,

[90] Wen, H.M. (2000). Predicting the penetration and perforation of FRP laminates struck normally by projectiles with different nose shapes. Composite Structures, **49**, 321-329.

[91] Islam, W., Gama, B. (2005). A quasi-static penetration model for ballistic energy absorption of thick section composite. Research Reviews, University of Delaware.

[92] Sun, C.T, Potti, S.V. (1996). A simple model to predict residual velocities of thick composite laminates subjected to high velocity impact. International Journal of Impact Engineering, **18**, 339-353.

[93] Nemes, J.A, Eskandari, H., Rakitch, L. (1998). Effect of laminate parameters on penetration of graphite/epoxy composites. International Journal of Impact Engineering, **21**, 97-112.

[94] Gama, B.A, Gillespie, J.W. (2008). Punch shear based penetration model of ballistic impact of thick-section composites. Composite Structures, **86**, 356–369.

[95] Xiao, J.R, Gama, B.A, Gillespie, J.W. (2007). Progressive damage and delamination in plain weave S-2 Glass/SC-15 composites under quasi-static punch-shear loading. Composite Structures, **78**, 182–196.

[96] Potti, S.V., Sun, C.T. (1997). Prediction of impact induced penetration and delamination in thick composite laminates. International Journal of Impact Engineering; **19**, 31-48.

[97] Goldsmith, W. Dharan, C.K.H, Chang, H. (1995). Quasi-Static and Ballistic Perforation of Carbon Fiber Laminates. International Journal of Solids Structures; 32:89-103.

[98] He, T., Wen, H.M., Qin, Y. (2007). Penetration and perforation of FRP laminates struck transversely by conical-nosed projectiles. Composite Structures, **81**, 243–252.

[99] Wen, HM. (2001). Penetration and perforation of thick FRP laminates. Composites Science and Technology, **61**, 1163–1172.

[100] Caprino, G., Langella, A., Lopresto, V. (2003). Indentation and penetration of Carbon fibre reinforced plastic laminates. Composites: Part B, **34**, 319–325.

[101] Wardle, B.L., Lagace, P.A. (2007). On the use of quasi-static testing to assess impact damage resistance of composite shell structures. Mechanics of Composite Materials and Structures, 5, 103-119.

[102] Yahaya, R., Sapuan, S.M, Jawaid, M., Leman, Z., Zainudin, E.S. (2014). Quasi-static penetration and ballistic properties of kenaf–Aramid hybrid composites. Materials and Design, **63,** 775–782.

[103] Jordan, J.B., Naito, C.J., Haque, B.Z. (2014). Quasi-static, low-velocity impact and ballistic impact behavior of plain weave E-Glass/phenolic. Journal of Composite Materials, **48**, 2505–2516.

[104] Yang, S,H., Sun, C.T. (1982). Indentation law for composite laminates. Composite materials: Testing and design (sixth conference), 425-449.

[105] Herb, V., Couégnat, G., Martin, E. (2010). Damage assessment of thin SiC/SiC composite plates subjected to quasi-static indentation loading. Composites: Part A, **41**, 1677–1685.

[106] Lee, S.M, Zahuta, P. (1991). Instrumented Impact and Static Indentation of Composites. Journal of Composite Materials, **25**, 204-222.

[107] Jackson, W.C, Poe, C. (1992). The Use of Impact Force as a Scale Parameter for the Impact Response of Composite Laminates. NASA Technical Memorandum 104189,

[108] Hongkarnjanakul, N., Rivallant, S., Bouvet, C., Miranda A. (2014). Permanent indentation characterization for low-velocity impact modelling using three-point bending test Journal of Composite Materials, **48**, 2441–2454.

[109] Kwon, Y.S, Sankar, B.V. Indentation Damage in Graphite/Epoxy Laminates. (1991). Proceedings of the American Society for Composites, Sixth Technical Conference. 483–492.

[110] Kaczmarek, H., Maison, S. (1994). Comparative ultrasonic analysis of damage in CFRP under static indentation and low-velocity impact. Compos. Sci. Technol, **51**, 11–26.

[111] Aoki, Y., Suemasu, H., Ishikawa, T. (2007). Damage propagation in CFRP laminates subjected to low velocity impact and static indentation. Adv. Compos. Mater, **16**, 45–61.

[112] Lagace, P.A, Williamson, J.E, Wilson, P.H, Wolf, E., Thomas, S.A. (1993). Preliminary Proposition for a Test Method to Measure (Impact) Damage Resistance. J. Reinf. Plast. Compos, **12**, 584-601.

[113] Highsmith, A.L. (1997). A Study of the Use of Contact Loading to Simulate Low Velocity Impact, NASA Contractor Report, **97**, 206121

[114] Elber, W. (1983). Failure Mechanics in Low-Velocity Impacts on Thin Composite Plates, NASA Technical Paper, 2152.

[115] Marom, G., Fischer, S., Tuler, R.F., Wagner, H.D. (1978). Hybrid effects in composites: conditions for positive or negative effects versus rule-of-mixtures behavior. Journal of Materials Science, **13**, 1419–1426.

[116] Stevanovic, M.M., Stecenko, T.B. (1992). Mechanical Behaviour of Carbon and Glass Hybrid Fiber Reinforced Polyester Composites, Journal of Material Science, **27**, 941–946.

[117] Yamashita, S., Hatta, H., Sugano, T., Murayama, K. (1989). Fiber Orientation Control of Short Fiber Composites: Experiment, Journal of Composite Materials, **23**, 32–41.

[118] Nakanishi, E., Suzuki, J., Isogimi, K. (1998). Microscopic Observations in Cutting of Aramid-Glass Hybrid FRP, First Asian-Australasian Conference on Composite Materials, ACCM-1, 225.1–225.4.

[119] Schijve, J., Vanlipzig, H.T.M., Vangestel, G.F.J.A., Hoeymakers, A.H.W. (1979). Fatigue Properties of Adhesive-Bonded Laminated Sheet Material of Aluminum Alloys, Engineering Fracture Mechanics, **12**, 561–579.

[120] Lee, S.H, Aono, Y., Noguchi, H. (2003). Damage Mechanism of Hybrid Composites with Nonwoven Carbon Tissue Subjected to Quasi-static Indentation Loads. Journal of Composite Materials, **37**, 4, 333-349

[121] Yeter, E. (2014). Buckling behavior of laminated hybrid composites. PhD Thesis in Mechanical Engineering, Gaziantep University.

[122] ASTM D 732–02. (2002). Standard Test Method for Shear Strength of Plastics by Punch Tool.

[123] Deka, L. (2008). Multi-site impact response of laminated and sandwich composites. PhD dissertation, University of Alabama at Birmingham.

[124] Lee, S.R, Sun, C.T. (1993). A Quasi-static penetration model for composite laminates. Journal of Composite Materials, **3**, 251-271.

[125] Dong, C., Davies, I.J. (2013). Flexural properties of glass and carbon fiber reinforced epoxy hybrid composites. Proceedings of the Institution of Mechanical Engineers, Part L: Journal of Materials Design and Applications, **227,** 308-317.

[126] Dong, C., Sudarisman, Davies, I.J. (2013). Flexural properties of E glass and TR50S carbon fiber reinforced epoxy hybrid composites. Journal of Materials Engineering and Performance, **22**, 41-49.

[127] Dong, C., Davies, I.J. (2012). Optimal design for the flexural behaviour of glass and carbon fibre reinforced polymer hybrid composites. Materials & Design, **37**, 450-457.

[128] Dong, C., Ranaweera-Jayawardena, H.A., Davies, I.J. (2012). Flexural properties of hybrid composites reinforced by S-2 glass and T700S carbon fibres. Composites Part B: Engineering, **43**, 573-581.

[129] Dong, C., Duong, J., Davies, I.J. (2012). Flexural properties of S-2 glass and TR30S carbon fiber-reinforced epoxy hybrid composites. Polymer Composites, **33**, 773-781.

[130] Dong, C., Davies, I.J. (2014). Flexural and tensile strengths of unidirectional hybrid epoxy composites reinforced by S-2 glass and T700S carbon fibres. Materials & Design, **54**, 955-966.

[131] Jeng, S.T, Jing, H.S, Chung, C. (1994). Predicting the ballistic limit for plain woven glass/epoxy composite laminates. International Journal of Impact Engineering, **4**, 451-464.

[132] Cristescu, N, Malvern, L.E, Sierakowski, R.L. (1975). Failure mechanism in composite plates by blunt-ended penetrators. American Society for Testing and Materials, ASTM, STP, **568**, 159–172.

[133] Marom, G., Fischer, S., Tuler, F.R, Wagner, H.D. (1978). Hybrid effects in composites: conditions for positive or negative effects versus rule-of-mixtures behaviour. Journal of Materials Science, **13**, 1419—1426.

[134] Aktas, A., Aktas, M., Turan, F. (2013). The effect of stacking sequence on the impact and post-impact behavior of woven/knit fabric glass/epoxy hybrid composites. Composite Structures, **103**, 119–135.

[135] Muhi, R.J, Najim, F., Moura, M. (2009). The effect of hybridization on the GFRP behavior under high velocity impact. Composites: Part B, **40**, 798–803.

[136] Ikeda, M., Kusumoto, Y., Yakushijin, Y., Somekawa, S., Ngweniform, P., Ahmmad, B. (2007). Hybridized synergy effect among TiO2, Pt and graphite silica on photocatalytic hydrogen production from water–methanol solution. Catalysis Communications, **8**, 1943–1946.

[137] Szeluga, U., Kumanek, B., Trzebicka, B. (2015). Synergy in hybrid polymer/nanocarbon composites. A review. Composites: Part A, **73**, 204–231.

CIRRICULUM VITAE

PERSONAL INFORMATION

Name and Surname: Mehmet BULUT

Nationality   :T.C.

E-mail: mbulut@gantep.edu.tr

EDUCATION

	Graduate School	Year
Master	Gaziantep Univeristy, Mechanical Engineering Department	2013
Bachelor	Balıkesir University	2005
High School	Sivas Cumhuriyet High School	1998

WORK EXPERIENCE

	Place	Enrollment
2010-Present (35.)	Gaziantep Univeristy, Mechanical Engineering Department	Research Asst.
2010-Present	Hakkari University, Mechanical Engineering Department	Research Asst.

PUBLICATIONS

Papers Published in International SCI indexed Journals

1) O.Y. Bozkurt, A. Erklig, M. Bulut. Hybridization effects on charpy impact behavior of basalt/aramid fiber reinforced hybrid composite laminates. Polymer Composites, 2016, DOI 10.1002/pc.23957.

2) A. Erklig, M. Bulut. Experimental investigation on tensile and charpy impact behavior of Kevlar/S-Glass/Epoxy hybrid composite laminates. Journal of Polymer Engineering, 2016. DOI:10.1515/polyeng-2015-0538,

3) M. Bulut, A. Erkliğ, E. Yeter. Hybridization effects on quasi-static penetration resistance in fiber reinforced hybrid composite laminates. Composites Part B: Engineering, 2016, 98, 9-22,

4) A. Erklig, M. Al-Saadi, M. Bulut. A comparative study on industrial waste fillers affecting mechanical properties of polymer matrix composites. Materials Research Express, 2016, 3, 105302,

5) Erklig, A., Bulut, M., Yeter, E. The effect of hybridization and boundary conditions on damping and free vibration of composite plates. Science and Engineering of Composite Materials, 2015, V22(5), 565–571,

6) E. Yeter, A. Erklig, M. Bulut. Hybridization Effects on Lateral Buckling Behavior of Laminated Composite Plates. Polymer Composites, 2015, DOI: 10.1002/pc.23438,

7) M. Bulut, O.Y.Bozkurt, A. Erklig. Damping and vibration characteristics of Basalt-Aramid/Epoxy hybrid composite laminates. Journal of Polymer Engineering, 2015, 36(2), 173-180,

8) M Bulut, A Erkliğ, E Yeter. Experimental investigation on influence of Kevlar fiber hybridization on tensile and damping response of Kevlar/glass/epoxy resin composite laminates. Journal of Composite Materials, 2015, 50, 1875-1886,

9) Ahmet Erkliğ, Mehmet Bulut and EyüpYeter. Natural frequency response of laminated hybrid composite beams with and without cutouts. Journal of Polymer Engineering, 2014, 34(9), 851–857,

10) Eyüp Yeter, Ahmet Erkliğ and Mehmet Bulut. Hybridization Effects on the Buckling Behavior of Laminated Composite Plates. Composite Structures, 2014, 118,19–27,

11) Ahmet Erklig, Eyüp Yeter and Mehmet Bulut. The effects of cut-outs on lateral buckling behavior of laminated composite beams. Composite Structures, 2013, 104, 54-59,

12) Ahmet Erkliğ, Mehmet Bulut and Eyüp Yeter. Effects of cutouts on natural frequency of laminated composite plates. Science and Engineering of Composite Materials, 2012, 20(2)-179–185.

International Conference Papers Published in Proceedings

1) A. Erkliğ, M. Bulut. Influence of perlite particle inclusion with adhesively bonded single strap repairs on tensile properties of S-glass/epoxy composite laminates. 3rd International Conference on Advanced Technology & Sciences (ICAT 2016), Konya/Turkey, 2016.

2) A. Erkliğ, M. Bulut. International conference on Structural Engineering, New Technology and Methods (ICSENM'2016), Prague, Czech Republic, 2016.

3) O.Y. Bozkurt, M. Bulut, Ö. Özbek. Effect of Fibre Orientations on Damping and Vibration Characteristics of Basalt Epoxy Composite Laminates. International conference on Structural Engineering, New Technology and Methods (ICSENM'2016), Prague, Czech Republic, 2016.

4) A. Erklig, M. Bulut. Tek tesirli yapıştırma bağlantılarında epoksi yapıştırıcı içerisindeki mikro boyuttaki perlitin hasar yüküne etkileri. International Conference on Welding Technologies and Exhibition (ICWET'16), 2016

5) O.Y. Bozkurt, Ö. Özbek, M. Bulut. Damping and Vibration Behavior of Adhesively Bonded Composite Laminates. International Conference on Welding Technologies and Exhibition (ICWET'16), 2016

6) Ahmet Erklig, Yousif Jaber al-ani, Mehmet Bulut, M. Akif Kütük. The effect of micro-particle-reinforced adhesive on tensile strength of double lap joints. 2nd International Conference on Engineering and Natural Sciences (ICENS 2016)

7) Mehmet Bulut and Ahmet Erkliğ. Free Vibration of Composite Plates With Cut-outs.2nd International Conference on Computation for Science and Technology, 9-11 july, 2012, Niğde.

National Conference Papers Published in Proceedings

1) M. Bulut, M. Şenyurt, A. Erkliğ.Tabakalı Kompozit Plakaların Yarı Statik Penetrasyon Yükleri Altındaki Davranışlarının Araştırılması. XIX. Ulusal Mekanik Kongresi (Trabzon),

2) M. Bulut, A. Erkliğ, E. Yeter.Kevlar ve S-Cam ile Güçlendirilmiş Hibrit Kompozitlerin Titreşim Özelliklerinin Belirlenmesi. XIX. Ulusal Mekanik Kongresi (Trabzon).